ADVANCES IN PHYSICS, 2000, VOL. 49, NO. 3, 257–320

Heavy fermion semiconductors

PETER S. RISEBOROUGH
Polytechnic University, Six Metro Tech Center, Brooklyn, NY 11201, USA

[Received 27 May 1999; revised 11 October 1999; accepted 14 October 1999]

Abstract

The heavy fermion semiconductors, or Kondo insulators, are very narrow gap semiconductors in which the properties show unusual temperature dependencies. We shall review their properties and show how they can be interpreted in terms of an electronic band structure, with a temperature dependent hybridization gap together with temperature dependent quasi-particle lifetimes. The properties of these semiconductors are very sensitive to impurities, which can enhance the incipient antiferromagnetic correlations and precipitate a magnetic instability.

Contents

1. Introduction

The class of materials known as heavy-fermion semiconductors, or alternately as Kondo insulators [1], is mainly comprised of materials which contain at least one element per formula unit with a partially filled localized f (or d) shell in addition to elements from the p or d series of the periodic table. A partial list of materials which

have, at one time or the other, been assigned to this class includes SmB_6 [2–4], $Ce_3Bi_4Pt_3$ [5], $Ce_3Sb_4Pt_3$ [6–8], $Ce_3Sb_4Au_3$ [6, 7], $CeFe_4P_{12}$ [9, 10], CeNiSn [11], CeRhSb [12], CeRhAs [13], YbB_{12} [14, 15], $U_3Sb_4Pt_3$ [16, 17], $U_3Sb_4Pt_3$ [16], $U_3Sb_4Pd_3$ [16], UNiSn [18–20], URhSb [18], UPtSn [18], UFe_4P_{12} [9, 21–24], FeSi [25] etc. All of these materials have cubic symmetry, except for the orthorhombic systems CeNiSn, CeRhSb and CeRhAs. The class of materials is characterized by their electronic properties, which at high temperatures is associated with a set of independent localized (f) moments interacting with a sea of conduction electrons, while at low temperatures the electronic properties resemble those of narrow gap semiconductors. The principal interest in these materials is due to the existence of large many-body renormalizations. For example, the gaps inferred from optical, magnetic, transport and thermodynamic properties are usually almost an order of magnitude smaller than those inferred from local density functional approximation (LDA) electronic structure calculations [26–35]. The existence of significant many-body effects is also signalled by unusual temperature dependencies. For example, in the high temperature state the resistivity exhibits a logarithmic dependence characteristic of the scattering of the conduction electrons from a set of independent local moments, and in the low temperature region the experimentally determined semiconducting gap shows a strong temperature dependence. Also the spectral densities inferred from optical, magnetic and electron spectroscopies indicate the existence of an extremely temperature dependent narrow f feature in the electronic density of states close to the top of the valence band, which may be identified with a band of heavy quasi-particles. As these materials are semiconducting, the properties of this filled quasi-particle band are not directly amenable to thermodynamic probes. However, by doping these materials it could be hoped that carriers could be introduced into the bands allowing the quasi-particles to be probed directly. Doping studies have shown [36–38], that on replacing the f ions with non-f ions, the specific heat rises towards the values expected for mixed valent materials. This is interpretable in terms of the disorder causing the coherence of the quasi-particle states to be disrupted and introducing impurity states with energies that fall within the band gap. These impurity states are known as Kondo hole states. For sufficiently high impurity concentrations these Kondo hole states form an impurity band and give rise to non-analytic dependencies on the impurity concentrations [39–42].

These materials were first designated as Kondo insulators [1] because the experimental properties of the high temperature phase were reminiscent of the Kondo effect, in which the conduction electrons interact with the degrees of freedom associated with dilute local moments. In the Kondo effect, the low temperature state of a single local moment may be described in terms of the formation of a spin singlet bound state involving the local moment and a conduction electron that screens the local moment [43]. The binding energy of the Kondo singlet is related to the Kondo temperature, T_K. As the temperature is increased to about T_K the electron in the bound state can be viewed as being thermally excited into the conduction band continuum, which has the consequence that the screening polarization cloud around the local moment is progressively diminished. The picture, which was evoked to describe the low temperature semiconducting phase, was that of a set of impurity local moments and a set of conduction electrons each bound to a local moment in the Kondo singlet state. In the limit of one electron per local moment the resulting state might be insulating [44], and the energy associated with the gap would be of the order of the Kondo temperature. The Kondo temperatures are in accord with the

small magnitude of the gaps observed for this class of materials. However this description suffers from the shortcoming that in these materials the local moments are quite concentrated so that the interactions and interference between the compensating polarization clouds should not be neglected. Inclusion of the interactions between two Kondo impurities is far from trivial and can lead to properties quite different from isolated impurities [45]. A proper treatment of these materials should include the periodic array of the local moments from the outset.

In fact, the experimental determined properties of the pure and impure heavy-fermion semiconductors can be understood within the framework of the periodic Anderson lattice model, at half filling. This model is often used as a basis for discussing the electronic properties of heavy fermion materials [46]. The main feature of this model is the existence of a very narrow f band cutting across and hybridizing with a conduction band. The net result is that the model has an indirect (hybridization) gap between bands of mixed f and conduction band character. When the bands are filled with a fractional number of electrons per f ion, the Fermi level lies inside one of the bands and the system is metallic. When the f occupancy, n_f, is close to unity, the lattice system is expected to exhibit strong Coulomb correlations similar the type that occurs in the single impurity Anderson model. It is this expectation which has led to the investigation of the model in the context of heavy fermion phenomena. At precisely half filling, the chemical potential lies within the gap making the system semiconducting [47–49]. The strong Coulomb correlations associated with the f character of the states at both edges of the band gap, are also assumed to be responsible for the unusual temperature dependencies exhibited by this class of materials.

Although SmB_6 was the first of these materials to be discovered [2–4], and has been most extensively investigated, there are difficulties in fitting it within the standard framework [50, 51]. One difficulty concerns the degeneracy of the Sm 4f shell configuration, and a second concerns its strong mixed valent and localized character. Similar difficulties may also occur in YbB_{12} [51–53]. Therefore, in this article, we shall focus most of our discussion on $Ce_3Bi_4Pt_3$ and FeSi, which not only fit nicely within the standard model, but also have gaps which are sufficiently large to be observed directly in spectroscopic studies. We shall also discuss the orthorhombic materials CeNiSn and CeRhSb which were, at one time, considered to be examples of heavy fermion semiconductors with extremely small gaps, of the order of 10 K. It was originally supposed that the impurity effects masked the true nature of the semiconducting phase of CeNiSn and resulted in metallic properties. However recent improvements in sample quality, combined with a better understanding of the materials properties, has resulted in these materials being characterized as semi-metals in which there is only a small overlap between the valence and conduction bands. This can be modelled as a hybridization gap semiconductor or semi-metal, in which the hybridization matrix element is zero at appropriate places in the Brillouin zone. There are uranium-based compounds, such as UNiSn, URhSb and UPtSn with much larger gaps, of the order of 0.12, 0.34 and 0.44 eV [18, 54–56]. However, on decreasing temperature, the electronic correlations responsible for the interesting properties can only develop over a limited temperature range before the gap arrests their further development. Since Yb has an almost full f shell it can be considered as the electron–hole symmetric partner of Ce, which has an almost empty f shell. From this viewpoint it may be reasonable to assume that Yb based heavy-fermion systems, including YbB_{12} [14, 15], also fit within the standard framework. However, this

viewpoint has been challenged by Kasuya, who pointed out that the electronic characters of SmB_6 and YbB_{12} are more localized than in the Ce-based semiconductors and semi-metals. In particular, in these low carrier density systems the effect of the screening of the long-ranged Coulomb interaction is very important. Kasuya has developed a model based on a local description of the Kondo effect which allows the effect of electron screening to be explicitly taken into account [51, 52], and has shown how the excitation spectra of these materials can be described [53]. For a fuller account, we refer the interested reader to the original papers.

We shall also refrain from extensively discussing the properties of materials like $CePd_3$, which once was regarded as an archetypical mixed valent compound [57], but also has long defied both experimental and theoretical characterization. This material does show characteristic enhanced Fermi-liquid behaviour at low temperatures, in the specific heat [58], magnetic susceptibility and electrical resistivity. The resistivity shows the characteristic low temperature T^2 variation expected from Fermi-liquid theory, goes through a maximum at around 120 K, and decreases at higher temperatures as expected from conduction electrons scattering from a set of independent Kondo impurities [59]. The substitution of only 13% of Ag impurities for Pd results in superunitary scattering, producing a maximum instead of a minimum in the resistivity at zero temperature [58]. Also the change in the low temperature resistivity produced by the substitution of a fixed concentration of non-magnetic impurities for Ce is anomalously large and has been shown to be independent of the solute [60]. The large magnitude of the Hall constant [61] is indicative of a significantly reduced carrier density. Frequency dependent conductivity measurements [62–65] indicate enhanced Fermi-liquid behaviour at low temperatures. However, these same measurements confirm that a strong reduction of the carrier density occurs at low temperatures [66]. The spectral density of magnetic fluctuations, as inferred from inelastic neutron scattering experiments [67–71], do show the characteristics broad response expected from the single impurity Kondo model with a characteristic energy of 60 meV and $n_f \approx 0.9 \pm 0.1$. But, Gd electron spin resonance (ESR) measurements [72], which show similar characteristic fluctuations of the local f moments, also show that the line width does not follow the linear Korringa relation. The deviation from the linear T Korringa is interpreted as being due to a reduced conduction density of states near the Fermi energy. Thus, there are strong indications that $CePd_3$ has a low carrier density and may also have its properties determined by physics similar to that of the heavy fermion semiconductors.

Here, we shall describe a few of the most salient experiments on the pure and doped heavy fermion semiconducting and semi-metallic systems, outline the standard theoretical framework for interpreting the experimental findings, and then discuss a select few of the more novel alternative theoretical approaches.

2. Thermodynamic measurements

2.1. *Specific heat measurements*

The experimentally determined temperature dependence of the specific heat of the heavy fermion semiconductors shows a Schottky-like anomaly, and at very low temperatures has a residual heat capacity which is linear in T. The peak could be viewed as being due either to excitation of a thermally activated gas of heavy quasi-

particles which is frozen out for temperatures below the gap energy, or to excitation of damped paramagnetic spin fluctuations which also have a gap in their excitation spectrum. These seemingly two different descriptions are not as disparate as they may seem at first sight. In fact for heavy fermion systems, it is believed that the large quasi-particle masses inferred from specific heat and de Haas–van Alphen measurements [73] originate from the entropy of the high temperature local moments. For metallic heavy fermion systems, it is believed that the fluctuations of the local spins produce an additional contribution to the specific heat, which can be found from the exact expression for the free energy

$$\Delta F(T) = -\frac{1}{2\pi}\int_{-\infty}^{+\infty} \mathrm{d}\omega \coth\left(\frac{\omega}{2k_{\mathrm{B}}T}\right) \sum_{q} \int_{0}^{U} \mathrm{d}U' \,\mathrm{Im}\,[\chi^{+,-}(q,\omega+\mathrm{i}\delta)]|_{U'}, \quad (1)$$

where U is the interaction strength between the f electrons and $\chi^{+,-}(q,\omega)$ is the dynamic spin-flip susceptibility. The data on UPt_3 shows a large linear T term and the existence of a $T^3 \ln T$ term [74] which also results from analyses of the above expression [75].

Brown has measured the specific heat of $Ce_3Bi_4Pt_3$ between 50 and 300 K. The Schottky-like anomaly occurs near 50 K [76]. The low temperature linear T coefficient is quite small considering the unusually large linear terms expected from materials containing f electrons. The value of the linear T coefficient, 3.3 mJ (mole Ce)$^{-1}$ K^{-2}, is about a third of the value for $La_3Bi_4Pt_3$ which contains no f electrons. The $Ce_3Bi_4Pt_3$ value is sample dependent, and is found to vary with the square root of the concentration of impurities substituted on the Ce sites [77]. From this one may infer that the residual linear T term is extrinsic and is due to the formation of impurity electronic states within the gap [41, 42]. The Schottky-like anomaly in the specific heat of FeSi has been fit by assuming that there is a gap in the magnetic excitation spectrum [25]. This produces a specific heat of the form

$$\Delta C = Nk_{\mathrm{B}}\left(\frac{\Delta E}{k_{\mathrm{B}}T}\right)^2 \frac{(2J+1)\exp\left[\Delta E/k_{\mathrm{B}}T\right]}{(2J+1+\exp\left[\Delta E/k_{\mathrm{B}}T\right])^2} \quad (2)$$

shown in figure 1. The best fit to the model is with a spin $J = \frac{1}{2}$, and the value of the inferred gap $2\Delta E$ is 1500 K. A similar activated behaviour can be obtained from assuming the existence of a gap $2\Delta E$ in the one electron density of states per spin $\rho(\epsilon)$, as

$$\Delta C = 2k_{\mathrm{B}} \frac{\int \mathrm{d}\epsilon f(\epsilon)\left(\frac{\partial \rho(\epsilon-\mu)^2}{\partial \epsilon}\right) \int \mathrm{d}\epsilon f(\epsilon)(\partial\rho/\partial\epsilon) + \left[\int \mathrm{d}\epsilon f(\epsilon)\left(\frac{\partial\rho(\epsilon-\mu)}{\partial\epsilon}\right)\right]^2}{T\int \mathrm{d}\epsilon f(\epsilon)(\partial\rho/\partial\epsilon)}, \quad (3)$$

where the temperature dependence of the prefactor strongly depends on the form of the density of states in the vicinity of the band edges. This expression reduces to the previous expression, with $J = 0$, for a very sharply peaked density of states. On substitutional doping with Al on the Si sites in FeSi [78] the specific heat acquires an additional term linear in temperature. This is indicative of a finite electronic density of states at the Fermi level, as expected from the formulae,

$$\lim_{T\to 0} \frac{\Delta C}{T} = \frac{2\pi^2}{3} k_{\mathrm{B}}^2 \rho(\mu), \quad (4)$$

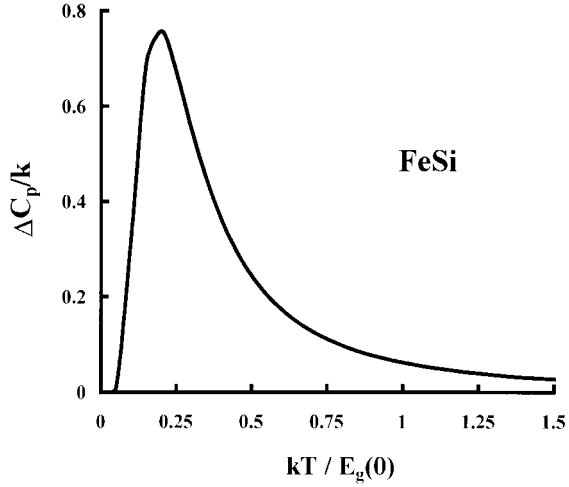

Figure 1. The temperature dependence of the specific heat anomaly in FeSi, as determined in [25]. The quantity $E_g(0)$ is the energy gap.

valid for non-interacting electrons. On assuming an eightfold band degeneracy one finds an effective mass roughly equal to 14 free electron masses, a similar conclusion holds for an analysis of the susceptibility of the doped sample, based on the non-interacting approximation

$$\lim_{T\to 0} \chi(T) = 2\mu_B^2 \rho(\mu). \tag{5}$$

The large effective masses could be the consequences of many-body enhancements with a Wilson ratio, $\lim_{T\to 0} T\chi(T)k_B^2\pi^2/3C(T)\mu_B^2$, of order unity.

The situation is slightly different for CeNiSn, which was once thought to be a heavy fermion semiconductor. The specific heat of CeNiSn has a similar temperature dependence to that of LaNiSn between 80 and 20 K. The contribution of the Ce electrons is assumed to give rise to a peak in $\Delta C/T$ near $T = 6$ K, with a value of $0.21\,\mathrm{J\,mole^{-1}\,K^{-2}}$ [11]. The specific heat drops sharply with decreasing temperature. The electronic specific heat, $\Delta C(T)$, can be fit by the sum of a linear T and a T^2 law [79] above 1 K. A naive Sommerfeld analysis indicates that the material has a pseudo-gap, in which the density of states almost vanishes at the Fermi energy, $\rho(\mu) \approx 0$, and the first derivative also has a discontinuity.

$$\rho(\epsilon) = \rho(\mu) + \left|\frac{\partial\rho(\epsilon)}{\partial\epsilon}\right| |\,\epsilon - \mu\,|\,. \tag{6}$$

As the magnitude of the coefficient of the linear T term is sensitive to the purity of the sample it was initially attributed to impurities. The picture of a gross V-shaped density of states near the Fermi energy [80] has been confirmed by other techniques such as nuclear magnetic resonance (NMR) [81, 82]. However, it is now accepted by most that for the pure materials the density of states at the Fermi level is not zero but has a small but finite value. Below 1 K the linear T term has a coefficient of the order of $28\,\mathrm{mJ\,mole^{-1}\,K^{-2}}$ [83]. The experimental results taken together with LDA electronic structure calculations produce a picture in which CeNiSn is a semi-metal, in which two different bands just slightly overlap at the Fermi energy. This picture of

CeNiSn [84] is now settled, however there does remain some debate as to whether the system possesses a significant amount of dynamic antiferromagnetic short-ranged order at low temperatures [85, 86]. The effect of a magnetic field on the specific heat and resistivity is consistent with the reduction of the pseudogap [79, 87]. While the specific heat measured at temperatures above 2 K and magnetic fields up to 14 T is reasonably described by a Zeeman splitting of the rigid V-shaped density of states [88, 89], the low temperature specific heat shows a slight initial decrease with increasing field not explainable by a pure Zeeman splitting of the density of states [90, 91].

The physical properties of CeRhSb are very similar to those of CeNiSn [12]. The specific heat or rather C/T [92, 93] shows a peak around 10 K with a peak height of $0.102\,\mathrm{J\,K^{-2}}$, which is a factor of about 1.6 less than the corresponding peak of CeNiSn. The C/T ratio then drops as the temperature is lowered further, consistent with the existence of a V-shaped pseudo-gap as in CeNiSn. The shape of the density of states, inferred from the fitting of the T^3 NMR relaxation rate in CeRhSb [94], is in good accord with the same fitting of the specific heat [95]. The drop in the specific heat is arrested at a sample dependent [95, 96] residual C/T ratio of less than $20\,\mathrm{mJ\,K^{-2}}$ at 2 K, which suggests that there is a small residual density of states within the pseudogap [95]. The effect of a magnetic field is to increase the residual C/T ratio and decrease the value of the pseudogap [97]. Although the C/T ratio of CeRhAs [13] has a similar T variation as CeRhSb the residual density of states seems to be practically zero. The small value of the residual density of states in the gap correlates with the large value of the gap obtained from resistivity measurements on CeRhAs [13], which is an order of magnitude bigger than the pseudogaps of CeNiSn and CeRhSb.

The specific heat of SmB_6, when the lattice contribution is estimated from LaB_6 and EuB_6 and subtracted out, also shows a large broad maximum [3] near 40 K. The entropy under the curve corresponds to the combination of entropy of the mixture of $0.6\,Sm^{+3}$ and $0.4\,Sm^{+2}$ configurations and the entropy associated with the degeneracy of the $J = \frac{5}{2}$ moments of the Sm^{+3} ions. This is quite consistent with SmB_6 being a homogeneous strongly mixed valent material. The estimate of the valence is in accord with the high temperature magnetic susceptibility and lattice constant measurements.

The specific heat of YbB_{12} [15] appears to be quite similar to those of $Ce_3Bi_4Pt_3$ and SmB_6 except that, instead of a single Schottky-like peak at 50 K, the specific heat of YbB_{12} has a second broader peak at 250 K. An analysis of the entropy of YbB_{12} indicates that the ground state may consist of a Γ_8 quartet and that the specific heat peak at 50 K is due to excitations to the Γ_6 and Γ_7 doublets [38]. If the system is modelled by a narrow electronic band density of states, which is split by a gap, the analysis of the specific heat data suggests that the low temperature gap in the density of states is temperature dependent. The inferred value of the gap is roughly 200 K at low temperatures and decreases to 140 K at 40 K. On substitution of Yb with Lu, the magnitude of the Schottky anomaly decreases. The ratio C_p/T per mole of Yb plotted against T^2 extrapolates to a sizeable low temperature intercept of $100\,\mathrm{mJ\,(mole\ YbB_{12})^{-1}\,K^{-2}}$, for concentrations of Lu around 12%. This observation suggests that the thermally excited f electrons or f holes in the stoichiometric compound have moderately heavy effective masses.

The specific heat of UNiSn follows that of ThNiSn quite closely [98–100], except for a sharp peak due to antiferromagnetic ordering of the U moments at $T_N = 43$ K.

The antiferromagnetic nature of the transition was confirmed by neutron diffraction measurements [101, 102]. The low temperature electronic contribution to the specific heat is proportional to T and has a coefficient of 20 mJ (mole UNiSn)$^{-1}$, which is 21 times larger than the corresponding linear T term in ThNiSn. This may indicate the existence of a narrow f band with modest mass enhancements at the Fermi energy [55]. The effect of Th substitution for U results in a very rapid decrease in the magnitude of the linear T term which suggests the disappearance of the density of states at the Fermi energy. This is consistent with the variation of resistivity with doping [103]. The specific heat experiments clearly indicate that the low temperature phase has a finite density of states at the Fermi energy, and that any semiconducting phase has to occur above the magnetic ordering temperature T_N.

2.2. *Susceptibility measurements*

The static magnetic susceptibilities of the rare earth based heavy fermion semiconducting systems [5] shows a significant deviation from the susceptibility of the FeSi system. In the systems containing Ce, the high temperature magnetic susceptibility obeys a Curie–Weiss form,

$$\chi(T) = \frac{n_f g^2 \mu_B^2 J(J+1)}{3k_B(T+\Theta)}, \quad T > \Theta, \tag{7}$$

in which the Curie constant contains nearly the full magnetic moment of the Ce $(4f)^1$ configuration, with $J = 5/2$. For $Ce_3Bi_4Pt_3$ the antiferromagnetic Curie–Weiss temperature is $\Theta \approx 125$ K. As the temperature is decreased the susceptibility goes through a maximum of 4×10^{-3} emu mole^{-1} at 80 K and subsequently decreases. For $Ce_3Bi_4Pt_3$ the experimentally measured data, shown in figure 2, goes through a minimum and has a low temperature Curie tail. The low temperature Curie tail is extrinsic, due to the presence of rare earth impurities. Indeed the extrapolation to $q \to 0$ of the q dependent static susceptibility $\chi(q,\omega = 0)$ obtained by integrating the inelastic neutron scattering spectrum shows that this tail is not a bulk property [104].

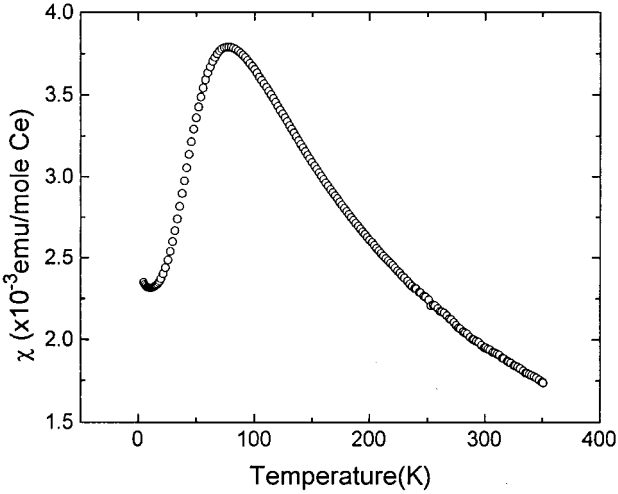

Figure 2. The temperature dependence of the magnetic susceptibility, $\chi(T)$, of $Ce_3Bi_4Pt_3$ as measured by Hundley *et al.* [5].

After subtracting out the Curie tail due to impurities, one finds that the susceptibility saturates to a low temperature value of roughly one half of its value at the maximum, i.e. $\chi(0) = 2.3 \times 10^{-3}$ emu mole^{-1}. In fact R. Modler and J. D. Thompson have made unpublished measurements of the magnetization, for $4 < T < 200$ K. Even at low temperatures, M is linear in H up to $H = 50$ T, which shows that there is a large residual value of $\chi(0)$ which is not due to free Ce moments. This low temperature value can be attributed to Van Vleck magnetism [105]. The band Van Vleck contribution to the susceptibility of Ce heavy fermion semiconductors has been modelled [49] as being due to the f and conduction electrons coupling to the magnetic field via different g factors. The application of a magnetic field then produces a relative shift of the unhybridized bands, and thereby results in a conversion between f and d character in the field split sub-bands.

By contrast in FeSi [25], where one expects the orbital contribution to the d shell moments to be quenched, the Van Vleck term is absent and the bulk susceptibility (corrected for a Curie tail) appears to vanish as T approaches zero, according to the activated expression

$$\chi(T) = g^2\mu_B^2 \frac{J(J+1)}{3k_BT} \frac{2J+1}{2J+1+\exp[\Delta E/k_BT]}. \tag{8}$$

This interpretation is completely consistent with the results on FeSi, where one would expect the orbital angular momentum to be quenched by crystal field effects, leaving a spin only moment. The g factors of the conduction and d states would then, effectively, cancel and give a value of zero for the zero temperature susceptibility of the semiconductor. The value of the activation energy obtained, ΔE, from this fit is 750 K. The susceptibility was fit to the expression,

$$\chi(T) = -\frac{g^2\mu_B^2}{2} \int d\epsilon \rho(\epsilon) \frac{\partial f(\epsilon)}{\partial \epsilon}, \tag{9}$$

assuming that the susceptibility originates from thermal population of electron and holes electronic excitations in narrow density of states, $\rho(\epsilon)$, containing a small band gap. Good agreement was obtained [106] with band gaps in the range of 950–1100 K which is equivalent to the range of activation energies 475–550 K. A more intricate analysis [107] found smaller band gaps, in the range of 700–820 K, and carrier masses of the order of 31 free electron masses.

The magnetic susceptibility of CeNiSn exhibits considerable anisotropy [11], which becomes more distinct at low temperatures. The susceptibility along the orthorhombic a-axis, $\chi_a(T)$, has a maximum of about 8.7×10^{-3} emu mole^{-1} at $T = 12$ K, and decreases to below 6.5×10^{-3} emu mole^{-1} at the lowest measured temperatures for the better crystals [80]. The susceptibilities on the other two principal axis do not exhibit any maxima. These susceptibilities do show slight Curie law upturns at low temperatures; the upturns have almost vanishing strength for the better samples. The susceptibilities in the two principal directions b and c, respectively, extrapolate to 2×10^{-3} emu mole^{-1} and 3×10^{-3} emu mole^{-1} at zero temperature [80]. An analysis of the a-axis susceptibility by Ikeda and Miyake [84] indicates that the quasi-particle density of states at the Fermi level does not account for the magnitude of $\chi_a(0)$, but that an additional Van Vleck contribution is required.

Measurements of the susceptibility of polycrystal samples of CeRhSb show broad peaks at 117 K [108]. Single crystal measurements [93] show that the susceptibility is extremely anisotropic, and the a-axis is the easy axis as in

isostructural CeNiSn. The a-axis susceptibility has a relatively sharp peak at 13 K [93], similar to the a-axis peak observed at $T = 12$ K in CeNiSn. The magnitude of the a-axis susceptibility maximum is of the order of 3.5×10^{-3} emu mole^{-1}, which is about a factor of 2.6 less than the corresponding peak in CeNiSn [96]. This comparison of the specific heat and susceptibility of these two materials suggests that if a gas of thermally excited heavy quasi-particles is formed above 12 K (i.e. above the gap temperature) then CeNiSn would have larger mass enhancements and would have more dynamic magnetic correlations than CeRhSb. This is supported by the lattice constant measurements [109], which indicates that Ce is almost trivalent in CeNiSn while CeRhSb has intermediate valence, since it is expected that the temperature scale for the magnetic fluctuations should vary as $(1 - n_f)$. The mixed valent nature of CeRhSb is not amenable to confirmation by the high temperature behaviour of the susceptibility. As the paramagnetic Curie–Weiss temperature is as large as $\Theta \approx 324$ K, the effective Curie constant cannot be accurately extracted from the high temperature susceptibility. The value of the Curie constant obtained from this fit is, in fact, larger than that of trivalent Ce.

The magnetic susceptibility of SmB_6 has a broad maximum at 50 K, and for higher temperatures can be represented as the weighted sum of the Curie susceptibility due to the $J = \frac{5}{2}$ moments of Sm^{+3} and the (ionic) Van Vleck susceptibility of the Sm^{+2} ions [110]. The weights of the two configurations Sm^{+3} and Sm^{+2} are 0.7 and 0.3, respectively. At lower temperatures the susceptibility saturates to a finite value. Because of the relatively large mixed valent character, SmB_6 behaves differently from other heavy fermion semiconductors which are usually close to having an integer valence.

The temperature dependence of the magnetic susceptibility in YbB_{12} [14] has a similar shape to $Ce_3Bi_4Pt_3$. The high temperature data is consistent with a Curie law, where the effective magnetic moment is $4.4\mu_B$ and a Curie–Weiss temperature, $\Theta \approx 100$ K. On using the ionic ground state value of $J = 7/2$ for the one hole configuration of Yb, one finds that the high temperature Yb valence is +2.95. The susceptibility exhibits a maximum of 10^{-2} emu mole^{-1} at about 70 K. Dilution studies [111] show that the temperature of the maximum and the value of the high temperature valence are almost independent of the degree of substitution of Lu for Yb. The susceptibility of polycrystalline samples shows a large low temperature Curie tail. However, most of this is ascribed to an impurity Yb_2O_3 phase or included Yb defects, as chemically treated samples and single crystal measurements [112] show much smaller Curie tails. These single crystal studies also show that the susceptibility of YbB_{12} extrapolates to a non-zero value for temperatures below 15 K. The Knight shift observed in NMR measurements on ^{11}B [113] is consistent with the above identification. Thus, like $Ce_3Bi_4Pt_3$, the susceptibility of YbB_{12} is also consistent with it containing an appreciable Van Vleck component of the order of 4×10^{-3} emu mole^{-1}.

The high temperature magnetic susceptibility of UNiSn follows a Curie–Weiss law. The effective magnetic moment extracted from the Curie constant is 3.08 μ_B and the Curie–Weiss temperature $\Theta \approx 75\,K$ [55, 99, 103, 114]. This is indicative that the f electrons are predominantly in the $5f^2$ configuration. The susceptibility shows a non-analytic upturn at the Néel temperature where $\chi(T_N) \sim 11 \times 10^{-3}$ emu/mole and saturates at a value of $\chi(0) \sim 15 \times 10^{-3}$ emu mole^{-1}. The abrupt increase in the susceptibility at the Néel temperature is quite different from the cusp like variation of $\chi(T)$ observed in materials which order antiferromagnetically. This may be due to

the increase in the number of effective magnetic degrees of freedom which occurs at the semiconducting–metal transition.

2.3. *Elastic properties*

The Gruneisen parameter, Ω, is defined by the relation with the specific heat C, thermal expansion coefficient α_V and the isothermal compressibility κ_T and the molar volume V_M, given by

$$\Omega = V_M \frac{\alpha_V}{\kappa_T C}. \tag{10}$$

The thermal expansion coefficient should track the specific heat if the Gruneisen parameter is approximately constant. Typical values of the Gruneisen parameter are around 2, and are relatively independent of the material, except for heavy fermion materials where Ω increase strongly with decreasing temperature below 10 K and saturates at large values.

The measured lattice constants in cubic $Ce_3Bi_4Pt_3$ shows that an anomalous thermal expansion occurs below 100 K where the expansion coefficient peaks around 50 K [115]. This could be indicative of a temperature dependent valence of the Ce ions. This interpretation is supported by an analysis where the thermal expansion coefficient of $La_3Bi_4Pt_3$, which has no f electrons, is subtracted from the coefficient of the analogous Ce compound. The resulting broad peak in the f contribution to the thermal expansion coefficient closely resembles the temperature dependence of the specific heat of $Ce_3Bi_4Pt_3$. The f electron Gruneisen parameter $\Omega = -\partial \ln (T_{sf})/\partial V$ extracted from the data via scaling arguments [116, 117] has a large value of $\Omega = 36$. This value is consistent with a moderately heavy fermion metal or strongly enhanced mixed valent metal which has a characteristic spin fluctuation temperature T_{sf} of 300 K, and as is well known, in mixed valent metals the values of the valence varies slightly with temperature [57]. The temperature dependence of the lattice constant is empirically found to track the temperature dependence of $T \times \chi(T)$, which, when combined with an approximate Curie law valid above 100 K, also would suggest a variation of the effective valence [118]. The variation of the valence with temperature has been observed in X-ray absorption measurements [119] near the Ce L_{III} edge, where n_f is found to be 0.9 at $T = 10$ K and increases towards unity as T increases.

The thermal expansion coefficient of FeSi when referenced to CoSi [106, 120] shows an electronic contribution that mirrors the specific heat, as expected if the electronic Gruneisen parameter is approximately constant. Analysis of the Schottky-like anomaly yields an activation energy of 540 K, which falls within the range of activation energies of 750–475 K obtained from the specific heat [25, 106], and also yields a large value for the Gruneisen constant $\Omega \approx 7$. This relatively large value of the Gruneisen constant is a further indicator of the similarity between FeSi and the heavy fermion semiconductors. The elastic constants have been measured by ultrasonic methods [106, 121]. The electronic contribution can be fit by invoking a strain dependence of the band energies and a gap of the order of 1250 K in the electronic density of states. The attenuation rate exhibits a peak at a temperature of 340 K, which is about half the gap energy inferred from resistivity measurements. This suggests that the rate is dominated by electron–phonon scattering and is limited by the threshold energy for electronic excitations.

The coefficients of linear expansion for CeNiSn are highly anisotropic. The linear expansion coefficients along the a and c axes have broad maxima at 45 and 175 K,

respectively [122]. The high temperature maxima are attributed to crystalline electric field effects. At low temperatures all three linear expansion coefficients show anomalies around 6 K, which is of the same order of magnitude as the pseudogap. The intensity of the 6 K peak is reduced with increasing pressure [123], which is consistent with the gap closing as pressure increases. The volume thermal expansion coefficient α_V shows a sharp asymmetric peak at this temperature. The linear T term extracted from α_V is generally associated with the existence of a high density of states at the Fermi level. The value of the linear coefficient, extrapolated from high temperatures, would seem to be indicative of an enhancement of the Fermi-level density of states occurring at temperatures above those at which the pseudogap forms. The extrapolated value of the linear T dependence of α_V decreases with increasing pressure [123]. The Gruneisen parameter found from the data [124] is of the order of 15 above a temperature of 5 K and drops to a negative value below 1 K, although this could be an artifact due to sample quality. The magnetic Gruneisen parameter has been obtained from magneto-restriction experiments on the same crystals [124], using the approximate temperature dependence of the magnetic susceptibility, $(\partial M/\partial T)_{P,H} = 0$. The analysis is based on the expression

$$\Omega_{\mathrm{B}} = V_M \frac{(\partial V/\partial H)_{P,T}}{\kappa_T H (\partial M/\partial H)_{P,T}} \tag{11}$$

and reproduces the high T behaviour, the low temperature drop and the change of sign. When a magnetic field is applied, this low temperature change of sign is suppressed and Ω attains values comparable to those of highly enhanced heavy fermion metals. This can be interpreted as the suppression of the pseudogap behaviour and the formation of a heavy fermion state by magnetic fields of order 8 T.

The elastic constants of CeNiSn, found by ultrasonic measurements [125], show a broad maximum in the longitudinal stiffness constants C_{22} and C_{11} at temperatures of 200 and 230 K, and a minimum at 40 K. A shoulder occurs in C_{22} and C_{11} near 8 K, while no anomalies were found in C_{44} and C_{66}. The low temperature hardening is attributed to the freezing of the electronic excitations below the characteristic pseudogap energy, thereby leading to a loss electronic of screening of the inter-atomic forces [126]. The field dependence of C_{11} and C_{33} at temperatures lower than 1 K show a kink for fields of 8.7 T, which is accompanied by a peaking of the ultrasonic attenuation. This may be a signal of a meta-magnetic transition associated with the loss of short-ranged antiferromagnetic correlations [125].

The temperature dependence of the lattice constants of SmB_6 [127, 128] shows the existence of a minimum at $T = 150$ K. The negative value of the thermal expansion coefficient is related to a change in the Sm valence from 2.6 to 2.53. The value of the bulk modulus of SmB_6 is relatively small, compared to other rare earth hexaborides [129]. The smallness is related to a pressure induced valence change associated with the lanthanide contraction. The temperature dependence of the bulk modulus shows a pronounced minima at 60 K characteristic of a valence fluctuating system [130]. The elastic constants have been fit by a phenomenological two band model including the effect of the coupling of the f electrons to the lattice [131], giving a gap energy of 160 K. A negative thermal expansion coefficient, which is similar to SmB_6, has been found in YbB_{12} [113].

The temperature dependence of the lattice parameters of UNiSn show that the system abruptly deforms from a cubic structure in the semiconducting phase to a

tetragonal structure in the metallic–magnetic phase [132]. However, the transverse elastic constant C_T shows a softening which occurs between 150 K and T_N as expected for a second order transition. The application of a magnetic field results in the separation of the first order structural change from the antiferromagnetic transitions [20], as evidenced by the thermal expansion [133] and the susceptibility [134].

3. Transport measurements

3.1. *Electronic transport properties*

The electrical resistivity, Hall coefficient and thermoelectric power have been measured for $Ce_3Bi_4Pt_3$ [135]. The resistivity and Hall coefficient show a thermally activated behaviour for temperatures above 45 K, with an activation energy of roughly 50 K. This activation would correspond to a gap of 100 K if the Fermi level lies symmetrically within the gap. The resistivity below $T = 45$ K increases less rapidly and perhaps saturates, indicating that in this regime extrinsic carriers dominate the conduction process, see figure 3. The room temperature resistivity is large ($\rho(T = 300\,\text{K}) = 220\,\mu\Omega\text{cm}$) and has a temperature dependence similar to the logarithmic T dependence expected from the Kondo effect. The Seebeck coefficient, S, has the general $1/T$ variation expected for ordinary semiconductors. The values of the gaps extracted from the resistivity and S have similar magnitudes, and are also found to have a temperature dependence. The gap decreases with increasing temperature [136] as shown in figure 4. The gap value inferred from the data taken at the lowest temperatures was 120 K. For $Ce_3Bi_4Pt_3$ the temperature [136] and pressure dependence of the gap [135, 137] follows the same behaviour as expected for the singlet binding energy of the single impurity Anderson model, thereby suggesting that the variation is due to electronic correlations. The transverse magneto-resistance [138] is positive for all fields at temperatures above 75 K, similar to the behaviour found in $La_3Bi_4Pt_3$. However, the magneto-resistance develops a large negative

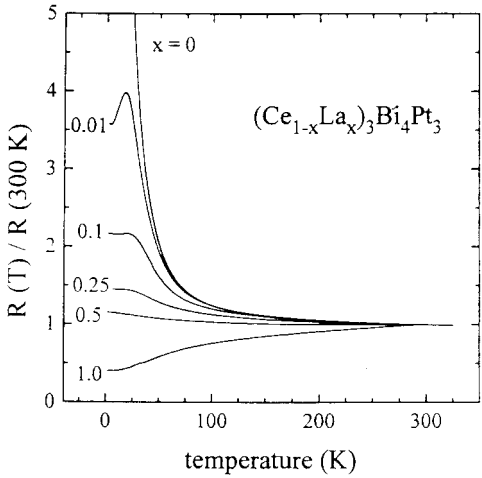

Figure 3. The normalized electrical resistivity, $\rho(T)$, of La-doped $(Ce_{1-x}La_x)_3Bi_4Pt_3$ for six different values of the impurity concentration x, as measured by Hundley *et al.* [77]. The room temperature resistivity is the same, within a factor of 2, for all concentrations.

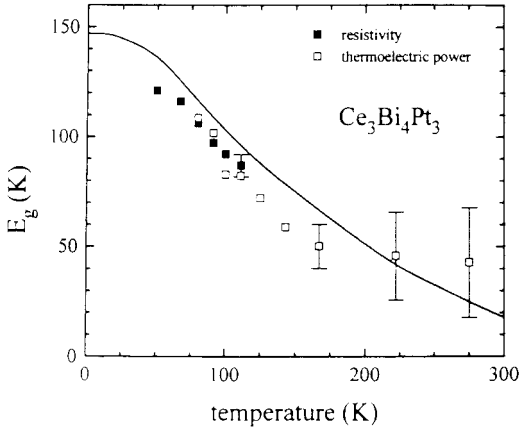

Figure 4. The temperature dependence of the gap in the mean field solution [49, 323] fit to the activation energies extracted from the resistivity and thermopower of $Ce_3Bi_4Pt_3$ in [136].

component below 7 K. The dependence of the negative magneto-resistance on field is not totally inconsistent with the bands in the vicinity of the gap being subjected to a rigid Zeeman shift, but suggests a more complex mechanism for suppression of the gap [138]. The thermopower S and the Hall constant, if they are interpreted in terms of the expressions for a simple one band model of carriers of charge e and Fermi energy μ measured from the lower band edge, are given by

$$S = \frac{\pi^2}{2}\frac{k_B^2 T}{e\mu} \tag{12}$$

and

$$R_H = \frac{1}{ne}. \tag{13}$$

Thus, both S and R_H should yield the sign of the charge of the carriers. For $Ce_3Bi_4Pt_3$ both the experimentally determined S and R_H imply similar sign charges for the carriers [139], which is also the case in YbB_{12}. This sign of the charges, inferred from S and R_H, are of opposite sign, for both CeNiSn and CeRhSb.

FeSi shows an activated resistivity very similar to $Ce_3Bi_4Pt_3$, and a semiconducting gap of the order of 950 K [106, 140]. The resistivity of FeSi starts to saturate as the temperature is lowered below 10 K, and over a limited temperature range follows the $\rho(T) \sim \exp[(T_0/T)^{1/4}]$ law, expected for variable range hopping [141–143]. Substitution of Al for Si has the effect of reducing the activation energy [144], and also leads to a metal insulator transition of the impurity bands for concentrations of around 1% Al. On the metallic side of the transition, the resistivity shows a $T^{1/2}$ variation characteristic of strong electron–electron correlations in disordered materials [144]. The thermopower of FeSi varies as $1/T$ between $T = 50$ K and $T = 150$ K [140], and a value of the semiconducting gap can be estimated to be of the order of 800 K. However, below $T = 50$ K the thermopower ceases to vary as $1/T$ and falls to zero linearly with T as the temperature approaches zero, consistent with the variable range hopping behaviour of the resistivity [145]. Substitution of Si with Ge leads to a reduction of the peak in S, closes the gap, and also produces a T^3

variation typical of phonon drag [145]. The measured Hall [146] constant is positive between 55 and 30 K, at lower temperatures it behaves erratically and is negative between 10 and 4 K. The nonlinear variation with field in the low temperature regime is not well understood.

Early measurements of the resistivity of single crystals of CeNiSn [11] showed that below 10 K the resistivity was anisotropic and below 6 K followed an activated temperature dependence, as expected from a semiconductor with anisotropic gap energies of the order of 3–5 K. However, the resistivity has a remarkable sensitivity to impurities below 15 K [96]. Since the resistivities of the better crystals remain metallic, in contrast to the semiconducting temperature dependence observed in other samples, it appears that the material is intrinsically metallic. Below $T \approx 2\,\mathrm{K}$ the resistivities along the three principal axes satisfy the inequalities $\rho_a(T) < \rho_b(T) < \rho_c(T)$. The resistivities along the b and c axes, respectively, have minima at $T = 3\,\mathrm{K}$ and $T = 2\,\mathrm{K}$, and then increase at lower temperatures. The inference of the intrinsic metallic nature of the systems is supported by the observation that the resistivity along the a-axis shows a T^2 term below 5 K indicative of electron–electron scattering at a Fermi surface. However, the value of the density of states estimated from the T^2 coefficient, assuming an isotropic Fermi-liquid theory, would be an order of magnitude larger than that estimated from the linear T coefficient of the specific heat [80]. This could reflect the anisotropy of the electronic states and suggests the gap may vanish only for some directions. The underlying metallic behaviour is seen more clearly when the resistivity is measured under pressure [147, 148]. The low temperature resistivities along the b and c axes show that the rapid increase with decreasing T is suppressed by the application of pressure. The decrease in the low temperature resistivity with increasing pressure corresponds to a monotonic collapse of the pseudogap. The suppression of the pseudogap under increasing pressure is also inferred from Hall coefficient measurements [149] which show an increase in the number of carriers. The low temperature variation of all three components of the resistivity almost follows a T^2 law, at a pressure of 20 kbar. The higher temperature behaviour still shows a broad peak and a quasi-logarithmic T dependence expected from heavy fermion materials with a crystal field splitting of the order of 100 K. The existence of a crystal field splitting is supported by the observation [109] that 20% substitution of La on the Ce site produces two different temperature ranges where the resistivity varies logarithmically with T. The ratio of the coefficients of the $\ln(T)$ terms reflect the ratio of the effective spin degeneracy at temperatures above and below the crystal field splitting.

The thermopower of CeNiSn is also anisotropic and is large and positive for the temperature range investigated, $300\,\mathrm{K} > T > 2\,\mathrm{K}$, but shows a sharp minimum at $T = 5\,\mathrm{K}$ [150, 151]. The Hall coefficient, R_H, becomes negative below 3 K, where the anisotropy becomes amplified [152]. The anisotropy is largest with respect to the orientation of the field relative to the principal directions, but not on the orientation of the current in the plane spanned by the other two principal directions. One particular interesting observation is that the number of carriers inferred from the (isotropic) one band analysis of the Hall coefficient, for carriers of charge e, anti-correlates with the variation of the resistivity

$$\rho(T) = \frac{m}{ne^2\tau}, \tag{14}$$

when the sample quality is varied [96, 153]. This implies that the effect of improvements in sample quality on the resistivity is primarily due to a dramatic reduction of the impurity scattering rate. The addition of less than 5% of Co or Cu impurities [154] does confirm that the resistivity does increase with doping while the Hall constant decreases. The dramatic increase in scattering rate could be interpreted in terms of quasi-one-dimensional conduction along the *a*-axis [154]. A Drude analysis of the real and imaginary parts of the microwave conductivity [155] of CeNiSn indicates that the scattering rate does indeed rapidly decrease below 10 K for pure single crystals. Thus, the presence of additional impurity scattering could be responsible for keeping the scattering rate large in disordered materials, thereby resulting in the resistivity increasing as the temperature is lowered.

The magneto-resistance of CeNiSn is also remarkably anisotropic [80, 96, 156]. When the applied field is perpendicular to the easy axis, the magneto-resistance is large and positive when the current is perpendicular to the magnetic field, and is small when the current is parallel to the field. On the other hand when the applied field is along the easy axis the magneto-resistance is always negative. Sugiyama *et al.* [157] have measured the longitudinal magneto-resistance in fields up to 35 T, where it becomes large and negative for all directions. These authors argue that although the quenching of spin flip scattering may describe the results at high fields, this description may not be valid at low temperatures where the change in the pseudogap structure should be involved. Inada *et al.* [156, 158] have pointed out that the large positive transverse magneto-resistance can be understood by assuming that the electron and hole Fermi surfaces are closed. On assuming that the number of electrons balances the number of holes, one finds that the transverse magneto-resistance increases with H according to a power law H^n, where $n > 1$. Furthermore, the longitudinal magneto-resistance is small as it measures the deviation of the Fermi surfaces from being spherically symmetric. These authors [156] also relate the negative magneto-resistance for fields applied along the easy axis to the reduction of the pseudogap which occurs with increasing field.

The resistivity of polycrystalline samples of CeRhSb shows a broad maximum at 113 K, below which it starts to decrease [12]. The Kondo-like temperature variation of the resistivity above 113 K and the subsequent decrease below the maximum is similar to the behaviour often found in heavy-fermion or mixed valent compounds. The maximum may be related to a crystal field splitting since substitution of 15% Pd on the Rh sites produces two well defined regions where the resistivity shows a logarithmic T dependence, similar to a single ion Kondo effect combined with crystal field splitting [159]. However the similarity to a heavy-fermion metal ends near 10 K, where the resistivity suddenly starts to show a large increase that is similar to a semiconducting temperature variation. An activation energy of 6.2 K was inferred from the resistivity between 10 and 4.2 K [12, 159] or 4 K from the lower temperature range of 2 to 8 K [97]. These values suggest that the pseudogap does not have a uniquely defined value, but is of the same order as the value of the pseudogap of 12 K inferred from NMR [94] and specific heat measurements [95]. The magneto-resistance is quite anomalous at low temperatures [97]. At 2 K there is a slight positive magneto-resistance for small fields, which changes sign and has a large magnitude at fields of 5 T. At the slightly higher temperature of 4.5 K the magneto-resistance is large and positive for all measured fields. At even higher temperatures the magneto-resistance remains positive, however, the magnitude decreases as temperature is increased. Resistivity measurements on single crystals show an

anisotropic variation. As in CeNiSn, the low temperature resistivity of CeRhSb is smallest along the *a*-axis, which also coincides with the magnetic easy axis. The low temperature *a*-axis resistivity is at least one order of magnitude smaller than the resistivity of the polycrystalline samples, and shows a sample dependent weak increase with decreasing T which is consistent with CeRhSb having an intrinsic metallic behaviour for conduction along the *a*-axis [93]. The striking similarity between CeNiSn and CeRhSb does not extend to the pressure dependence of the resistivity, the Hall coefficient and the thermopower as the pseudogap does not monotonically decrease with increasing pressure. Instead, the pressure dependence of the resistivity of CeRhSb [160] seems to imply that the pseudogap initially increases with the application of pressure, goes through a maximum around 30 kbar and finally closes at 60 kbar. For CeRhSb, the Hall coefficient remains positive in the entire temperature range investigated [96], while the thermopower is anisotropic and positive at high temperatures but changes sign below 5 K [93, 139]. The increase in the Hall coefficient induced by increasing pressure [161] is much larger than the corresponding change in the resistivity, suggesting that a change in carrier concentration is not responsible for the change in the resistivity. Analysis of the resistivity and the number of carriers inferred from the Hall effect in CeRhSb,

$$\frac{R_{\mathrm{H}}}{\rho(T)} = \frac{e\tau}{m}, \tag{15}$$

suggests that the scattering rate changes rapidly at low temperatures [96, 162].

In contrast to the semi-metallic compounds CeNiSn and CeRhSb, the properties of CeRhAs have not been extensively studied. The resistivity of CeRhAs does show an increase with decreasing temperature and then saturates at low temperatures. The estimated gap energy of 144 K, obtained from the temperature dependence of the resistivity [13] between 40 and 130 K, is an order of magnitude larger than the pseudogaps of CeNiSn and CeRhSb. The Hall coefficient has been measured at a limited number of temperatures, where it was found to be positive.

The resistivity of SmB_6 has been measured by numerous groups over time [2, 4, 163–167]. The results show that a large increase in the resistivity occurs at temperatures below 50 K and saturates to a high residual value at the lowest temperatures. The value of the residual resistivity indicates that the scattering is superunitary and incompatible with metallic conduction [4]. The residual resistivity is sample dependent and increases when the quality of the sample is improved, as either implied by successive passes through zone refinement [168] or as evidenced by the smallness of the low temperature Curie tail in the susceptibility [169]. The residual resistivity was observed to increase through 8, 30 and 70.7 Ω cm after, respectively, undergoing, one, three and four passes through zone refinement [168]. The origin of the low temperature conductivity is not well understood [170]. Although a variable range hopping regime can be found in the resistivity at ambient pressures, the application of slight pressure changes the sign of the low temperature $\rho(T)$ [171]. In the higher temperature regime, the resistivities of the better quality samples [167] have minima near 50 K followed by broad maxima at 150 K. Activation energies can be inferred from the temperature variation of the resistivity between 4 and 14 K. Activation energies ranging between 21 and 48 K have been reported in the literature. The Hall coefficient is positive at high temperatures and changes sign at a temperature about 62 K [4, 163], after which it remains negative down to the lowest measured temperatures [4, 165]. An activation energy of 21 K can

be obtained from the Hall data in the temperature range between 4 and 13 K [4], whereas analysis of the variation of the sample's resistivity over the same temperature range yields an activation energy of 31 K. The magnitude of the Hall coefficient, $|R_H|$, has a maximum at 4 K and saturates at lower temperatures [165]. The effect of pressure is that of decreasing the energy gap [164] and of producing an abrupt transition to a metallic state near 53 kbar [165, 172]. The magnitude of the low temperature Hall coefficient decreases on increasing pressure, indicating an increase in the number of carriers which exactly coincides with the decrease in the number of f electrons inferred from X-ray absorption measurements over the same pressure range. The temperature dependence of the magneto-resistance is remarkable [166, 172, 173]. Generically it is negative and shows a H^2 variation. The magnitude of the magneto-resistance is relatively small at $T = 2.5$ K, but it is large at $T = 4$ K, $\rho(H)$ dropping to 80% of the $H = 0$ value at $H = 50$ T. The inferred activation energy varies only weakly with applied fields [166], decreasing proportionally to H^2 and thus is not consistent with a rigid Zeeman splitting of the density of states. On the application of pressure, the temperature range, where the H^2 variation occurs, is restricted to temperatures lower than the gap energy, and crosses over to a $H^{3/2}$ variation at temperatures higher than the gap energy [166, 174].

The electrical resistivity of YbB_{12} has been measured [113] between 5 and 300 K and shows a change by 5 orders of magnitude in this temperature range [112]. Although a resistivity that exhibits such a large variation in size is expected to be thermally activated, no unique activation energy has been identified. For example, an activation energy of 68 K was obtained from the resistivity in the temperature range $7\,\text{K} < T < 15\,\text{K}$, however, the activation energy deduced from the higher temperature range of $15\,\text{K} < T < 40\,\text{K}$ only has the value of 25 K. The Hall coefficient, R_H, also shows a similar type of activation to the resistivity in the same two temperature ranges. The values of the activation energies deduced from the Hall coefficient in these two temperature ranges were found to be 90 K and 20 K respectively. The trend of decreasing gaps with increasing temperature is consistent with the gap inferred from specific heat measurements on YbB_{12}, and is qualitatively similar to the behaviour observed in $Ce_3Bi_4Pt_3$ [136]. Measurements of the gap under pressures up to 80 kbar, show that the gap decreases slightly with a linear dependence on pressure [175]. The low temperature magneto-resistance is large and negative [176–178], indicating that the effect of an applied magnetic field is that of reducing the activation energy [176]. If the reduction of the gap is interpreted on the basis of a Zeeman split hybridization gap model, the value of $gJ = 1.9$ is found. However, the gap is first closed and completely metallic behaviour only occurs at fields as high as 50 T [177, 178].

The properties of UNiSn do not fall into the same pattern, as the activated resistivity [18, 19] is observed above 125 K but the increase in resistivity is interrupted by an antiferromagnetic transition around $T = 50$ K. Below this temperature the resistivity plummets down, reaching metallic values at $T = 43$ K when the ordering is complete. Sample quality affects the magnitude of the gap [179], suggesting that the intrinsic gap is of the order of 100 meV, whereas the smaller activation energy of 38–40 meV [100, 114] could represent the energy separation of impurity states from the gap edges. The density of carriers inferred from the Hall coefficient [179] at temperatures above T_N is low, of the order of $10^{19}\,\text{cm}^{-3}$ consistent with the semiconducting behaviour of the resistivity in the same temperature range. The Hall coefficient changes sign at a temperature around 200 K and is positive at low

temperatures. The number of carriers inferred from the Hall coefficient shows a decrease below 100 K consistent with the thermal depopulation expected in a semiconductor and falls to half its value just above T_N. The number of carriers exhibits an anomaly at the magnetic ordering temperature. Below the Néel temperature the number of carriers increases at lower temperatures but only recovers to a value similar to that found at 100 K. The very gradual and modest increase in the number of carriers is offset in the resistivity by an abrupt and large increase in the low temperature mobility $e\tau/m$. The mobility increases by an order of magnitude over a very narrow temperature range. The magneto-resistance shows an H^2 variation above T_N and a more complex field dependence at lower temperatures [179], possibly due to spin disorder scattering and a field dependent antiferromagnetic band structure. The Seebeck coefficient S is negative above 150 K, where it shows a gradual decrease in magnitude with decreasing T [114]. The measured S shows a large positive peak with a maximum a few degrees below T_N, perhaps due to the development of an antiferromagnetic super-zone boundary gap.

3.2. *Thermal conductivity*

The thermal conductivity, $\lambda(T)$, of FeSi seems to be dominated by the phonon contribution at low temperatures [141], where the electronic contribution is frozen out. The electronic contribution to the thermal conductivity was estimated, by assuming the validity of the Wiedemann–Franz rule. The estimated electronic contribution was at most 10^{-4} times smaller than the phonon contribution. The phonon contribution vanished at low temperatures as a power law of the temperature, for $T < 0.2$ K. The exponent found from the data was close to the three representing the $\lambda(T) \sim T^3$ variation expected from the thermal population of phonons and the mean free path was of the order of the linear dimensions of the sample.

Thermal conductivity measurements have been performed on single crystals of CeNiSn [180] and CeRhSb [181]. For CeNiSn the thermal conductivity, $\lambda(T)$, is anisotropic, being largest along the b-axis. For all three principal axes $\lambda(T)$ decreases with increasing temperature and shows a knee-like anomaly near 5 K. This was interpreted on the basis that the electronic contribution to the thermal current is small due to the small value of the electronic density of states at the Fermi energy and the large electronic scattering rate, so the phonon contribution dominates. This is in accord with earlier estimates based on polycrystalline sample measurements [182]. The enhancement of $\lambda(T)$ at 6 K was related to the opening of a pseudogap which would result in a decrease in the rate of scattering of phonons, due to the freezing out of the electron–phonon scattering mechanism [180]. The relationship between the enhancement of $\lambda(T)$ and the pseudogap is borne out by experiments [181] in which 5% Co or Cu is substituted on the Ni sites, which is known to close the pseudogap. Likewise, the application of an applied field of 15 T completely suppresses the anomaly [181]. The thermal conductivity of CeRhSb shows a similar knee-like anomaly at 12 K [181].

The thermodynamic and transport properties typically show some type of thermally activated behaviour from which an activation energy relating to the gap can be extracted. The magnitude of the gap has been the subject of some interest, primarily due to the temperature dependence as inferred by Hundley *et al.* [136], and also by the different values inferred from different measurements made at similar temperatures. One source of these second types of differences may be found in the

differences between thermodynamic quantities and spectroscopic properties. Thermodynamic properties usually correspond to one particle correlation functions, and as in the Fermi function, the activation energy corresponds to the energy difference between the edge of the density of states and the chemical potential. For a pure intrinsic semiconductor in which the chemical potential lies at the exact middle of the gap, the activation energy should correspond to half of the value of the gap. For doped semiconductors, with impurity bands within the gap, the activation energy could be expected to correspond to the minimum separation of the impurity band to the edges of the host bands. Spectroscopic properties that correspond to two particle correlation functions generally should show a gap which has the magnitude of the energy separation between the empty and filled bands, and thus be at least a factor of two larger than the activation energy obtained from the thermodynamics.

4. Spectroscopies

Inelastic neutron scattering, infrared absorption and photo-electron spectroscopic measurements have been made on some of the heavy fermion semiconducting materials. In the case of $Ce_3Bi_4Pt_3$ [104, 183–185], UNiSn [186], FeSi [187–191], SmB_6 [192–194] and YbB_{12} [195, 196] spectroscopic measurements have shown clear evidence of gaps in the spectra. The direct observability of the gaps in these materials is due to the magnitude of the gaps lying within the region of energies which are accessible to the experimental techniques.

4.1. *Optical spectroscopy*

The response of a system to a weak externally applied transverse electromagnetic field is given by the frequency dependent conductivity $\sigma(q,\omega)$. This conductivity has an imaginary part and a real part that characterizes the excitation of the electronic system caused by the absorption of photons. The real and imaginary parts are related through the Kramers–Kronig relation, which is an expression of causality. A quite common method of determining the complex conductivity for strongly absorbing sample is that of reflectivity. The major drawback of these methods lay in their sensitivity to sample surface quality. The real and imaginary parts can be obtained quite directly in oblique incidence reflectivity measurements where the reflectance of the two polarization components of the incident beam are measured, or via ellipsometry. However, the most common method used is that of normal incidence reflection. In principle it would be necessary to measure the reflectance and absorption in order to determine the complex conductivity. However, it suffices to measure the reflectance over a very wide frequency range and then deduce the absorption using the Kramers–Kronig relations.

The frequency dependence of the conductivity expected for a generic metal consists of a Drude peak,

$$\sigma(\omega) = \frac{(ne^2\tau/m)}{(1+\omega^2\tau^2)}, \tag{16}$$

which extrapolates at $\omega \to 0$ to the dc conductivity $\sigma(0)$. A Fermi-liquid analysis appropriate to heavy-fermion materials shows that the dc conductivity should exhibit no enhancement as the effective mass and the quasi-particle lifetime are expected to be renormalized by the same factor, $Z(\omega)$ which is related to the one electron self-energy $\Sigma(\omega)$ via

$$Z(\omega) = 1 - \mathrm{Re}\left[\frac{\mathrm{d}\Sigma(\omega)}{\mathrm{d}\omega}\right]. \tag{17}$$

The renormalized scattering rate τ^* and renormalized quasi-particle mass m^* are related to the unrenormalized scattering rate and band mass m_B via

$$\tau^* = Z(0)\tau \tag{18}$$

and

$$m^* = Z(0)m_B. \tag{19}$$

Thus, the renormalization in the numerator and denominator of the factor τ^*/m^* in the dc conductivity should nearly drop out resulting in the approximate expression $\sigma(0) = ne^2\tau/m_B$. Roughly speaking, for heavy fermion materials the electronic correlations are localized, thus, the self-energy becomes roughly k independent but is a strongly varying function of frequency at low temperatures. The rapid frequency dependence causes the simultaneous enhancements of the effective mass, and also reduces the scattering rate $\hbar/\tau(\omega) = 2\,\mathrm{Im}\,[\Sigma(\omega)]$ via the factor $Z(\omega)$. The vertex function in the conductivity also is expected to be relatively k independent and hence drops out of the expression for the conductivity. As the only place that the many-body correlations occur is through the multiplicative factor $\omega Z(\omega)$, it seems natural that the dc limit of the conductivity should remain unrenormalized. However, the low temperature Drude peak should therefore exhibit an anomalously narrow width of

$$1/\tau^* \approx \frac{2\,\mathrm{Im}\,[\Sigma(0)]}{\hbar Z(0)} \tag{20}$$

associated with the enhanced quasi-particle lifetime, and as the enhancement is reduced with increasing temperature, the Drude peak should also broaden. This type of temperature dependence of the Drude peak is often observed in heavy fermion metals [197, 198]. For a recent review of the electrodynamic response of heavy fermion compounds the reader is referred to the article by Degiorgi [199]. In a conventional semiconductor one expects that at low temperatures there is a threshold energy for optical absorption. For a direct gap semiconductor the threshold energy would correspond to the direct ($q = 0$) excitation of an electron–hole pair which carry the same momenta. In an indirect gap semiconductor the threshold corresponds to the indirect gap, in which a phonon carries away the momentum difference between the final state electron–hole pair.

The conductivity is defined in terms of the causal relation between the spatial and time dependence of the current response, $J_i(r,t)$ to the vector potential $A_j(r',t')$ applied at an earlier time t'. These are related via the Kubo formula, which can be expressed as

$$J_i(r,t) = \sum_j \int_{-\infty}^{+\infty} \mathrm{d}t' \int \mathrm{d}^3r' R_{i,j}(r-r',t-t')A_j(r',t'). \tag{21}$$

The correlation function in the above expression is given by the sum of a paramagnetic current–current correlation function and a diamagnetic term via

$$R_{i,j}(r-r',t-t') = -\mathrm{i}\theta(t-t')\langle[j_i(r,t),j_j(r',t')]_-\rangle - ne\delta_{i,j}\delta(r-r')\delta(t-t'). \tag{22}$$

On performing Fourier transforms in space and time one obtains the relation

$$J_i(q,\omega) = \sum_j R_{i,j}(q,\omega) A_j(q,\omega), \tag{23}$$

which defines the frequency dependent conductivity as the response to an electric field $E_j(q,\omega) = \mathrm{i}\omega A_j(q,\omega)$ as

$$\sigma_{i,j}(q,\omega) = \frac{R_{i,j}(q,\omega)}{\mathrm{i}\omega}. \tag{24}$$

In the independent electron approximation, the tensor $R_{i,j}(q,\omega)$ is given by a Lindhard expression involving inter-band and thermally excited intra-band excitations. If one assumes that the f electrons are almost localized and have negligible band dispersion, then the current is carried by the conduction electrons. In this case, the appropriate expression for the tensor $R_{i,j}(q,\omega)$ is

$$R_{i,j}(q,\omega) = -e^2 \sum_{k,\alpha,\beta,\sigma} v_i^{\alpha,\beta}(k+q/2) v_j^{\beta,\alpha}(k+q/2)^* \times |B_\alpha(k)|^2 |B_\beta(k+q)|^2 \left(\frac{f_{k,\alpha,\sigma} - f_{k+q,\beta,\sigma}}{\omega + \epsilon_{k+q,\beta,\sigma} - \epsilon_{k,\alpha,\sigma} + \mathrm{i}\tau^{-1}} \right), \tag{25}$$

where the factors $|B_\alpha(k)|^2$ projects the conduction electron character out of the state k,α, and $v_i^{\alpha,\beta}(k)$ is the ith component of the velocity vector. Due to the large magnitude of the speed of light and our interest in relatively low frequency phenomena, one can often approximate the incident vector potential as having $q = 0$. This would indicate that the inter-band spectrum should have a threshold at an energy corresponding to the value of the direct gap. However, many-body interactions should result in the spectrum having a non-zero intensity above a threshold corresponding to the indirect gap. This intensity should be low if the states involved are mostly of f character. The intra-band contributions are expected to yield a thermally activated Drude peak which extends to energies lower than the gap in the low temperature spectra associated with the inter-band excitations.

Infrared reflectivity measurements have been performed on $Ce_3Bi_4Pt_3$ [183], and FeSi [187]. The real part of the frequency dependent conductivity $\sigma(\omega)$ has been extracted from the data. The measurements shown in figure 5 show that at low temperatures the materials exhibit a gap in the conductivity between $\omega = 0$ and a threshold energy. Above the threshold, the spectrum for $Ce_3Bi_4Pt_3$ shows a gradual increase before saturation [183]. The unusual shape of this spectrum allows the flexibility of defining two characteristic energies related to the gap, and could cause some confusion in defining the relative magnitude of charge and spin gaps, see figure 6. As we shall comment on later, this might be evidence for the indirect nature of the gap, the saturation of the spectra being associated with the gap expected in direct optical absorption, while the tail in the spectra represents indirect process which culminate at the indirect gap. As the temperature is increased the gap in the spectrum is progressively filled in and the spectrum above the gap, in an energy interval corresponding to three or four times the low temperature gap energy, shows insignificant temperature variation. The filling in of the gap region can be understood in terms of the development of a low frequency Drude peak due to an increasing population of thermally activated electron–hole pairs, or due to the temperature dependence of the gap, as inferred from dc transport measurements [136].

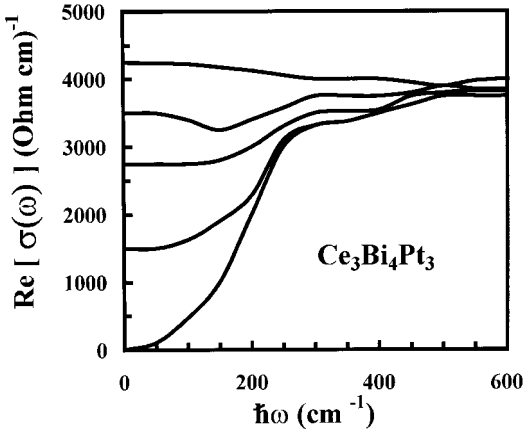

Figure 5. The real part of the optical conductivity, $\sigma(\omega)$, of $Ce_3Bi_4Pt_3$ for five different temperatures, $T = 25\,\mathrm{K}$, $T = 50\,\mathrm{K}$, $T = 75\,\mathrm{K}$, $T = 100\,\mathrm{K}$ and $T = 300\,\mathrm{K}$. The measurements were made by Bucher *et al.* [183].

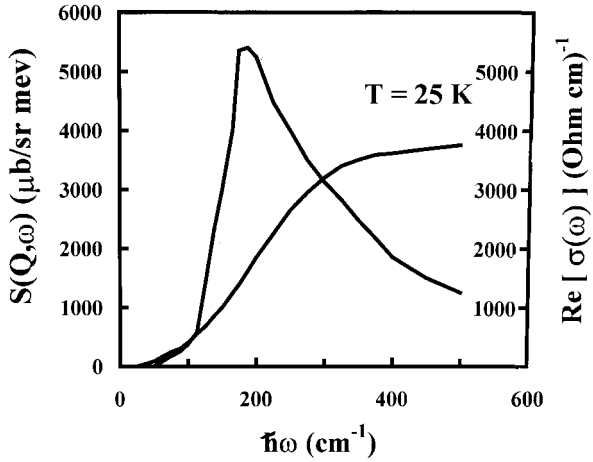

Figure 6. The inelastic neutron scattering measurements of Severing *et al.* [104] made on $Ce_3Bi_4Pt_3$ at $T = 25\,\mathrm{K}$, $S(Q,\omega)$ superimposed on the $T = 25\,\mathrm{K}$ results for the real part of $\sigma(\omega)$ from [183].

The measurements on FeSi are quite similar [187], and show marked deviations from the spectrum calculated using the LDA [29, 200], which again is evidence for a strong many-body renormalization of the gap. In fact experiments on FeSi [201, 202] show that, in addition to spectral weight filling in the gap, the gap edge moves to a slightly lower frequency as the temperature is increased. The motion of the gap edge is also a signature of many-body effects. The magnitude of the gap is estimated to be of the order of 50–70 meV [201, 203–205]. The temperature dependence of the gap spectral weight in both FeSi and $Ce_3Bi_4Pt_3$, shows a strong correlation with the formation of magnetic moments, seen through analysis of the static susceptibility [187]. An alternate viewpoint is that of Degiorgi *et al.* [206] who suggest that the anomalous properties of FeSi may be the consequences of Anderson localization. By examining the conductivity at microwave frequencies as well as in the far-infrared

range, these authors find that the low temperature low frequency optical conductivity follows the expression

$$\sigma(\omega) = \sigma(0) + A\omega^2[\ln(\omega/\omega_0)]^4 \tag{26}$$

expected for photon activated hopping. This viewpoint has been challenged [142] by an analysis of the frequency dependence of the real and imaginary parts of the microwave conductivity. In this analysis it is found that the low temperature conductivity has a power law frequency dependence with an exponent characteristic of hopping conduction, but crosses over to a completely metallic behaviour for $T > 25\,\mathrm{K}$. Resistivity measurements [144] on $FeSi_{1-x}Al_x$ show that even though an extrinsic impurity band may occur within the gap, Coulomb interactions also play an important role.

The frequency dependent conductivity should satisfy the optical f sum rule at all temperatures [207], which states that the integral

$$\int_0^\infty \mathrm{d}\omega\sigma(\omega) = \frac{\pi n e^2}{2m} \tag{27}$$

is a constant. Consideration of the integrated intensity of the absorption spectrum suggests that in order to satisfy the f sum rule, the lost spectral weight in the gap region at high temperatures, evident in figure 5, must reappear at other energies. One possibility is that the weight was transferred to lower energies and appears as a delta function spike at $\omega = 0$, as happens in superconductors. Another possibility is that the spectral weight has been moved to higher energies. It appears that the latter case is appropriate for these materials as experiments on FeSi show [146, 206, 208] that the spectral weight is transferred to energies roughly 3 to 4 times higher than the gap energy. As the temperature change, which causes the evolution from the low temperature spectrum to the high temperature spectrum, is comparable to the gap energy, at first sight it seems unlikely that such a small change could move large amounts of spectral weight to a much higher energy range. However, as the conductivity is related to a two-particle correlation function, the thermal disorder introduced by a small temperature change can and does significantly alter the spectrum of allowed excitations between initial and final states. In fact a temperature change of 300 K does result in a significant redistribution of spectral weight in SmB_6 which extends out to at least 1.5 eV.

The real part of the conductivity extracted from reflectivity measurements on SmB_6 [209–212] shows the opening of a gap in the low frequency part of the spectrum, as the temperature is lowered from 300 to 4 K. Two gap energies have been identified at low temperatures, the smaller value is estimated as 4 meV, while the larger value is found to be 14 meV. The absorption edge at 4 meV has been attributed to absorption by impurity states that exist in the intrinsic gap, and the 14 meV value has been identified as the intrinsic gap. An analysis of the residual Drude peak observed for temperatures below 15 K shows a thermally activated population of carriers [213], originating from a donor band at about 3 meV below the conduction band. This interpretation has been confirmed by sub-millimetre transmission experiments [193] which indicate that the carriers in the conduction band have very large effective masses of the order of 100 free electron masses, indicating the importance of electron correlations. The 13 K data [210] also shows the existence of a peak at about 120 meV and a second peak at an energy of

roughly 0.5 eV. In the hybridization gap interpretation, the energy of the first peak ($\approx$120 meV) may be tentatively identified as the direct gap, which when broadened by the emission and absorption of collective boson fluctuations gives rise to the absorption spectrum which has a low energy tail that commences at the indirect gap energy. The second peak may be assigned to inter-band excitations. On increasing the temperature from 13 to 300 K the two distinct peaks which were separated by 0.38 eV can no longer be resolved.

In YbB_{12} the observed frequency dependent conductivity [195, 214] follows the generic pattern of heavy fermion semiconductors. A gap develops in the low temperature conductivity, as the temperature is lowered from 290 to 20 K. The spectrum has a gap estimated to be 25 meV, above which the spectrum increases until it hits a shoulder at 40 meV and then flattens off. The conductivity also has a pronounced peak above 0.2 eV. An analysis of the 0.2 eV peak indicates that the 40 meV shoulder is actually a peak, similar to the 0.12 eV feature observed in SmB_6. Although a peak is expected to occur at the energy of the direct gap, this identification would require an extremely small dispersion of the conduction band. Alternatively, since this energy is roughly twice the gap energy it could be related to the threshold of incoherent excitations. This continuum should be separated from the threshold of quasi-particle excitations by the smallest collective excitation energy, similar to the separation of the zero phonon and multi-phonon lines in semiconductors. The 25 meV value of the optical gap is much larger than the gaps inferred from thermodynamic and transport measurements, such as the 12 meV inferred from the resistivity [112, 113]. This points to the pinning of the Fermi level to states within the gap, possibly of extrinsic character. In this picture the value of the intrinsic gap would be 25 meV and the partially occupied impurity states would be separated from one of the edges of the gap by an energy of 6 meV.

The optical conductivity of UNiSn [186, 215] exhibits a peak at 100 meV (800 cm^{-1}) with a peak value of order 1500 $\mu\Omega cm^{-1}$ at room temperature. The low frequency conductivity ($\omega < 130\,cm^{-1} \approx 17$ meV) shows a marked decrease as the temperature is decreased in the range $300\,K > T \gg T_N$, which indicates the presence of a gap in the excitation spectrum in the paramagnetic phase. The conductivity shows a threshold at $\omega = 480\,cm^{-1}$ that could be identified with the gap energy. The spectrum in the low frequency gap region is filled in for temperatures below $T = 43$ K where the antiferromagnetism sets in. This is in accord with the results of the thermodynamic and transport measurements [19, 20]. In the low temperature antiferromagnetic phase a sharp mode is found at an energy $\omega = 18\,cm^{-1}$ ($\omega = 2.3$ meV) which corresponds to half the Néel temperature and may reflect a pinned spin density wave.

Very interesting microwave conductivity measurements [155] have been made on a single crystal of CeNiSn, for frequencies of 14 and 9.6 GHz. By measuring the surface impedance both the real and imaginary parts of the conductivity can be found. The real part of the conductivities for each principal axis superimpose on the corresponding dc conductivity, for temperatures above 10 K. However, considerable deviation occurs below 10 K, which is surprising since the characteristic microwave frequency is of the order of 1 K. This could be indicative that the frequency dependence is enhanced by the wave function renormalization from ω to $\omega Z(\omega)$, where $Z(\omega)$ is responsible for the quasi-particle mass enhancements of almost localized electron systems and also shows up in the optical conductivity as a narrowing of the Drude peak [197, 198]. The authors [155] analyse their data on

the basis of the Drude model; by taking the ratio of the real and imaginary parts of the conductivity they separate the carrier density from the transport scattering rates for the various directions. The scattering rates drop by an order of magnitude as the temperature is reduced from 10 to 2 K. This drastic reduction in the scattering rate results in the metallic conductivity, even though the number of carriers inferred from the Hall effect decreases as the temperature is decreased [96].

The angular momentum selection rules involved in the absorption of a photon restrict the electronic excitations to occur predominantly between states that differ by angular momentum of unity. The angular momentum is manifest by the vector character of the velocity appearing in the interaction. Raman scattering is a higher order process involving the absorption and emission of another photon, and is complementary to absorption in that it involves states that differ by either zero or two units of angular momentum, and is also able to better access a lower range of excitation energies.

The Raman scattering spectra of FeSi is interesting [216] in that it shows that a gap opens up in the electronic continuum below a temperature of the order of 250 K. As the temperature is lowered, the spectral weight below an energy of $800\,\mathrm{cm}^{-1}$ ($\approx 100\,\mathrm{meV}$) is depleted and a peak grows at an energy of $1200\,\mathrm{cm}^{-1}$ ($\approx 150\,\mathrm{meV}$). Unlike the optical absorption, the spectral weight in the Raman scattering process is not governed by the optical sum rule. The shape of the Raman spectrum is consistent with the initial to final state excitation being an indirect process, in that it contains no clear signature of a unique gap energy but has a long tail with a threshold somewhere above $200\,\mathrm{cm}^{-1}$. However, a temperature dependent characteristic energy can be defined, which separates the region of spectral depletion from spectral growth. This energy shows a rapid increase from zero to saturation as the temperature is lowered below 250 K.

Raman scattering experiments have been performed on CeNiSn and CeRhSb [217]. The phonon spectra of both materials are similar, and most phonon lines show an increase in energy with increasing temperature. However, other peaks which involve the vibrations of Ce behave anomalously. These peaks ride on the back of a broad continuous spectrum presumably due to electronic excitations. At 5 K the broad continua of CeNiSn and CeRhSb, respectively, can be fit by V-shaped spectra with pseudogaps of 28 and 36 K. These estimates of the pseudogap energies are similar to those obtained from NMR [94] and specific heat [95] measurements.

The electronic continuum seen in the Raman scattering of SmB_6 also shows a temperature dependent evolution [218]. For temperatures below 70 K, the spectrum is depleted for energies below $290\,\mathrm{cm}^{-1}$ ($\approx 36\,\mathrm{meV}$) and the spectrum is enhanced at an energy of $350\,\mathrm{cm}^{-1}$ ($\approx 43.4\,\mathrm{meV}$). The value of the gap inferred from the Raman scattering experiments of 36 meV is much greater than the gap energy of 4 meV inferred from transport measurements [4] and the 4–14 meV inferred from the optical absorption spectrum. A value between 100 and $150\,\mathrm{cm}^{-1}$ (12.5–18.5 meV) may be more consistent with the tail of the indirect spectrum. A second feature of $d_{x^2-y^2}$ symmetry starts evolving in the spectrum at a temperature just slightly lower than the temperature where the gap starts developing. This feature has a characteristic energy of $130\,\mathrm{cm}^{-1}$ ($\approx 16\,\mathrm{meV}$) just slightly higher than the energy of the feature observed in inelastic neutron scattering experiments [194, 219, 220].

4.2. *Tunnelling spectroscopy*

Electron tunnelling measurements provide a method of probing the energy gap in the electronic density of states, giving information similar to optical absorption. In these experiments the junction is formed consisting of an (α) electrode made of the material being investigated which is separated by an insulating barrier from another electrode (β), which may be either a metal or another semiconductor. A bias voltage V is applied across the junction and the resulting current flow I is measured. The linear response relationship between I and V can be expressed in terms of the tunnelling Hamiltonian H_t which transfers electrons between the two electrodes. The tunnelling Hamiltonian is given by

$$H_t = \sum_{k\,k'} [\Lambda_{k,\alpha;k',\beta} a^+_{k,\alpha} a_{k',\beta} + \text{h.c.}], \tag{28}$$

which in the interaction representation can be written as

$$H_t(t) = A(t)\,\exp[-ieVt/\hbar] + A^+(t)\exp[+ieVt/\hbar], \tag{29}$$

where the operator $A(t)$ is given in terms of the tunnelling matrix elements $\Lambda_{k,\alpha;k',\beta}$ by

$$A(t) = \sum_{k\,k'} [\Lambda_{k,\alpha;k',\beta} a^+_{k,\alpha}(t) a_{k',\beta}(t)]. \tag{30}$$

The single particle tunnelling current is given by the two particle Green's function

$$I(V) = \left(\frac{2e}{\hbar^2}\right) \text{Re}\left[\int_{-\infty}^{+\infty} dt' \exp[-ieV(t-t')/\hbar]\theta(t-t')\langle[A(t), A^+(t')]\rangle\right] \tag{31}$$

similar to the optical conductivity. In the non-interacting electron approximation, the tunnelling current reduces to

$$I(V) = \frac{4\pi e}{\hbar} \sum_{k\,k'} |\Lambda_{k,\alpha;k',\beta}|^2 [f(\epsilon_\alpha(k)) - f(\epsilon_\beta(k'))]\delta(\epsilon_\alpha(k) - \epsilon_\beta(k') + eV), \tag{32}$$

which at low temperatures resembles the joint density of states for the junction. For smooth interfaces and isotropic systems, the component of the Bloch wave vector k parallel to the surface is conserved in tunnelling processes. As the tunnelling matrix elements behave similarly to group velocities, a cancellation with the energy dependence of the density of states may occur in elastic tunnelling with ideal junctions. For point contact tunnelling spectroscopy the effect of the barrier vanishes and there is no conservation of $k_{||}$, so the energy dependence of the density of states may be observed. These measurements depend extremely sensitively upon the quality of the junctions interfaces, their exposure and their orientation. Unfortunately, tunnel junctions are not directly amenable to *in situ* characterization.

Break junction tunnelling [221] and point contact spectroscopy [222] measurements have been performed on $Ce_3Bi_4Pt_3$. At low temperatures the differential conductance dI/dV shows typical semiconducting behaviour. As the temperature is increased the gap structure is washed out. In the interpretation of the point contact spectroscopy measurements [222], the gap edges are defined as coinciding with the maxima of d^2I/dV^2. The value of the gap $T = 1.5\,\text{K}$ obtained in this manner is 9.7 meV, which is in agreement with a gap of 8–10 meV inferred from the activation of the resistivity in the same low temperature range [135, 136]. The finite value of the zero bias resistance is attributed to an impurity band within the gap, and its temperature dependence tracks that of the dc resistivity.

Scanning tunnelling microscope (STM) measurements have been performed on FeSi [223], which showed strong non-ohmic variation due to the formation of a Schottky barrier. Using the Schottky barrier transmission coefficient known at room temperatures, a temperature dependent quasi-particle density of states was inferred from the differential conductivity. The temperature dependence of the integrated intensity of the quasi-particle density of states was found to resemble the mean-field approximation for an order parameter at a second order phase transition, with transition temperature of 200 K. The quasi-particle density of states had the form of a symmetric two peaked structure, with a peak-to-peak separation of 110 meV. The height of the two peaks and the magnitude of the dip separating the peaks increased as the temperature was lowered from 300 to 4 K, but the zero bias conductance remained finite. The authors [223] infer that a gap of $\approx$50 meV occurs in FeSi, which is comparable with the ranges of 50–70 meV inferred from optical spectroscopy [201, 204] and the range of 60–82 meV inferred from the resistivity using different fitting procedures [78, 106].

Break junction experiments on the orthorhombic systems CeNiSn [224, 225] and CeRhSb [224, 226] show tunnelling spectra that exhibit two types of pseudogaps which culminate in peaks, corresponding to intra-grain and grain boundary tunnelling. The peak-to-peak separations differ by a factor of 2 and the smaller values are identified with semiconductor–insulator–metal tunnelling and the larger values are associated with semiconductor–insulator–semiconductor tunnelling. The smallest peak-to-peak separation in the tunnelling density of states of CeNiSn yields a gap of 10 meV, which is significantly larger than the largest gap of 4 meV of the largest intensity feature observed in inelastic neutron scattering experiments on polycrystals [227]. Similar tunnelling experiments on single crystals of CeNiSn [228] show only the larger peak-to-peak separations, which should correspond to twice the gap energy. The gap inferred from these experiments is also in the range of 8 to 10.5 meV. The low temperature values of the characteristic energies inferred from tunnelling, for both systems, are roughly equal to the Kondo temperature [224]. The temperature dependence of the characteristic tunnelling energy of CeNiSn shows a similar type of temperature dependence to that of the transport gap in $Ce_3Bi_4Pt_3$ [77]. Although the characteristic tunnelling energy of CeRhSb also decreases with increasing temperature, the shape of the curve is qualitatively different from $Ce_3Bi_4Pt_3$. The field dependence of the characteristic energy of polycrystalline CeNiSn shows a slight initial increase with increasing fields and then shows a decrease [225] as qualitatively expected from a Zeeman splitting. Similar experiments on single crystals of CeNiSn [228] shows a large anisotropic dependence on the direction of the field. No notable dependence was observed in the I–V characteristics for fields in the b-direction, but the peak-to-peak energy was observed to decrease on applying fields parallel to the a-direction, simultaneously with an enhancement of $\mathrm{d}I/\mathrm{d}V$ at $V = 0$. As the square root of the zero bias value tracks the C/T ratio at 1.7 K, it may reflect the density of states at the Fermi energy, and suggests that either the appropriate tunnelling matrix elements $\Lambda_{k,\alpha;k',\beta}$ or the many-body vertex function is actually a smooth function of k and k'. In either case, the evolution of the $V = 0$ peak in $\mathrm{d}I/\mathrm{d}V$ found on increasing the field could represent the formation of a heavy fermion metallic state.

Early point contact tunnelling experiments [229] on SmB_6 have shown that the differential conductivity $\mathrm{d}I/\mathrm{d}V$ shows a minimum at zero bias, $V = 0$, with a width of 4.6 meV, as determined by the peak-to-peak separation in $\mathrm{d}^2V/\mathrm{d}I^2$. This value is

similar to estimates made from tunnelling measurements [230] where the full width at half minimum of the gap was reported as 2.7 meV, which implies a full width of 5.4 meV. These values are considerably smaller than the 16 meV obtained from later measurements on, presumably, better samples [231, 232]. The smaller value of 4.6 meV is in reasonable agreement with the range of values of 41–48 K (≈3.4–4.1 meV) obtained from the resistivity measurements [165, 167]. The variation in the gap energies inferred from tunnelling spectroscopies can be systematized according to the quality of the samples, in which the smaller value of the gap of 4 meV corresponds to tunnelling to impurity states in the gap, whereas 14 meV is a measure of the full intrinsic gap. The gap starts developing at a temperature around 40 K, but the depletion in the zero bias conductance is small (approximately only 30%) as the temperature is reduced to 10 K [232].

Point contact tunnelling measurements on YbB_{12} at 4.2 K [233] yield an estimate of the gap as 6.5 ± 0.5 meV, which is in the same range as estimates based on the resistivity and optical absorption, 3 to 12 meV. On the other hand, break junction measurements on YbB_{12} [234] are not well understood, as the inferred characteristic tunnelling energies are in the range of 220–260 meV which is at least an order of magnitude larger.

4.3. *Inelastic neutron scattering spectroscopy*

One of the most direct ways of measuring the magnetic excitations of a system is through the scattering of low energy neutrons. The neutrons interact with the magnetic moments in the system via a weak dipole–dipole interaction. In inelastic neutron scattering spectroscopy, one measures the differential scattering cross-section, as a function of the momentum and energy transferred between the neutrons and the electronic system (Q,ω). The inelastic differential cross-section for an unpolarized beam of neutrons is given by the expression,

$$\frac{\mathrm{d}^2\sigma}{\mathrm{d}\Omega\,\mathrm{d}\omega} = \frac{k'}{k}\sum_{i,j}(\delta_{i,j} - \hat{Q}_i\hat{Q}_j)\left(\frac{g_N e^2}{mc^2}\right)^2 S^{i,j}(Q,\omega), \tag{33}$$

where k and k' are the initial and final momenta of the neutron. The scattering function $S^{i,j}(Q,\omega)$ is related to the imaginary part of the dynamic magnetic susceptibility, via

$$S^{i,j}(Q,\omega) = \frac{2}{\pi}\left(\frac{F(Q)}{g\mu_B}\right)^2 [1 + N(\omega)]\,\mathrm{Im}\,[\chi^{i,j}(Q,\omega)], \tag{34}$$

in which $F(Q)$ is the magnetic form factor and g_N is the gyromagnetic ratio the neutron. The dynamic susceptibility is given by the Fourier transform of the two-time spin correlation function

$$\chi^{i,j}(r - r', t - t') = \frac{\mathrm{i}}{\hbar}\theta(t - t')\langle[S^i(r,t), S^j(r',t')]_-\rangle. \tag{35}$$

In the independent electron approximation, the longitudinal dynamic susceptibility is given by a Lindhard expression involving inter-band and intra-band excitations. If one assumes that the magnetic moment resides mainly on the f electrons and neglects the spin of the conduction electrons, the appropriate expression is

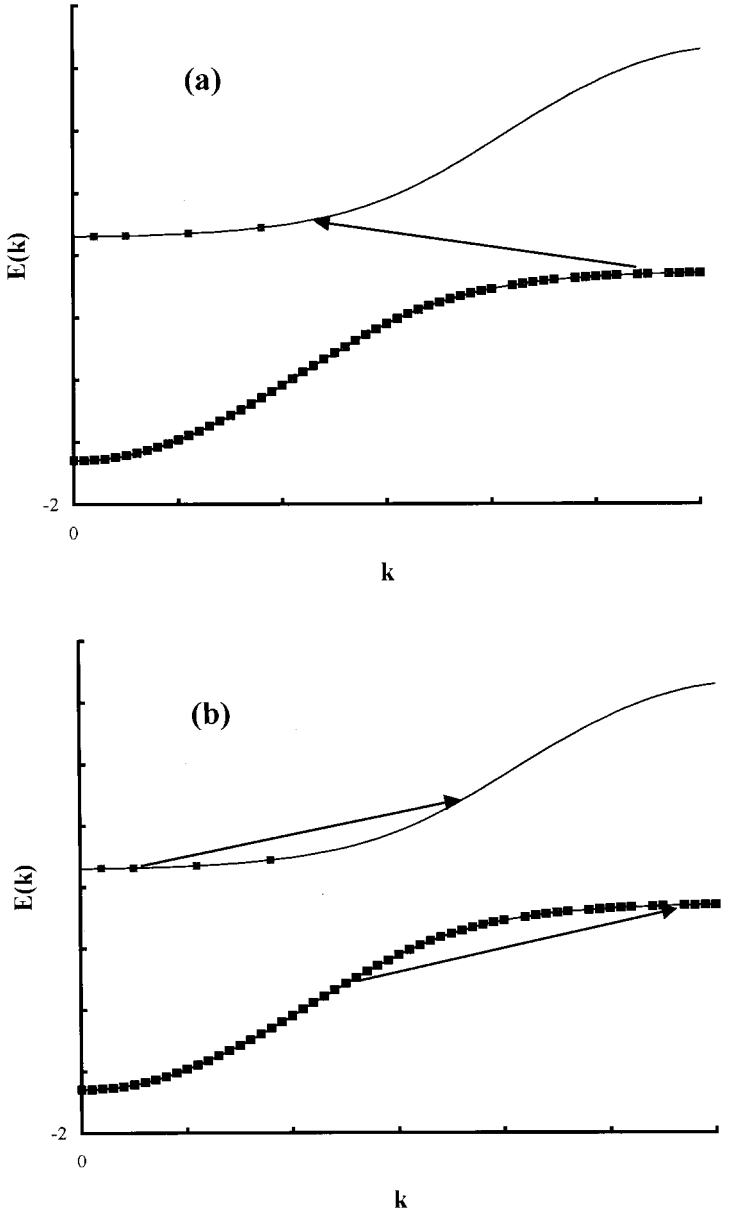

Figure 7. The finite Q inter-band Stoner excitations depicted in (a) have a threshold energy, while the intra-band excitations depicted in (b) have a quasi-elastic form but have a thermally activated intensity when integrated over ω.

$$\chi^{z,z}(Q,\omega) = \sum_{k,\alpha,\beta,m} m^2 |A_\alpha(k)|^2 |A_\beta(k+Q)|^2 \left(\frac{f_{k,\alpha,m} - f_{k+Q,\beta,m}}{\omega + \epsilon_{k+Q,\beta,m} - \epsilon_{k,\alpha,m}} \right), \qquad (36)$$

where the factors $|A_\alpha(k)|^2$ projects the f character out of the state k,α. For FeSi where the orbital moment is quenched these factors would be replaced by unity. As in the case of the optical conductivity, the susceptibility has inter-band and

intra-band contributions to $\mathrm{Im}\,[\chi(Q,\omega)]$. These finite Q excitations are shown schematically in figure 7. The inter-band excitations should be responsible for the low temperature spectrum which has a gap below the threshold for the excitation of electron–hole pairs, and has a continuous form at higher energies which forms the Stoner continuum. The Stoner continuum should peak at those energies where there are large f contributions to the density of electron or hole states. The intra-band spectrum should have a thermally activated integrated intensity, and should have the form of a quasi-elastic spectrum which also exists within the gap region. The above form of the single or quasi-particle contribution to the susceptibility neglects the effect of collective spin-wave excitations which are produced by an additional residual interaction which couples the quasi-particles. This interaction is expected to be weak for f electron heavy fermion materials where the response function has a large Q independent component that can be fit to the relaxational form

$$\chi(Q,\omega) = \frac{\chi_0 \Gamma}{\Gamma - \mathrm{i}\omega}. \tag{37}$$

As most of the integrated intensity expected from sum rules is tied up in the above response there is little intensity left to assign to smaller Q dependent contributions which peak at non-zero Q, indicating antiferromagnetic correlations [235, 236]. The low ω and Q peak expected from the Pauli-paramagnetic quasi-particle contribution is suppressed. This implies strong spin–orbit coupling between the f quasi-particles of a Fermi liquid, and that most of the response is of local origin.

Inelastic neutron scattering measurements have been performed on $Ce_3Bi_4Pt_3$ [104], FeSi [188, 189], CeNiSn [85, 86, 227, 237, 238], SmB_6 [194, 219, 220] and YbB_{12} [196]. These experiments measure the dynamical magnetic susceptibility $\chi(Q,\omega)$ which is the spectrum for the magnetic excitations. The experiments on polycrystalline $Ce_3Bi_4Pt_3$, in the low temperature regime, shown in figure 6, show clear evidence of a gap in the spectrum of spin-flip magnetic excitations and, to within the determination of the experimental background, no states within the gap. The magnitude of the observed gap in the spectrum is approximately twice the activation energy inferred from thermodynamic and electron transport measurements. Thus, the gap in the magnetic spectrum is consistent with that expected with (Stoner) single electron excitations over the band gap, and the spin gap and the charge gap are of comparable magnitude [184]. For example, at 2 K the gap observed in on $Ce_3Bi_4Pt_3$ [104] is 12 meV or 140 K, which is quite similar to the gap of 120 K found from transport measurements [136]. The range of momentum transfer accessed by the inelastic neutron scattering measurements on polycrystalline samples is of the order of half a reciprocal lattice vector. Thus, the observed gap could correspond to the minimum energy spin-flip process exciting an electron from the filled valence band to an empty conduction band in an indirect semiconductor. Mason and collaborators have performed inelastic neutron scattering experiments on Canfield's biggest single crystal investigating the Q dependence. Although most of the Brillouin zone was probed, excluding small momentum transfers, there was very little Q dependence of the gap [239]. This is consistent with the published results on powdered samples [104, 184, 240]. Any Q independence of the gap does not necessarily imply that the system is a direct gap and not an indirect gap semiconductor. This is because, like in $Q = 0$ optical absorption, indirect processes, involving the participation of low energy boson excitations with large momentum transfers, can result in the $Q = 0$ neutron excitations having a threshold which

corresponds to the indirect gap. However, the shape of the spectrum above threshold should have a characteristic shape. As the temperature is increased the gap in the magnetic spectrum is filled in. Again this could be interpreted either in terms of a quasi-elastic peak due to neutrons scattering off from the thermal equilibrium distributions of electrons in the conduction band and holes in the valence band, or due to the collapse of the gap with increasing temperature. Substitution of La on the Ce sites has the effect of rapidly moving the gap edge to lower energies [184], and the statistics are not inconsistent with the appearance of states within the gap as the concentration of La is increased. At high temperatures ($T > 300\,\mathrm{K}$) the inelastic neutron scattering experiments on FeSi [188, 189] shows a quasi-elastic scattering peak which has a strongly Q dependent energy width. The intensity of this peak, when integrated over ω, is strongly temperature dependent and scales with $3k_{\mathrm{B}}T\chi(T)$ indicating that the scattering is due to a thermally excited population of magnetic moments. At a temperature of 300 K the spectrum taken at $Q = (1.2,1.2,0)$ shows evidence for the existence of an additional contribution to $S(Q,\omega)$ which has the form of a small feature with a threshold of order 20–30 meV. This feature was attributed to electronic spin-flip excitations across the band gap. An interesting characteristic of the results on FeSi is that although the scattering function is strongly peaked about ferromagnetic Q vectors, the value of the instantaneous correlation function

$$S(Q,t=0)/|F(Q)|^2 = \int_0^\infty \mathrm{d}\omega S(Q,\omega)/|F(Q)|^2, \tag{38}$$

is almost Q independent due to the strong Q dependence of the peak widths. Thus it is concluded that there is no evidence for non-local correlations at any of the measured temperatures. A similar absence of a Q dependence in $\mathrm{Re}\,[\chi(Q,\omega=0)]$ has been inferred for CeNiSn [86] based on a Kramers–Kronig analysis of $\mathrm{Im}\,[\chi(Q,\omega)]$ which would also indicate the absence of any preferential response of the paramagnetic system to any type of staggered ordering field.

The inelastic neutron scattering data on CeNiSn [86], taken at $T = 1.4\,\mathrm{K}$ can be interpreted as showing a minimum in $S(Q,\omega)$ near zero energy transfer. For Q values near $Q = (0,0,1)$ the spectra shows a fairly sharp intense and asymmetric peak at 2 meV, which was taken as indicative of a threshold for inelastic scattering. The close proximity of the threshold to the inelastic scattering peak makes the determination of whether a true gap exists difficult. For Q values further from $Q = (0,0,1)$ the peak broadens and becomes less intense. The spectra is extremely anisotropic as no structure is observed for $Q = (1,0,0)$. The polarization of the magnetic fluctuations is mainly along the a-axis consistent with the identification, based on static susceptibility measurements [11], of the a-axis as being the easy axis. The difficulty in ascertaining whether these systems are narrow gap semiconductors or anisotropic semi-metals from the neutron scattering data is not surprising, as the magnitude of the characteristic activation energy inferred from transport measurements is only 3.4 K. In fact later experiments by Raymond *et al.* [241] on single and polycrystalline samples show that the 2 meV peak rides upon the back of a Q independent quasi-elastic peak of the sort found by Mason *et al.* [86]. The quasi-elastic peak within the 2 meV 'threshold' carries over 2/3 of the intensity of the magnetic signal.

As the temperature is increased from $T = 1.4\,\mathrm{K}$ to $T = 15\,\mathrm{K}$ the 2 meV peak in CeNiSn broadens and loses intensity, so that the low energy spectrum evolves into a quasi-elastic peak. A stronger second asymmetric excitation peak is found [227, 237]

at low temperatures in powdered samples. In single crystals this $\omega = 4$ meV peak is found at $Q = (Q_a, \frac{1}{2}, Q_c)$, for arbitrary Q_a and Q_c [85, 238]. For ω below 3 meV the peak loses intensity, such that its shape resembles the 'threshold peak' at 2 meV and $Q = (0,0,1)$, as just discussed. Since the value of Q for the 4 meV peak has a value close to the magnetic modulation wave vectors of isostructural antiferromagnetic compounds, and because the intensity grows below $T = 15$ K, this has been attributed [85, 238] to the growth of one-dimensional antiferromagnetic correlations. However, as the application of high magnetic fields [242, 243] do not lead to an increase in the excitation energy but only a (symmetric) broadening of the peak, an assignment as a simple antiparamagnon type of spin fluctuation mode is questionable. As pointed out by Sato *et al.* [85] these excitations do not have the character of crystal field excitations [244, 245], which indeed were later discovered [246, 247] to occur at much higher excitation energies of the order of 40 meV. The field dependence of the 4 meV peak seems more consistent with a Zeeman splitting of a smeared (anisotropic) hybridization gap of the type considered by Ikeda and Miyake [84]. Such an interpretation is also consistent with the observation that intensity of the peak drops as the coherence of the sample is interrupted by either Co doping [248, 249] or Cu doping [250]. As NMR measurements on Co-doped materials show [251, 252], the results of doping [248, 249] is also consistent with the loss of antiferromagnetic correlations as the f states become more mixed valent. The increase of mixed valent character is manifested by the existence of a first order isostructural valence transition to a strongly mixed valent phase [253, 254] in $CeNi_{0.65}Co_{0.35}Sn$. Also substitution of Cu for only 13% of the Ni leads to the complete loss of the inelastic peaks leaving only a quasi-elastic peak [250]. The quasi-elastic peak has a maximal intensity at $Q = (0,1/2,1)$ consistent with the long-ranged antiferromagnetic ordering [83]. On the other hand, under pressure the 4 meV mode moves to higher energies and its width remains constant [255, 256], while transport measurements indicate that the pseudogap closes [147–149]. The 2 meV mode does not broaden as rapidly as the 4 meV mode when the field increases [242, 243], but appears to show an increase in frequency with increasing field and a loss of integrated (over ω) intensity as expected for antiferromagnetic spin fluctuations. Due to the absence of spectral weight being shifted to lower energies, the 2 meV peak is incompatible with a triplet excitation of an electron–hole pair in rigid Zeeman split density of states.

Although the resistivities and anisotropic magnetic susceptibilities of CeNiSn and CeRhSb are quite similar, and NMR experiments indicate that they both have a pseudogap at the Fermi energy [94], the high energy magnetic excitation spectra are quite different [257]. In CeRhSb the scattering cross-section shows a broad peak centred at 40 meV with a comparable width, and does neither show the existence of low energy excitations nor features similar to the unusual 4 and 2 meV gap structures of CeNiSn.

The high energy transfer region of the inelastic neutron scattering data on polycrystalline SmB_6 confirms the mixed valent nature of the ground state [219, 258]. In these experiments distinctive peaks of magnetic origin were observed at $\hbar\omega \approx 36$ meV and at $\hbar\omega \approx 115$ meV which, respectively correspond to the inter-term transition $^7F_0 \rightarrow {}^7F_1$ of Sm^{2+} and $^6H_{5/2} \rightarrow {}^6H_{7/2}$ of Sm^{3+}. The Q dependence of the form factors for these excitations are quite similar to the atomic from factors for the respective inter-multiplet transitions [219]. The average valence obtained from the intensity of these peaks yields $0.5f^6$ and $0.5f^5$. The large widths of these peaks

(~30 meV) have been attributed to the unrenormalized hybridization width ($\Delta = \pi|V|^2\rho(\mu)$).

In addition to these high energy excitations, a remarkable sharp magnetic excitation at energy transfers of 13 meV has been identified in the data taken at temperatures between 20 and 4.5 K [219]. The Q dependence of this low energy peak is sharper than the form factors associated with the f electrons. Measurements on single crystals [194, 220, 259] show that the integrated intensity (integrated over ω) of the 14 meV peak increases dramatically as the temperature is reduced from 40 to 20 K, and that the line width is only reduced from 3 to 1.5 meV in the same temperature range. The energy of the peak only shows a slight reduction as the temperature is changed from 50 to 2 K [220]. The dependence of the integrated intensity versus Q, shows a strong dependence on the magnitude of Q consistent with the admixture f with the B d or p electrons, and also shows an anisotropy within the reduced Brillouin zone. The intensity of the peak is maximum along the direction $Q = (q,q,q)$ at a q value corresponding to the corner of the Brillouin zone. The excitation energy also shows a small dispersion which is slightly greater than the peak width. At $T = 2$ K the dispersion is of the order of 2 meV and produces a minimum in the excitation energy at the corner of the Brillouin zone. The amount of dispersion increases with decreasing temperature. The 14 meV excitation has the right sort of atomic form factor, Q dependent intensity and dispersion expected from a transition between the hybridization split quasi-particle peaks of mixed f and d intensity. However, the magnitude of the indirect gap of 13 meV needed for this interpretation is in conflict with some assignments [209, 260] of the magnitude of the intrinsic optical gap as 3–4 meV, but agrees with other assignments which are closer to 14 meV [192]. However, as previously mentioned, the smaller value may be associated with transitions from impurity states, whereas the larger value may be the value of the intrinsic gap. Additional encouragement for assigning the indirect gap energy at 14 meV is given by the comparison of the unrenormalized hybridization width of 30 meV found at relatively high energy transfers, which would suggest a many-body renormalization of a factor of the order of 2. The trends of the temperature dependence of the integrated intensities and the widths of the quasi-particle peaks are in accord with the expectations of many-body effects. However, the temperature dependence of the dispersion relation is neither consistent with the low temperature evolution of mass enhancements nor the opening of a gap. Therefore, this excitation may tentatively be considered to be a branch of excitations of magnetic character which is split off from the Stoner continuum of particle–hole spin-flip excitations which occur between the two hybridized bands [49]. The branch of collective excitations can be considered to be a consequence of short-ranged antiferromagnetic correlations. The main difference between this type of magnetic excitation and antiparamagnons in metals [75] is that the lifetime broadening is suppressed in the region where the mode falls in the gap below the Stoner continuum. The temperature dependence of the dispersion relation is consistent with the softening of the mode as the antiferromagnetic correlations develop. An alternate explanation that has been suggested [261] involves a homogeneous mixed valent state of excitonic character in which the f orbital is mixed with a bound state residing on the neighbouring B atoms. This excitonic ground state has low lying excited states corresponding to the reorientation of the orbital and spin angular momenta. Since these excitations have a bound state character, the discreteness of the localized eigenvalue could be responsible for the sharpness of the 14 meV feature.

Inelastic neutron scattering experiments have been performed on a polycrystalline sample of YbB_{12} [196]. A large peak was identified at an energy transfer of 15.5 meV which coincides with the smaller phonon peak of LuB_{12}. The width of this peak corresponds to the experimental resolution, and the integrated intensity has a Q dependence which falls off more rapidly than expected from the 4f form factor alone. In addition to this narrow peak, the magnetic spectrum exhibits two broader asymmetric peaks located at $\omega \approx 20$ meV and $\omega \approx 37$ meV, which generally follow the form factor (apart from some oscillations seen in the 20 meV peak). The integrated intensity of the 20 meV peak decreases with increasing temperature, over the range 100 to 150 K. The energy of this feature shows a substantial decrease from $\omega = 20$ to 10 meV in the same temperature range. The shape of the curve is reminiscent of the temperature dependence of the gap in $Ce_3Bi_4Pt_3$ inferred from transport measurements [136]. The energy of the 15 meV peak remains constant over the same temperature range, however, its intensity drops rapidly at $T = 50$ K where the energy of the broad '20 meV' peak coincides with that of the narrow 15.5 meV peak. The energy of the 40 meV peak also shows a strong decrease with increasing temperature, which saturates to a value of 20 meV, however, its integrated intensity doubles between 2.5 and 40 K. This peak has an energy which is significantly lower than the energy of the crystal field excitations which are estimated to be around 60 meV. The temperature dependence of the energy and the intensity suggests that this peak is related to the 20 meV peak. A possible interpretation that suggests itself is that the narrow peak 15.5 meV represents an unbroadened antiparamagnon which is split off from the bottom of the Stoner continuum of spin-flip f quasi-particle excitations which peaks up at 20 meV. The temperature dependence of the energy and intensity of the 2 meV feature simply follows from the temperature dependence of the hybridization gap. The intensity of the spin exciton state should decrease and rapidly broaden as it merges with the continuum. This interpretation is consistent with the assignment made from optical conductivity of the intrinsic gap of 25 meV. The origin of the 40 meV peak is a more subtle issue, but its energy does coincide with the energy of the shoulder seen in the optical conductivity.

Inelastic neutron scattering experiments are not very effective at very low energy transfers, because of the large elastic peak due to nuclear scattering. The region of low frequency spin dynamics is more effectively probed by ac susceptibility measurements [182], and nuclear or muon magnetic resonance measurements.

4.4. *Magnetic resonance measurements*

Important information about the spectrum of magnetic excitations can also be obtained from various magnetic resonance measurements. In nuclear magnetic resonance experiments an ac magnetic field causes a resonant excitation of the nuclear spins between the nuclear Zeeman levels split by an applied static magnetic field. Two important quantities can be measured which provide information about the spectrum of magnetic excitations, the Knight shift and the nuclear magnetic relaxation rate. The Knight shift, K_s is the relative change in the nuclear magnetic resonance frequency caused by the coupling of the nuclear spins to the magnetic polarization of the electrons, via the hyperfine interaction, H_{hf}. If the electronic spin polarization dominates the polarization, the main contribution to the Knight shift is from the electronic magnetic susceptibility. Hence, one expects to find the linear relation

$$K_s(T) = \left(\frac{H_{hf}}{g\mu_B}\right) \mathrm{Re}\,[\chi^{z,z}(0,0)]. \tag{39}$$

The linearity between the susceptibility and the Knight shift can break down if the strength of the transferred hyperfine coupling to the electronic states varies, with temperature or energy.

The nuclear magnetic relaxation rate $1/T_1$ is the rate with which the z component of the nuclear magnetic moment decays, and is a measure of the fluctuations of the hyperfine field at the nuclear site. These fluctuations are driven by the spontaneous fluctuations of the electronic magnetic moments. The rate is usually given by the expression

$$\frac{1}{T_1} = 2k_B T \left(\frac{g_N \mu_N}{g\mu_B}\right)^2 \sum_q |H_{hf}(q)|^2 \,\mathrm{Im}\left[\frac{\chi^{+,-}(q,\omega_N)}{\omega_N}\right], \tag{40}$$

where $H_{hf}(q)$ is the Fourier transform of the effective field which represents the hyperfine interaction, and ω_N is the nuclear Larmor frequency which is usually much slower than the relevant electronic frequency, and thus can be set to zero. If the hyperfine interaction is approximated by a local field, then the q dependence of the hyperfine field $H_{hf}(q)$ can be neglected. The neglect of the q dependence of the hyperfine field is a good approximation for most rare earth and mixed valent systems. Furthermore, if the susceptibility is also approximated by a quasi-particle susceptibility, the relaxation rate can be reduced to an expression which is linearly proportional to the temperature and the square of the density of states at the Fermi energy, $\rho(\mu)^2$.

Nuclear quadrupole resonance (NQR) measurements are also useful as they provide information about the electric field gradient at the probing nucleus, and therefore has contributions from both the lattice and electronic charge density. The quadrupole resonance frequency is particularly sensitive to the 4f charge distribution via the direct electronic charge distribution and also through changes in the lattice constant [262].

NMR and NQR measurements have been performed on $Ce_3Bi_4Pt_3$ [263]. The Knight shift was found to be extremely anisotropic and temperature dependent. The isotropic part almost scales with the susceptibility over the entire temperature range, but the anisotropic component shows marked deviations below about $T = 80$ K. Below 80 K the linear T dependence of $1/T_1$ expected from a Korringa law fails, indicative of the gap opening up in the electronic density of states. The NQR frequency for $Ce_3Bi_4Pt_3$ is found to have a variation similar to that of $La_3B_4Pt_3$ at temperatures above 100 K, however, on decreasing the temperature the quadrupole frequency for $Ce_3Bi_4Pt_3$ shows a drop and saturates at low temperatures. After the temperature dependence of the lattice constant was taken into account, the drop is attributable to the freezing of the metallic $T^{3/2}$ contribution below 100 K.

The Knight shift of ^{29}Si in the NMR of FeSi tracks the bulk susceptibility over the temperature range 100–300 K, but the behaviour at lower temperatures becomes uncertain due to a change of line shape and the low temperature sample dependent Curie tail in the static susceptibility [264]. The relaxation rate $1/T_1$ is small and almost temperature independent for temperatures below 75 K, while the rate shows a rapid increase as the temperature is raised above 70 K. The low temperature relaxation rate was interpreted in terms of extrinsic localized states within the gap, and the rapid increase above 70 K is indicative of the fluctuating hyperfine field

induced by the spin fluctuations of the gas of thermally excited highly correlated electrons and holes.

The NMR of ^{119}Sb in CeNiSn shows a relaxation rate $1/T_1$ which starts to drop rapidly below 30 K at T^3 dependence below 1 K [81, 82], instead of the linear T dependence expected from the usual Korringa law. However, if instead of using a constant one electron density of states at the Fermi level a V-shaped density of states $\rho(\epsilon)$ which vanishes at the Fermi level, the Korringa expression

$$\frac{1}{T_1} = H_{\mathrm{hf}}^2 \int \mathrm{d}\epsilon \rho(\epsilon)^2 f(\epsilon)[1 - f(\epsilon)], \tag{41}$$

which results in a T^3 variation similar to that observed below 1 K. A similar conclusion of the inapplicability of the usual Korringa relation has been formed on the basis of electron spin resonance experiments on CeNiSn [265]. Cu substitution on the Ni sites is found to suppress the pseudogap [266]. Below $T = 0.3$ K the relaxation rate for stoichiometric crystals of CeNiSn then follows a linear T dependence which is consistent with a finite density of states at the Fermi level for both single and polycrystalline samples [94, 252]. However, neither the density of states inferred from the T^2 coefficient of the resistivity, nor that inferred from $1/T_1T$ agree [80, 252], to within an order of magnitude, with that inferred from the specific heat. The field dependence of the $1/T_1$ relaxation rate has been measured, for fields up to 11.2 T [267], and were analysed on the basis of the spin split Korringa expression,

$$\frac{1}{T_1} = H_{\mathrm{hf}}^2 T \int \mathrm{d}\epsilon \rho(\epsilon - gJ\mu_{\mathrm{B}}H)\rho(\epsilon + gJ\mu_{\mathrm{B}}H)\left[-\frac{\partial f(\epsilon)}{\partial \epsilon}\right]. \tag{42}$$

The results indicate that if the pseudogap is reduced by a Zeeman splitting of the rigid up and down spin bands, then the reduction of the gap $2g\mu_{\mathrm{B}}H$ involves a coupling of $gJ = 0.77$ instead of the values 1.29 expected from the crystal field splitting of the f electrons or the value of 1 expected from free electrons. The analysis also shows that the residual density of states within the pseudogap remains approximately constant for fields up to 2 T, and thereafter increases linearly so that the value is roughly tripled when the value of the field reaches 8 T. The measured Knight shifts on single crystals [268] were found to have the same temperature dependent anisotropy as the static susceptibility. The a-axis Knight shift tracks the a-axis susceptibility quite well, down to the lowest measured temperatures. On the other hand, the $1/T_1$ relaxation rate was found to have only a very weak anisotropy.

The temperature dependence of the ^{11}B relaxation rate in SmB_6 increases with increasing temperature above 10 K [269, 270]. The temperature dependence is exponential with an activation energy $\Delta E \approx 5.6$ meV. The rate decreases by almost two orders of magnitude between 300 K and 10 K. The relaxation rate seems to saturate at lower temperatures, however, below 10 K it also has a small sample dependent and field dependent temperature variation. Similar anomalies have been observed in the ESR spectra of SmB_6 [271]. Nevertheless, the NMR measurements clearly show the existence of a gap in the spectrum of the fluctuations of the magnetic moments of f origin.

The NMR on ^{117}Sn and ^{119}Sn in UNiSn shows a marked drop in intensity around the Néel temperature [272], where the ^{117}Sn signal is lost. The loss of intensity may be the result of the change in skin-depth occurring at the antiferromagnetic induced semiconductor–metal transition. The Knight shift shows a Curie–Weiss variation

between 300 and 52 K, and tracks the susceptibility down to 45 K. The relaxation rate $1/T_1$ decreases with decreasing temperature below 90 K, exhibits a minimum at 50 K followed by an upturn which occurs near the magnetic phase transition. Analysis based on the relation

$$1/T_1 \sim T\chi(T)/\Gamma \tag{43}$$

suggests that the relaxation rate is constant above the Néel temperature, as expected for local heavy fermion spin fluctuations, and that Γ is increased by a critical slowing down which occurs in the vicinity of the antiferromagnetic transition. The identification of the magnetic transition as being second order is in agreement with the neutron diffraction measurements of the temperature dependence of the magnetic Bragg peaks [101].

In muon spin rotation and relaxation (μSR) experiments a beam of spin polarized muons are injected into the sample and subsequently come to rest, retaining most of their initial spin orientation. The muons precess in the combined internal and external magnetic fields in the sample and are dephased by static inhomogeneities and dynamic fluctuations in the field. The muon then decays by emitting a positron in the direction of the muon spin. The time dependent asymmetry in the positron emission is then measured. Muon spin resonance experiments produce similar types of information as NMR, namely a change in the precession frequency due to the polarization of the spins in the sample, and a dephasing due to distributions of static magnetic fields and dynamically fluctuating fields. One important difference between μSR and NMR is that the muons do not reside on any well-defined lattice sites. Muons are also very sensitive to very weak magnetic correlations.

μSR measurements [273, 274] on CeNiSn indicate that as the temperature is lowered the magnetic fluctuations slow down giving rise to short-ranged correlations, but no static magnetic ordering occurs down to 10 mK. Doping studies also show that CeNiSn when doped with Pt or Cu on the Ni sites undergoes a transition to a magnetic phase [275–278], which for Pt doping is an incommensurate antiferromagnetic phase, and for Cu doping a spin-glass phase. The specific heat of the 5% Cu-doped samples shows a large low temperature C/T ratio just before the spin-glass phase occurs, as identified by μSR [83]. If this large γ value is identified with a heavy fermion mass enhancement, these experiments could be taken as indicative that CeNiSn is intrinsically a heavy fermion metal, were it not for the pseudogap in the one electron spectrum caused by the coherence of the lattice. Muon experiments [279] show that doping on the Ce sites seem to be much less effective in causing magnetic ordering. A concentration of U on the Ce sites as big as 20% is needed to produce an inhomogeneous weakly magnetic ordered state, which was previously inferred from transport properties [280].

4.5. *Photo-electron spectroscopy*

Valence band photo-emission is of great importance in determining the form of the occupied portion of the electronic density of states. In the sudden approximation and in the zero temperature limit, the valence band photo-emission spectrum is proportional to the imaginary part of the one electron Green's function, modified by photon energy dependent matrix elements related to the photon's cross-section. The imaginary part of the Green's function yields the spectral density of one electron excitations. In materials containing elements of the lanthanide series, the photo-

emission cross-section undergoes a strong absorption process $4d^{10}4f^n \rightarrow 4d^9 4f^{n+1}$ for photon energies of the order of 100 eV. The $4d^9 4f^{n+1}$ configuration subsequently decays by emitting a 4f electron. This resonantly enhances the f derived photo-emission spectrum and makes it possible to extract the partial f density of states by subtraction of the off-resonance spectrum from the on-resonance spectrum [281]. This process has been extensively used in metallic Ce compounds to deduce the portion of the f partial density of states which occurs below the Fermi energy. The f electron density of states for metallic Ce compounds, generically consists of two peaks. One broad f peak is found at an energy 2 eV below the Fermi energy and is considered to be located at the energy of the localized f level, E_f. The broadening of this f level is considered as being due to the decay of the final state f hole through the hybridization with the conduction band states, $\Delta = \pi |V|^2 \rho(E_F)$. The second f peak occurs at the Fermi energy μ, and generally has a small integrated intensity and is also relatively narrow. In angle resolved experiments, the peak at μ shows a slight dispersion in its energy and a marked periodic modulation in its intensity as the k vector is varied across successive Brillouin zones [282]. This f peak is regarded as being a coherent quasi-particle peak, the dispersion of the peak energy and the integrated intensity of the f peak closer to the Fermi level are indicators of states of itinerant character which are admixed with the localized f states. One important limitation of valence band photo-emission spectroscopy is that for the low energies, the emitted electrons originate near to the surface, and therefore this technique is extremely sensitive to the surface region and may not be representative of the bulk [283].

Valence band photo-emission experiments on the semiconducting materials should, in principle, yield a direct picture of the single electron density of states which terminates at the top of the valence band. The gap between the top of the valence band and the chemical potential is not directly observable, as the spectrum should be zero in this region for ideal materials. Therefore the gap has to be determined by comparison to a reference system with which the semiconductor is in equilibrium with. Such studies have been performed for $Ce_3Bi_4Pt_3$ [185, 284, 285] which show that the lowest binding energy peak is offset from the reference Fermi energy by an energy of roughly 20 meV, which is smaller than the experimental resolution. However, to date, clear evidence for a gap or more correctly a pseudo-gap forming in the low temperature phase has only been reported in FeSi [191, 286, 287]. The smallness of this feature, and the small value of the width of the observed pseudo-gap may be due to the surface region probed in photo-emission behaving rather differently from the bulk. Nevertheless, a strong temperature dependence has been observed in the near gap spectra of both $Ce_3Bi_4Pt_3$ [185] and FeSi [190, 191]. The degree of the temperature dependence of the photo-emission spectrum of metallic Ce heavy fermion compounds has been the subject of much controversy [282]. However, preliminary measurements on $Ce_3Bi_4Pt_3$ show one of the largest temperature dependencies observed to date [185], and is consistent with the results of theoretical studies of the lattice, as will be described later. The temperature dependence is particularly evident in the angle resolved experiments on FeSi [190], shown in figure 8. At low temperatures these measurements showed the existence of a very sharp asymmetric feature with only slight dispersion near the valence band edge. The dispersion of this feature is found to be less than 30 meV, which is significantly smaller than the calculated band widths of 200–500 meV near the top of the valence band found in electronic structure calculations. This discrepancy suggests

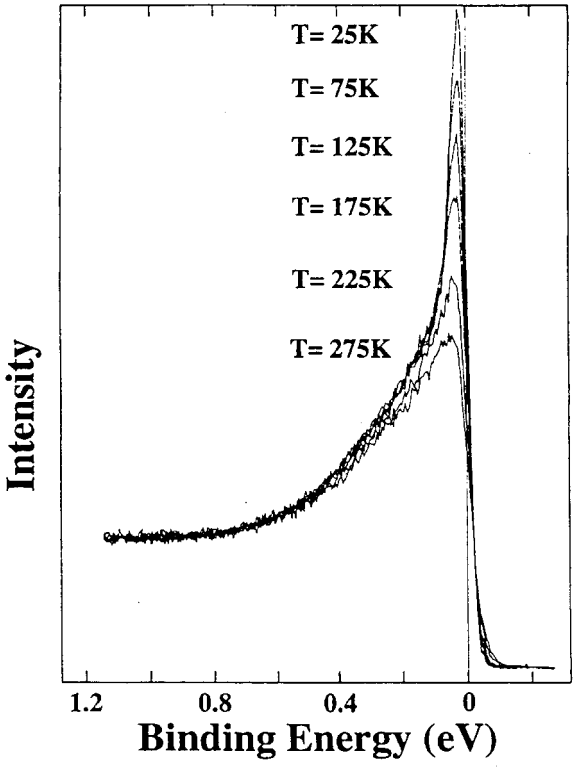

Figure 8. The temperature dependence of the angle resolved photo-emission spectrum of FeSi from reference [190]. The spectra were taken at angle $\Theta = 23$ at the temperatures $T = 25\,\mathrm{K}$ then at 75, 125, 175, 225 and 275 K.

the feature is actually a quasi-particle band that is subject to large many-body enhancements of the quasi-particle masses. The rapid broadening of the feature as the peak disperses from the top of the valence band also suggests that the width is due to strong electron–electron scattering which is suppressed for states at the top of the valence band, due to phase space limitations. The long asymmetric tail at higher binding energy is suggestive of the excitation of many final state electron–hole pairs, as expected from strongly correlated materials. As the temperature is increased from 25 to 275 K this peak rapidly broadens and loses intensity. The existence of this feature in the low temperature spectrum and its temperature dependence is consistent with the existence of a temperature dependent hybridization gap [191], and the presence of strong many-body renormalizations. The small integrated intensity of the quasi-particle feature and the existence of a large amount of incoherent scattering could be responsible for the apparent absence of structure observed in the angle integrated and polycrystalline measurements [286, 288, 289].

The very small magnitude of the pseudo-gap in CeNiSn is smaller than the current experimental resolution. Therefore, photo-emission studies do not directly yield very much information about the density of states in the low energy region [290–292]. However, measurements at $T = 20\,\mathrm{K}$ do indicate the existence of a depression in the density of states near the Fermi energy [293]. These resonant studies do confirm that the valence band does have the two characteristic f peaks

observed in many Ce compounds [282], as well as $Ce_3Bi_4Pt_3$ [185]. In CeNiSn [290] one peak is located at a binding energy of 2.7 eV below the Fermi level and is considerably broadened, while the second peak lies within 0.3 eV of the Fermi level [283]. The relatively small intensity of the 0.3 eV peak is suggestive of a small amount of mixed valent character [283]. The mixing is expected to occur both with the narrow Ni 3d band [291], that is clearly observed in the off-resonance spectra as a peak at roughly 1.5 eV below the Fermi energy, and the Sn 5p band. The on- and off-resonance spectra in the related compound CePdSn shows that the Sn 5p band stretches from binding energies of 2 eV up to the Fermi level [292]. The importance of the f hybridization with the Sn states compared to the hybridization with Ni states can be inferred from doping studies, [294, 295] where Co is substituted for 30% of the Ni atoms and the observed change in the f spectrum is minor. On the other hand the hybridization with Ni is sufficiently large to induce a small magnetic moment on the Ni site, which is observed in polarized neutron diffraction scattering [296, 297].

High resolution off-resonance photo-emission has also been carried out on CeRhSb and CeRhAs, as a function of temperature [298]. The off-resonance spectra are dominated by the conduction band density of states, and only a vestige of the sharp f peaks in the density of states can be observed. However, the raw spectrum at 13.5 K does show an anomalous depression near the Fermi energy, when compared to Au. The spectra develop asymmetrically around the Fermi energy as the temperature is decreased. The density of states obtained by dividing by an experimentally broadened Fermi function indicates that a pseudogap gradually develops in CeRhSb and CeRhAs, below the respective temperatures of 120 and 300 K. The reduction in the spectral weight occurs below the onset energies which are given, respectively, by 35 and 100 meV. These onset energies are much larger than the values of pseudogaps inferred from transport measurements. However, the depression in the density of states for CeRhAs is augmented at 13.5 K by a sharp dip of width 10 meV which is comparable to the gap of 12 meV found in transport measurements [13].

Due to the various admixtures of different ionic states of Ce in the ground state of a mixed valent compound the Ce *d* core-level photo-emission spectra should show features corresponding to the various ionic final states. Thus for Ce, one expects the initial state would correspond to an admixture of the ionic states where the f shell occupancies are predominantly composed of $4f^1$ and $4f^0$. After the d electron has been emitted from the full d^{10} shell, the final states would correspond to the ionic terms made from the ($d^9 4f^1$) and ($d^9 4f^0$) configurations. In the 3d and 4d core level spectroscopy measurements higher energies are involved than in valence band photo-emission, thus, the experiments probe deeper into the bulk. Thus, the CeNiSn d core hole spectra [290] give confirmation that the system is indeed mixed valent, but only slightly so as the number of f electrons per Ce ion is close to 1, i.e. $n_f > 0.95$ [291]. This value of n_f is quite consistent with the values found in most Ce heavy-fermion systems, and is also quite encouraging for the interpretation of CeNiSn as an asymmetric zero gap semiconductor. This is because theory implies that an approximate electron–hole symmetry should hold at high temperatures where n_f approaches 1.

The f photo-emission spectra of Yb compounds should resemble the inverse photo-emission or BIS spectra of Ce compounds, due to the approximate electron–hole symmetry associated with the filling of the f shell. However, in general, it is found that the Ce compounds have a f occupation number, n_f close to unity, while

the Yb compounds are in the mixed valent limit with the number of f holes in the range of n_f of 0.85. The valence band photo-emission measurements of poly-crystalline YbB_{12} [299] provide no exception. A broad asymmetric f peak is observed about 25 meV below the chemical potential. The inferred number of f holes puts YbB_{12} in the mixed valent regime, similar to SmB_6 [300, 301]. In the off-resonance valence band spectra there is a slight amount of missing weight near the chemical potential as referenced to Au or $Yb_{1-x}La_xB_{12}$, [300] due to the existence of the gap. The temperature dependence of the spectral weight [302] shows the gradual evolution of the depletion which starts at energies 100 meV below the reference Fermi energy. The depletion over the large energy range mainly occurs in the temperature range between 225 and 150 K. A sharp dip at μ, of width 10 meV, evolves in a lower temperature interval between 75 and 6 K. For both the two energy scales, the depletion of states with non-f character can be interpreted as being caused by the temperature dependence of an effective hybridization matrix element. The depletion over the 100 meV energy range can be interpreted as being due to the growth of the f quasi-particle peak and the level repulsion with the non-f valence band states, as found in the single impurity Anderson model. The depletion which occurs at the lower excitation energies would then be a manifestation of the hybridization gap caused by the coherence of the lattice.

5. Doping studies

Doping studies can shed light on the nature of the stoichiometric materials by allowing the magnetic and charge state to be separately varied [305]. For example, this type of approach allows one to establish that the existence of the gap depends on the coherence of the lattice. As previously mentioned, the gap in $Ce_{3-x}La_xBi_4Pt_3$ is reduced on increasing x and is due to the disturbance of the coherence of the lattice [77]. As reported in [135], the same effect is produced by the same level of doping with 7 rare earths, all of which produce the same residual value of C/T ratio. Similarly, substitution on the rare earth sites also produces a reduction of the gap and a metallic state in $Sm_{1-x}La_xB_6$ [303] and the f hole system $Yb_{1-x}Lu_xB_{12}$ [304]. However, Lu doping of YbB_{12} also produces a rapid reduction in the magnetic character of the system.

The effect of substituting Al for Si in FeSi has the effect of producing a finite density of states at the Fermi energy, as evidenced by the change in the susceptibility and specific heat. The quasi-particles introduced by doping have highly enhanced effective masses. The sign of the Seebeck coefficient indicates that the extra carriers introduced by the doping are hole-like [78]. The gap inferred from the Hall effect [145] is reduced by substituting Ge for Si, or by slightly varying the stoichiometry, thus it appears that the gap is related to the coherence of the lattice. The effect of introducing Co or Mn impurities on the Fe sites does induce magnetic ordering [306–309]. This magnetic ordering is not due to the localized transition metal impurity moments as doping FeSi with either Ru or Rh impurities, which have more delocalized d shells, also produces magnetic ordering [310]. These studies confirm that the weak nature of the magnetic interactions is intrinsic to FeSi [86], as a change in the number of d electrons systematically changes the type of the magnetic ordering from antiferromagnetic, to helical and ferromagnetic. The change in the nature of the magnetic correlations also shows up in the change in sign of the Curie–Weiss temperature of the low temperature Curie tail [308].

Studies where small concentrations of Co, Pd and Cu are substituted on the Ni sites in CeNiSn seem to indicate that the material is a compensated semi-metal. As these impurities have either, less, the same number or more electrons than Ni, the Hall coefficient may have been expected to reflect the charge of the extra holes or electrons introduced by the dopants. However, the net result [153] is that the Hall coefficient decreases for all these impurities, suggesting that the dominant effect of the impurities is the disruption of the coherence and the destruction of the pseudogap. Furthermore, the measurements also indicate that the change of electron number occurs within the f states. In fact, the disturbance of the approximate electron–hole symmetry of the parent compound by introduction of extra electrons or holes can be seen in the properties of the f electrons [94]. The increase in the number of electrons by substitution of Ni with 5% Cu does produce an instability to a magnetically ordered state [83, 94, 250], whereas the hole doping introduced by Co impurities decreases the short-ranged magnetic correlations and produces a first order valence transition [253, 254]. This suggests that the density of states is similar to a smeared version of the hybridization gap model, where the number of f electrons is close to unity and the density of states has a symmetric narrow f quasi-particle band just above and below the Fermi level. Substitution on the Ce sites by La has only a small effect on the transport properties similar to those of Co or Cu on the Ni sites [153]. Substitution of La [153, 182], tetravalent Zr [311] or U [279, 280] on the Ce sites, respectively, result in a reduction [109, 312] or increase in the magnetic character of the ground state similar to the addition of Co or Cu on the Ni sites.

The data on doped CeRhSb appears to yield similar trends, in that the addition of impurities suppresses the gap. For electron doping, the magnetic correlations are enhanced by substitution of Ni for Rh [313] and antiferromagnetic ordering occurs when Pd is substituted for Rh [314, 315]. On hole doping, by substituting La for Ce, no antiferromagnetic ordering was observed [109, 316]. However, unlike the corresponding CeNiSn case, the low temperature susceptibility of CeRhSb showed an initial enhancement for less than 10% La [109]

6. Theoretical description

The basic model that many authors have used to describe the properties of the heavy-fermion semiconductors is the Anderson lattice model. It consists of a set of localized f levels, hybridizing with a conduction band. This model is considered to provide the basic description of the electronic properties of heavy fermion materials. It can be argued, based on considerations of Luttinger's theorem, that the solution of the model at half filling is expected to exhibit an indirect gap in the density of states, where the chemical potential lies directly in the gap, making the system semiconducting. That is, if the non-interacting limit of the model contains four states per atom; two states per atom in the upper hybridized band and two states per atom in the lower hybridized band, then at half filling the two electrons per atom completely fill the doubly degenerate lower hybridized band and the non-interacting system is semiconducting. Luttinger's theorem implies that, if the interactions can be turned on adiabatically so that perturbation theory converges, the ground state of the interacting system will remain insulating.

The total Hamiltonian is written as the sum,

$$H = H_{\mathrm{f}} + H_{\mathrm{d}} + H_{\mathrm{fd}}, \tag{44}$$

where H_f is the Hamiltonian which describes the lattice of localized f electrons, H_d is the Hamiltonian describing the conduction electron states and H_{fd} describes the hybridization between the f orbitals and the conduction band. The localized electrons are both spin and orbitally degenerate, and are governed by H_f:

$$H_f = \sum_{i,\alpha} E_f f^+_{i,\alpha} f_{i,\alpha} + \sum_{i,\alpha,\beta} \frac{U_{ff}}{2} f^+_{i,\alpha} f^+_{i,\beta} f_{i,\beta} f_{i,\alpha}, \tag{45}$$

in which E_f is the binding energy of a single f electron to a lattice site, U_{ff} is the strength of the Coulomb repulsion between a pair of f electrons located on the same lattice site. The total degeneracy of each f orbital is 14 and is due to the spin and orbital degrees of freedom. However, this degeneracy may be lifted by the introduction of spin–orbit coupling and crystal field splittings, in which case the degeneracy of the lowest f multiplet may be reduced to N. We shall consider the case $N = 2$. The operators $f^+_{i,\alpha}$ ($f_{i,\alpha}$) respectively create (destroy) an f electron at site i with a combined spin–orbit label α. The summation runs over all lattice sites and all values of the degeneracy labels. The conduction electrons are described by the Hamiltonian H_d:

$$H_d = \sum_{\mathbf{k},\alpha} e_d(\mathbf{k}) d^+_{\mathbf{k},\alpha} d_{\mathbf{k},\alpha}, \tag{46}$$

where $e_d(\mathbf{k})$ is the dispersion relation for the d bands and the operators $d^+_{\mathbf{k},\alpha}$ ($d_{\mathbf{k},\alpha}$) respectively, create and annihilate an electron in the αth d sub-band state labelled by the Bloch wave vector $\mathbf{k}$. The hybridization between the f states and the states of the d band is governed by H_{fd}, where

$$H_{fd} = N_s^{-1/2} \sum_{i,\mathbf{k},\alpha} [V(\mathbf{k}) \exp(-i\mathbf{k} \cdot \mathbf{R}_i) f^+_{i,\alpha} d_{\mathbf{k},\alpha} + V^*(\mathbf{k}) \exp(i\mathbf{k} \cdot \mathbf{R}_i) d^+_{\mathbf{k},\alpha} f_{i,\alpha}]. \tag{47}$$

The first term represents a process in which a conduction electron in the Bloch state labelled by wave vector $\mathbf{k}$ hops onto the f orbital located at site i. The quantity α is conserved in this process. The second term is the Hermitean conjugate process, whereby an electron in the f orbital at site i tunnels into the conduction band state labelled by the Bloch wave vector $\mathbf{k}$. The summation runs over the total number of lattice sites, N_s and over the $\mathbf{k}$ values in the first Brillouin zone.

The non-interacting Hamiltonian, $U_{ff} \to 0$, is exactly soluble. The electronic states fall into two quasi-particle bands of mixed f and conduction band character. When the binding energy of the f levels fall within the width of the (unhybridized) conduction band, the bands are as shown in figure 9. In this case, the gap between the bands is indirect and is centred around E_f. The width of the indirect gap is found to be of the order of $2V^2/W$, where W represents about half of the total width of the conduction band, and the direct gap has a magnitude of $2V$. Each band can contain up to, at most, $2N$ electrons, so at precisely half filling the system is semiconducting. Martin and co-worker [317, 318] have argued, on the basis of Luttinger's work, that if the non-interacting system is semiconducting then the fully interacting system should also be semiconducting. Although the applicability of Luttinger's theory requires the convergence of the perturbation expansion in U_{ff}, fluctuation-exchange calculations indicate that there exists a region of convergence [319]. Furthermore, numerous other calculations [48] indicate that the conclusions of Martin and Allen may even be valid in the limit $U_{ff} \to \infty$. Ikeda and Miyake [84] use this same model

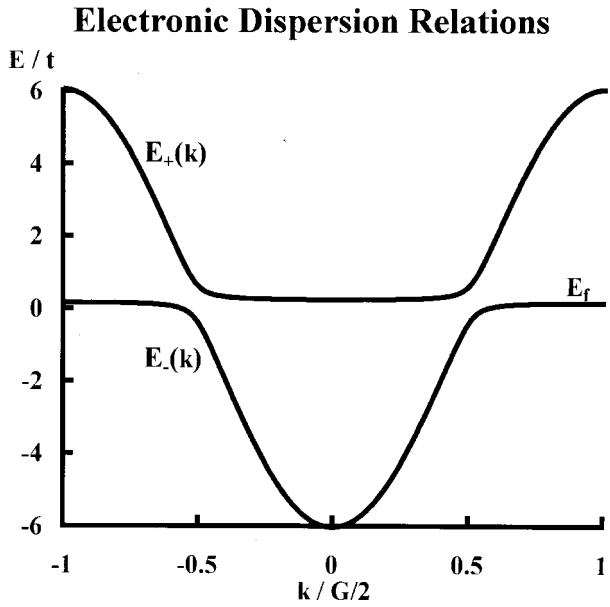

Figure 9. The hybridized band structure, for k vectors along the body diagonal of the first Brillouin zone. The dispersion relation has two branches $E_+(k)$ and $E_-(k)$, with a hybridization gap around E_f. The unhybridized conduction band is treated in the tight binding approximation and has a total width of $2W = 12t$. The indirect gap is between the zone boundary of the lower branch and the $k = 0$ state of the upper branch. The direct gap occurs for k values half-way along the body diagonal and has a magnitude of $2V$.

to treat CeNiSn, but assume that $V(\mathbf{k})$ is anisotropic and vanishes precisely along the z-axis. In their picture, this leads to CeNiSn being an anisotropic zero gap semiconductor. A closely related description of CeNiSn [320], starts from the usual picture of a Kondo insulator, but assumes that the Coulomb interactions completely suppress fluctuations of the charge distribution, represented by the charge monopole and multi-poles. This leaves three degenerate $J = 5/2$ configurations which can take part in the Kondo effect. A mean field treatment shows that interference between the sites can lead to the picture of Ikeda and Miyake, in which the hybridization vanishes along the z-axis, and becomes small near other $\mathbf{k}$ points.

6.1. *Mean-field approximation*

The simplest level of approximation to the $U_{ff} \to \infty$ limit is a mean field description which merely leads to a renormalization of the unperturbed bands. Two distinctive features of this renormalized band description are the renormalization of the hybridization matrix element from V to a reduced value of $(1 - n_f)^{1/2}V$ and the renormalization of the position of the bare f level from E_f below the chemical potential, μ, to a new position $E_f + \lambda$ which lies just above μ. The physical interpretation of the renormalization of V dates back to Gutzwiller. Gutzwiller noted that the Coulomb interaction reduces the probability of an electron hopping onto a localized f level will be reduced if the level is already occupied by one electron. Furthermore, in the $U_{ff} \to \infty$ limit, this will produce an average reduction of the hopping probability by a factor of $(1 - n_f)$. When this concept is applied to the

Anderson lattice model, it predicts the reduction of the effective hybridization matrix element which results in a further flattening of the bands near μ. The renormalization of the f level from its bare position E_f to $E_f + \lambda$ is a result of the minimization of the Coulomb interaction energy. The Coulomb interaction energy is minimized whenever it becomes improbable that there is more than one f electron per site, which can be achieved by reducing the f occupancy to a number less than unity. The resulting bands are interpreted as quasi-particle bands, and the flattening of the bands produces the enhancement of the quasi-particle masses. The renormalization of the quasi-particle mass can become quite significant in the Kondo limit, which corresponds to the position of the bare f level lying far below μ, in which case the total f occupancy is expected to be close to unity. In this case the quasi-particle bands will show f features located around the band gap. The weight associated with the f character of the quasi-particle bands is also reduced by a factor of $(1 - n_f)$. The mean field theory ignores the existence of the incoherent weight in the electronic spectrum, which could be expected to predominantly remain close to the binding energy of the bare f level.

One particular formulation of the mean-field approximation involves the slave boson technique [321]. This approach to the $U_{ff} \rightarrow \infty$ limit of the Anderson lattice model projects out the states of double f occupancy by introducing a dynamical constraint involving a slave boson field. This proceeds by replacing the f electron operators by a product of an f quasi-particle operator and a slave boson field,

$$\begin{aligned} f^+_{i,\alpha} &= \tilde{f}^+_{i,\alpha} b_i, \\ f_{i,\alpha} &= b^+_i \tilde{f}_{i,\alpha}, \end{aligned} \tag{48}$$

where the creation and annihilation operators for site i are represented by b^+_i and b_i respectively, and the f quasi-particle creation and annihilation operators are $\tilde{f}^+_{i,\alpha}$ and $\tilde{f}_{i,\alpha}$. This amounts to a projection on to the physical space for $U_{ff} \rightarrow \infty$, if these new operators satisfy the constraints

$$\sum_\alpha \tilde{f}^+_{i,\alpha} \tilde{f}_{i,\alpha} + b^+_i b_i = Q_i = 1, \quad \forall i.$$

This Hamiltonian has the same matrix elements as the initial one, as long as one stays within the manifold of states which satisfies the constraints [321, 322].

The slave boson field satisfies the equation of motion

$$i\hbar \frac{\partial}{\partial t}(b^+_i) = \lambda_i b^+_i + \frac{1}{N_s^{1/2}} \sum_{\mathbf{k},\alpha} V(\mathbf{k}) \exp[i\mathbf{k} \cdot \mathbf{R}_i] \tilde{f}^+_{i,\alpha} d_{\mathbf{k},\alpha}. \tag{49}$$

The lowest order approximation consists of only retaining the terms of zeroth order in the boson fluctuation operators B_i. If b_0 is found to be finite this will correspond to a time independent macroscopic occupation of the $k = 0$ state. This is equivalent to assuming that the boson field has undergone Bose–Einstein condensation. This implies that equation (49) becomes

$$\lambda_i b^*_0 = \frac{-1}{N_s^{1/2}} \sum_{\mathbf{k},\alpha} V(\mathbf{k}) \exp[i\mathbf{k} \cdot \mathbf{R}_i] \langle \tilde{f}^+_{i,\alpha} d_{\mathbf{k},\alpha} \rangle. \tag{50}$$

The above equation and equation (49) provide self-consistency equations from which b_0 and λ_i can be determined. In this renormalized band approximation

the Hamiltonian becomes quadratic and can be diagonalized. The fermionic Hamiltonian maps onto the non-interacting Anderson model, in which the hybridization matrix element is renormalized through

$$\tilde{V}(\mathbf{k}) = b_0 V(\mathbf{k}) \tag{51}$$

and the f level energy is also renormalized upward via

$$\tilde{E}_f = E_f + \lambda. \tag{52}$$

This moves the quasi-particle component of the f structure from the incoherent bare f level component of the density of states, to a position near the chemical potential. The quasi-particle dispersion relations are calculated as

$$E_{\pm}(\mathbf{k}) = \tfrac{1}{2}[\tilde{E}_f + e_d(\mathbf{k}) \pm ([\tilde{E}_f - e_d(\mathbf{k})]^2 + 4 \mid \tilde{V}(\mathbf{k}) \mid^2)^{1/2}]. \tag{53}$$

An interesting feature of this formulation is that the amplitude of the slave boson condensate b_0 is found to be temperature dependent, and for the semiconductor system vanishes at a critical temperature, T_c, given by [49, 323]

$$k_B T_c = 1.14W \exp\left[\frac{E_f - \mu}{N\Delta}\right], \tag{54}$$

where $\Delta = |V|^2/W$. This temperature is related to the Kondo temperature, in which the effect of both band edges are taken into consideration. The temperature dependence of the amplitude of the slave boson condensate corresponds to a temperature dependence of the indirect gap, via the renormalization factor $|b_0|^2$, and also the reduction in the f quasi-particle weight at the band edges. It is of interest to note that the activation energy observed in transport measurements shows a similar temperature dependence to the temperature dependence of the indirect gap found in the mean field approximation [136], as can be seen in figure 4. A similar non-magnetic temperature-driven metal to insulator transition has been found by a different approach [324, 325]. The slave boson mean field theory is expected to be exact in the limit that the degeneracy of the f level approaches infinity. However in order to describe the semiconducting state it is necessary to invoke spin–orbit and crystal field splittings to yield an effective degeneracy factor of only two, to obtain the observed low temperature behaviour. The convergence of the $1/N$ expansion has not been established for the Anderson lattice model. However, for the related Anderson impurity problem, the series appears to converge quite rapidly for $N = 6$, and if the series still converges for $N = 2$ then the rate of convergence appears to be slow. While that it is clear that the lower band is completely occupied for $Ce_3Bi_4Pt_3$, it is not so clear for SmB_6 where because of the multiply occupied character of the f levels, some methods of electron counting [50] lead to the conclusion that the lower band is only partially occupied.

The mean field description has been applied to the description of thermodynamic [49, 326, 327] and transport properties [323, 328] of the heavy fermion semiconductors. The temperature dependence of the electrical resistivity, Hall resistivity and thermopower have been calculated [323] using the Boltzmann equation with the mean field solution band structure and an inelastic scattering rate from random impurities. Both the resistivity and the Hall resistance were dominated by the exponential activated number of carriers, and the thermopower roughly followed

the $1/T$ relation expected for a normal semiconductor. However, the signs of the thermopower and Hall coefficient were inconsistent with a single band picture. In general, one expects that the heavier carriers should give rise to a larger contribution to S than R_H. The resistivity has also been calculated [328] for the case when the impurities are randomly substituted on the f sites. In this case, as shall be explained below, it is not sufficient to assume that the impurities do not affect the band structure. The results of the calculation of the temperature dependence of the resistivity [328], shows an exponential activated behaviour, but at very low temperatures the resistivity exhibits a maximum and then decreases towards the residual zero temperature value.

In the mean field approximation, the effect of the magnetic field is expected to give rise to a Zeeman splitting of the quasi-particle bands and hence lead to a reduction of the hybridization gap. The high field behaviour has been investigated by Saso [329] using the periodic Anderson lattice in the limit of infinite spatial dimensions, $d \to \infty$. The treatment suggests that the semiconductor-to-metal transition associated with the field induced closing of the gap may be of first order.

6.2. *The effect of impurities*

The effect of a small amount of impurities dominate the electronic properties of ordinary semiconductors at ambient temperatures; the same is true of heavy fermion semiconductors. In the heavy fermion materials, the properties associated with an uncorrelated impurity in a highly correlated and coherent host can lead to anomalies in the transport properties and has led to the concept of a 'Kondo hole' [330]. Sollie and Schlottmann [39, 40] have quantified this for the semiconductors. In this model, non-magnetic impurities substitute for the Ce sites. The f level at the impurity site is removed to high energies, thereby disrupting the coherence of the lattice. As a result of this, a bound state of mixed f and d character is produced at low temperatures. If the system has electron–hole symmetry, the spectral weight resides entirely on the neighbouring f ions. These bound states have energies equal to that of the renormalized f level, and therefore lie in the gap and pin the Fermi level. That is, the large impurity density of states stabilizes the position of the Fermi energy for a range of further doping which roughly corresponds to the number of Kondo holes. At high temperatures, where the coherence of the lattice disappears, these bound states merge into the band continuum.

A finite concentration of these impurities can lead to the formation of connected clusters of Kondo holes, which may percolate and form impurity bands. Due to the extended nature of an isolated Kondo hole the critical concentration for percolation is much smaller than for the classical percolation problem. Schlottmann has investigated the changes in the thermodynamic properties induced by the presence of Kondo hole impurity bands [41, 42, 331]. The finite concentration, c, of randomly distributed impurities was treated using the coherent potential approximation. The height and width of the impurity band were found to vary with impurity concentration as $c^{1/2}$. The impurity band gives rise to a term in the specific heat linear in T, and an additional contribution to the susceptibility which has the form of the Pauli paramagnetic susceptibility. The characteristic $c^{1/2}$ dependence has been identified in the specific heat of $Ce_3Bi_4Pt_3$ [77], and the results of this model are generally consistent with the effects of disorder in the heavy fermion semiconductors [17, 37, 38, 113, 332].

6.3. *Beyond the mean field approximation*

The mean field approximation is deficient in that it does not give rise to finite quasi-particle lifetimes, due to the neglect of the slave boson dynamics, and also does not yield collective excitations. Therefore, it is inappropriate for the description of some spectroscopies and also magnetic instabilities. The slave boson dynamics can be incorporated using the 1/N expansion techniques further developed by Millis and Lee [322]. To lowest order, the f quasi-particles become dressed by self-energy processes involving the emission and absorption of slave bosons. For the semiconducting system, the slave boson spectra exhibits a low energy gap [333] which suppresses the infrared divergence which plagues the metallic system [334]. The lifetime of a quasi-particle has the most dramatic effect on the infrared conductivity. In the mean field approximation, the optical conductivity of the pure system should correspond to $q = 0$ excitations of electrons, with d character, from the filled bands to the empty band. At zero temperature, the threshold for these direct process should correspond just to $2\tilde{V}$, which is the direct gap. This should give a square root singularity in the conductivity at threshold, however, by taking into account the emission and absorption of slave bosons [333], this square root singularity becomes smeared and develops a long tail which stretches down to the much smaller indirect gap. This process is analogous to the indirect absorption threshold in usual semiconductors, where phonons play the role of the slave bosons in assisting the indirect transitions. This interpretation leads to a different analysis of the infrared conductivity measurements, in which the assigned value of the gap would correspond to the direct gap, and the ω^2 variation below the direct gap would be attributed to the almost Fermi-liquid behaviour of the electron scattering rate. The scattering rate, and hence the intensity of the indirect absorption process should fall to zero precisely at the indirect gap. Rasul [335] has investigated the effect of impurities on the optical conductivity. His results show that the effects of impurities also produce a conductivity, $\sigma(\omega)$, that falls continuously to zero at the indirect gap, and that the spectral weight associated with the gap reappears at energies above the direct gap.

The higher order $1/N$ corrections can be used to generate spin dependent interactions between the quasi-particles [336, 337]. It has been suggested that these interactions can result in the existence of collective spin wave-like modes, even in the paramagnetic phase [49]. These excitations are not Goldstone modes as the system does not posses long-ranged magnetic order, but are due to temporal short-ranged magnetic order and are more like paramagnons. Indeed, at high excitation energies, these excitations should enter into the continuum of spin-flip electron–hole excitations and should become strongly damped. The surprising feature is that as the strength of the magnetic correlations increase, this branch of excitations should soften and fall below the threshold of electron–hole excitations, and therefore sharpen up. Although this discrete branch of spin excitations was also found for the Kondo lattice [338, 339], the discrete branch of the excitation spectra was not observed in inelastic neutron scattering experiments on $Ce_3Bi_4Pt_3$ [104]. However, this branch may have been observed in SmB_6 [194] and YbB_{12} [196]. Nevertheless, the magnetic interactions [340] should give rise to a soft Goldstone mode at magnetic instabilities. This is very appropriate as Dorin and Schlottmann [341] have analysed the finite U_{ff} limit of the model, using a different variant of the slave boson method. The results of the calculations show that the semiconductors can undergo a second order transition to an antiferromagnetic phase. The existence of antiferromagnetic correlations found by Dorin and Schlottmann is supported by the predictions of

Doniach and Fazekas [342], who find that small amounts of doping can lead to an antiferromagnetic instability. UNiSn is an example of such a semiconductor that does undergo a transition to an antiferromagnetic phase, and it might be possible to observe the softening of the discrete branch [49, 338] of the spin excitation spectrum at temperatures just above the transition temperature. One interesting question that remains open concerns why there is an apparent absence of a significant exchange interaction, $J(q)$, between the quasi-particles in materials such as $Ce_3Bi_4Pt_3$, CeNiSn and FeSi, as evidenced by the q independence of $\mathrm{Re}\,[\chi(q,\omega)]$ for small ω, while the interaction seems to be present in SmB_6 and YbB_{12}.

The incorporation of the boson dynamics is also crucial for the description of photo-emission spectra. The finite width of the main peak of the slave boson spectrum, at $\omega = \lambda$, is essential in obtaining a width of the bare f peak in the photo-emission spectrum which is similar to that of the single impurity Anderson model [343]. The temperature dependence of the integrated intensity of the quasi-particle peak situated close to the chemical potential, μ, follows from the mean field behaviour of $|b_0|^2$ similar to that shown in figure 4. However, the width of the quasi-particle peak near the gap and its unusual activated temperature dependence is a direct consequence of the emission and absorption of slave boson fluctuations. The calculations [343] also shows a small continuum structure which commences at energies slightly removed from the quasi-particle peaks. The energy offset corresponds to the minimum energy of the slave boson excitations, and the continuum spectra joins smoothly onto the incoherent bare f peak at E_f.

6.4. *Alternative approaches*

Other approaches based on an Anderson lattice model have been undertaken. One approach by Fu *et al.* [344] has used a parametrization of the Anderson lattice model based on LDA calculations [29]. The many-body effects, due to electron–electron interactions have been incorporated using second order perturbation theory, and by approximating the resulting self-energy by the expression appropriate for the limit of infinite spatial dimensions. This result does produce a temperature dependent renormalization of the gap and is consistent with the temperature dependent features seen in optical conductivity and the photo-emission spectrum. Good quantitative fits were not attained. It could be expected that inclusion of both higher order perturbation corrections and improvements to the $d \to \infty$ approximation should yield better agreement. Urasaki and Saso [200] obtained better agreement using self-consistent second order perturbation theory and the infinite dimension limit, and find a rapid filling of the gap with increasing temperature. Higher order terms in the self-energy were taken into account, albeit, with the simple two- and three-dimensional Anderson lattice model, by McQueen *et al.* [319], using the self-consistent fluctuation exchange approximation. These calculations confirmed the existence of a high temperature metallic state with no gap in the density of states, but a gap was found to open up at low temperatures. The gradual appearance of the gap was associated with the narrowing of the quasi-particle peaks in the spectral functions. Jarrell *et al.* have performed Monte Carlo calculations on the Anderson lattice model in the infinite d limit [345]. These calculations are essentially exact, and also show that a pseudogap opens up at low temperatures. However, the existence of a pseudogap, in which the density of states only shows a minimum instead of reaching zero for a finite energy range, may be traceable to the

nature of the gap in the non-interacting limit at $d \to \infty$, where the Gaussian tails and the density of states smear the gap.

Although there exist serious technical problems with trying to superimpose the solution of the single impurity Kondo model to describe the concentrated semiconducting systems [43, 45], it remains possible that the semiconductors may still be described by a periodic array of Kondo impurities. The solution of this model represents a very formidable many-body problem. Yu and White [339] have addressed a one-dimensional version of this problem using a numerical renormalization group procedure based on the density matrix and have found gaps in both the spectra of the charge and spin excitations. This work is very promising as it convincingly demonstrates that the gap remains in the lattice system, albeit a one-dimensional lattice. The results show that the system has very large antiferromagnetic correlations built into the ground state, as is commonly observed in heavy fermion systems. Furthermore, the differing value of the charge and spin gaps may be taken as an indication of spin–charge separation. Tsvelik [346] has investigated the same model using a semi-classical path integral approach. He showed that the system can have its low energy magnetic spectrum mapped onto the O(3) nonlinear sigma model. The spin excitations are massive, in agreement with the results of Yu and White [339]. Even though the characteristic energy gap, when expressed in terms of the coupling constant, has the formal appearance of the Kondo temperature, the gap is due to the antiferromagnetic coupling mediated by the conduction electrons and not to local spin screening. It remains to be seen whether these results hold for higher dimensions, where it could be expected that antiferromagnetic order is associated with the gapped phase.

Coleman *et al.* [347] have treated the $d = 3$ Kondo lattice using Majorana fermions to represent the localized spins, and found quite different results. This Majorana spin representation introduces three real component vectors at each lattice site and does not produce any states with unphysical spin properties, but is nevertheless over-complete. This over-completeness, is usually removed by enforcing a gauge condition. On performing a Hubbard–Stratonovich transformation and imposing a time independent auxiliary field they arrive at a mean field theory. This mean field theory has anomalous odd frequency pairing fields. In addition to the gapped excitations, there is a gapless branch that does not couple to charge or spin excitations for energies within the gap region. The upshot is that the properties of the mean field solution include a small linear T term for the specific heat, and a T^3 term for the NMR relaxation rate. However, the effect of the fluctuations and their interactions remain to be worked out, and could reintroduce a gap into the solution.

Since FeSi involves the partially occupied 3d shell, which is expected to be less localized than the 4f shell and also have a weaker Coulomb interaction strength, perhaps the Anderson lattice model may not form the most appropriate model to represent its properties. Several authors [29, 200, 348–352] have suggested that, for this d shell material, a spin fluctuation picture involving a more realistic band description may be a better representation.

7. Conclusions

In summary, the heavy fermion semiconductors have thermodynamic and transport properties that show a small temperature dependent gap, at low temperatures. This can be interpreted in terms of a hybridization gap model, in

which the magnitude of the indirect gap is strongly reduced from the values expected from LDA electronic structure calculations by electronic correlations. In this model, the temperature dependence is due to the many-body effects arising from the localized levels which also causes the reduction of the gap. The effects of impurities are important and are also very different from impurities in conventional semiconductors, as they can break the coherence that is responsible for the hybridization gap. In order to understand the spectroscopic properties, the effects of fluctuations and quasi-particle lifetimes have to be invoked. As a result, the properties associated with direct transitions become fluctuation assisted leading to a smaller threshold corresponding to the indirect gap. The residual interactions between the quasi-particles can result in a magnetic instability. In this situation, the magnetic excitation spectrum can exhibit a branch of collective excitations which is expected to soften at the instability, and perhaps is seen in SmB_6 [312] and YbB_{12} [196]. An ideal candidate for observation of this mode by inelastic neutron scattering could be UNiSn, which exhibits semiconducting behaviour at high temperatures but at low temperatures undergoes an antiferromagnetic phase transition and becomes metallic [18, 20]. The metallic phase occurring below the magnetic ordering temperature has planes in which the magnetic moments are aligned parallel [101, 102]. This could produce an effective ferromagnetic exchange field which might close the gap and therefore be responsible for the metal–insulator transition in UNiSn.

The physics of heavy fermion semiconductors may be considered as being relatively simple, due to the existence of gaps in the low temperature electronic and magnetic excitation spectral densities which suppresses fluctuations. In the standard description, the existence of such gaps occurs because of the assumed simple and non-degenerate nature of the (unhybridized) conduction band states in the vicinity of the gap and the condition of half filling of these bands. These are quite special and stringent conditions. One might speculate that there exist many materials in which these conditions just slightly fail to hold true, perhaps because of the existence of another band in the vicinity of the Fermi energy. In such cases, the system is not expected to have a semiconducting ground state but should be metallic instead, and as in CeNiSn in which the observed behaviour at finite temperatures is similar to that of the semiconducting compounds. This similarity may be caused by the limited phase space available for fluctuations associated with the reduced density of states near the Fermi energy. However, it is to be expected that the finite density of states will eventually drive the system to a metallic state, away from the fixed point of the semiconducting ground state. If this is the case one would be led to speculate that a reinvestigation of many of the mixed valent systems, such as $CePd_3$, may reveal that their finite temperature properties are dominated by essentially the same physics as the heavy fermion semiconductors.

Acknowledgements

I would like to acknowledge A. J. Arko, J. Cooley, Z. Fisk, M. Jarrell, J. J. Joyce, R. Modler, G. Sparn, A. Severing, J. L. Smith, T. Takabatake and J. D. Thompson for enlightening conversations. The article is dedicated to the memory of B. R. Coles who was instrumental in its inception. The work was supported by the US Department of Energy.

References

[1] AEPPLI, G., and FISK, Z., 1992, *Comments Cond. Mat. Phys.*, **16,** 155.
[2] MENTH, A., BUEHLER, E., and GEBALLE, T. H., 1969, *Phys. Rev. Lett.*, **22,** 295.
[3] KASUYA, T., TAKEGAHARA, K., FUJITA, T., and BANAI, E., 1979, *J. Phys. Coll.*, **C5,** 308.
[4] ALLEN, J. W., BATLOGG, B., and WACHTER, P., 1979, *Phys. Rev. B*, **20,** 4807.
[5] HUNDLEY, M. F., CANFIELD, P. C., THOMPSON, J. D., FISK, Z., and LAWRENCE, J. M., 1990, *Phys. Rev. B*, **42,** 6842.
[6] KASAYA, M., KATOH, K., and TAKEGAHARA, K., 1991, *Solid State Commun.*, **78,** 797.
[7] KATOH, K., and KASAYA, M., 1993, *Physica* B, **186–188,** 428.
[8] KASAYA, M., 1992, *J. phys. Soc. Jpn.*, **61,** 3841.
[9] MEISNER, G., TORIKACHVILI, M. S., YANG, K. N., MAPLE, M. B., and GUERTIN, R. P., 1985, *J. appl. Phys.*, **57,** 3073.
[10] MARTINS, G. B., PIRES, M. A., BARBERIS, G. E., RETTORI, C., and TORIKACHVILI, M. S., 1994, *Phys. Rev.* B, **50,** 14822.
[11] TAKABATAKE, T., TESHINA, F., FUJII, H., NISHIGORI, S., SUZUKI T., FUJITA, T., YAMAGUCHI, Y., SAKURAI, J., and JACAARD, D., 1990, *Phys. Rev.* B, **41,** 9607.
[12] MALIK, S. K., and ADROJA, D. T., 1991, *Phys. Rev.* B, **43,** 6277.
[13] YOSHII, S., KASAYA, M., TAKAHASHI, H., and MORI, N., 1996, *Physica* B, **223–224,** 421.
[14] KASAYA, M., IGA, F., NEGISHI, K., NAKAI, S., and KASUYA, T., 1983, *J. magn. magn. Matter*, **31–34,** 437.
[15] IGA, F., TAKAKUWA, Y., TAKAHASHI, T., KASAYA, M., KASUYA, T., and SAGAWA, T., 1984, *Solid State Commun.*, **50,** 903.
[16] TAKABATAKE, T., MIYATA, S., FUJII, H., AOKI, Y., SUZUKI, T., FUJITA, T., SAKURAI, J., and HIRAOKA, T., 1990, *J. phys. Soc. Jpn.*, **59,** 4412.
[17] CANFIELD, P. C., LACERDA, A., THOMPSON, J. D., SPARN, G., BEYERMANN, W. P., HUNDLEY, M. F., and FISK, Z., 1992, *J. Alloys Compounds*, **181,** 77.
[18] PALSTRA, T. T. M., NIEUWENHUYS, G. J., MYDOSH, J. A., and BUSCHOW, K. H. J., 1986, *J. magn. magn. Matter*, **54–57,** 549.
[19] BYKOVETZ, N., HERMAN, W. H., YUEN, T., JEE, C., LIN, C. L., and CROW, J. E., 1988, *J. appl. Phys.*, **63,** 4127.
[20] YUEN, T., LIN, C. I., SCHLOTTMANN, P., BYKOWETZ, N., PENAMBUCO-WISE, P., and CROW, J. E., 1991, *Physica* B, **171,** 362.
[21] TORIKACHVILI, M. S., ROSSEL, C., MCELFRESH, M. W., MAPLE, M. B., GUERTIN, R. P., and MEISNER, G. P., 1986, *J. magn. magn. Matter*, **54–57,** 365.
[22] TORIKACHVILI, M. S., CHEN, J. W., DALICHAOUCH, Y., GUERTIN, R. P., MCELFRESH, M. W., ROSSEL, C., MAPLE, M. B., and MEISNER, G. P., 1987, *Phys. Rev.* B, **36,** 8660.
[23] GUERTIN, R. P., ROSSEL, C., TORIKACHVILI, M. S., MCELFRESH, M. W., MAPLE, M. B., BLOOM, S. H., YAO, Y. S., KURIC, M. V., and MEISNER, G. P., 1987, *Phys. Rev.* B, **36,** 8665.
[24] NAKOTTE, H., DILLEY, N. R., TORIKACHVILI, M. S., BORDALLO, H. N., MAPLE, M. B., CHANG, S., CHRISTIANSON, A., SCHULTZ, A. J., MAJKRZAK, C. F., and SHIRANE, G., 1999, *Physica* B, **259–261,** 280.
[25] JACCARINO, V., WERTHEIM, G. K., WERNICK, J. H., and WALKER, L. R., 1967, *Phys. Rev.*, **160,** 476.
[26] TAKEGAHARA, K., HARIMA, H., KANETA, Y., and YANASE, A., 1993, *J. phys. Soc. Jpn.*, **62,** 2103.
[27] YANASE, A., and HARIMA, H., 1992, *Prog. Theor. Phys.*, **108,** 19.
[28] MATHEISS, L. F., and HAMMAN, D. R., 1993, *Phys. Rev.* B, **47,** 13114.
[29] FU, C., KRIJN, M. P. C. M., and DONIACH, S., 1994, *Phys Rev.* B, **49,** 2219.
[30] HAMMOND, T. J., GEHRING, G. A., SUVASINI, M. B., and TEMMERMAN, W. M., 1995, *Phys. Rev.* B, **51,** 2994.
[31] GALAKHOV, V. R., KURMAEV, E. Z., CHERKASHENKO, V. M., YARMOSHENKO, YU. M., SHAMIN, S. N., POSTNIKOV, A. V., UHLENBROCK, ST., NEUMANN, M., LU, Z. W., KLEIN, B. M., and SHI, Z.-P., 1995, *J. Phys. condens. Matter*, **7,** 5529.
[32] ANISIMOV, V. I., EZHOV, S. YU., ELFIMOV, I. S., SOLOVYEV, I. V., and RICE, T. M., 1996, *Phys. Rev. Lett.*, **76,** 1735.

[33] ALBERS, R. C., BORING, A. M., DAALDEROP, G. H. O., and MUELLER, F. M., 1987, *Phys. Rev.* B, **36,** 3661.
[34] ERIKSSON, O., ALBERS, R. C., and BORING, A. M., 1991, *Phys. Rev.* B, **43,** 5649.
[35] OPPENEER, P., YARESKO, A. N., PERLOV, A. YA., ANTONOV, V. N., and ESCHRIG, H., 1996, *Phys. Rev.* B, **54,** 3706.
[36] CANFIELD, P. C., THOMPSON, J. D., FISK, Z., HUNDLEY, M. F., and LACERDA, A., 1992, *J. magn. magn. Matter*, **108,** 217.
[37] HUNDLEY, M. F., CANFIELD, P. C., THOMPSON, J. D., FISK, Z., and LAWRENCE, J. M., 1991, *Physica* B, **171,** 254.
[38] IGA, F., KASAYA, M., and KASUYA, T., 1988, *J. magn. magn. Matter*, **76–77,** 156.
[39] SOLLIE, R., and SCHLOTTMANN, P., 1991, *J. appl. Phys.*, **69,** 5478.
[40] SOLLIE, R., and SCHLOTTMANN, P., 1991, *J. appl. Phys.*, **70,** 5803.
[41] SCHLOTTMANN, P., 1992, *Phys. Rev.* B, **46,** 998.
[42] SCHLOTTMANN, P., 1993, *Physica* B, **186–188,** 375.
[43] NOZIERES, P., 1985, *Ann. Phys.* (Paris), **10,** 19.
[44] SASO, T., and OGURA, J., 1993, *Physica* B, **186–188,** 372.
[45] JONES, B. A., VARMA, C. M., and WILKINS, J. W., 1988, *Phys. Rev. Lett.*, **61,** 125.
[46] LEE, P. A., RICE, T. M., SERENE, J. W., SHAM, L. J., and WILKINS, J. W., 1986, *Comments Cond. Mat. Phys.*, **3,** 99.
[47] MOTT, N. F., 1973, *Phil. Mag.*, **30,** 403.
[48] VARMA, C. M., and YAFFET, Y., 1976, *Phys. Rev.* B, **13,** 2950.
[49] RISEBOROUGH, P. S, 1992, *Phys. Rev.* B, **45,** 13984.
[50] COLES, B. R., 1997, *Physica* B, **230–232,** 718.
[51] KASUYA, T., 1994, *Europhys. Lett.*, **26,** 277.
[52] KASUYA, T., 1994, *Europhys. Lett.*, **26,** 283.
[53] KASUYA, T., 1996, *Physica* B, **223–224,** 402.
[54] HOCHST, H., TAN, K., and BUSCHOW, K. H. J., 1986, *J. magn. magn. Matter*, **54–57,** 545.
[55] PALSTRA, T. T. M., NIEUWENHUYS, G. J., VLASTUIN, R. F. M., VAN DEN BERG, J., and MYDOSH, J. A., 1987, *J. magn. magn. Matter*, **67,** 331.
[56] PALSTRA, T. T. M., NIEUWENHUYS, G. J., VLASTUIN, R. F. M., MYDOSH, J. A., and BUSCHOW, K. H. J., 1988, *J. appl. Phys.*, **63,** 4279.
[57] LAWRENCE, J. M., RISEBOROUGH, P. S., and PARKS, R. D., 1981, *Rep. Prog. Phys.*, **44,** 1.
[58] MIHALASIN, T., SCOBORIA, P., and WARD, J. A., 1981, *Valence Fluctuations in Solids*, edited by L. M. Falicov, W. Hanke and M. B. Maple (Amsterdam: North Holland).
[59] SCOBORIA, P., CROW, J. E., and MIHALASIN, T., 1979, *J. appl. Phys.*, **50,** 1859.
[60] LAWRENCE, J. M. , THOMPSON, J. D., and CHEN, Y. Y., 1985, *Phys. Rev. Lett.*, **54,** 2537.
[61] CATTANEO, E., HAFNER, U., and WOHLLEBEN, D., 1982, *Valence Instabilities*, edited by P. Wachter and H. Boppart (Amsterdam: North Holland); 1986, *Z. Phys.* B, **64,** 305.
[62] PINKERTON, F. E., WEBB, B. C., SIEVERS, A. J., WILKINS, J. W., and SHAM, L. J., 1984, *Phys. Rev.* B, **30,** 3068.
[63] WEBB, B. C., SIEVERS, A. J., and MIHALASIN, T., 1986, *Phys. Rev. Lett.*, **57,** 1951.
[64] BEYERMANN, W. P. , GRUNER, G. , DALICHAOUCH, Y., and MAPLE, M. B., 1988, *Phys. Rev. Lett.*, **60,** 216.
[65] AWASTHI, A., BEYERMANN, W. P., CARINI, J. P., and GRUNER, G., 1989, *Phys. Rev.* B, **39,** 2377.
[66] BUCHER, B., SCHLESINGER, Z., MANDRUS, D., FISK, Z., SARRAO, J., DITUSA, J. F., OGELSBY, C., AEPPLI, G., and BUCHER, E., 1996, *Phys. Rev.* B, **53,** 2948
[67] HOLLAND-MORITZ, E., LOWENHAUPT, M., SCHAMTZ, W., and WOHLLEBEN, D. K., 1977, *Phys. Rev. Lett.*, **38,** 983.
[68] SHAPIRO, S. M., STASSIS, C., and AEPPLI, G., 1989, *Phys. Rev. Lett.*, **62,** 94.
[69] SEVERING, A., and MURANI, A. P., 1990, *Physica* B, **163,** 699.
[70] MURANI, A. P., SEVERING, A., and MARSHALL, W. G., 1996, *Phys. Rev.* B, **53,** 2641.
[71] MURANI, A. P., RAPHAEL, R., BOWDEN, Z. A., and ECCLESTON, R. S., 1996, *Phys. Rev.* B, **53,** 8188.
[72] SCHAFER, H., and ELSCHNER, B., 1983, *Z. Phys.* B, **53,** 109.

[73] TAILLEFER, L., NEWBURY, R., LONZARICH, G. G., FISK, Z., and SMITH, J. L., 1987, *J. magn. magn. Matter*, **63–64,** 372.
[74] STEWART, G. R., FISK, Z., WILLIS, J. O., and SMITH, J. L., 1984, *Phys. Rev. Lett.*, **52,** 679.
[75] DONIACH, S., and ENGELSBERG, S., 1966, *Phys. Rev. Lett.*, **17,** 750.
[76] BROWN, S. E., private communication.
[77] HUNDLEY, M. F., CANFIELD, P. C., THOMPSON, J. D., and FISK, Z., 1994, *Phys. Rev* B, **50,** 18142.
[78] DITUSA, J. F., FRIEMELT, K., BUCHER, E., AEPPLI, G., and RAMIREZ, A. P., 1997, *Phys. Rev. Lett.*, **78,** 2831.
[79] TAKABATAKE, T., NAGASAWA, M., FUJII, H., KIDO, G., NOHARA, M., NISHIGORI, S., SUZUKI, T., FUJITA, T., HELFRISCH, R., AHLHEIM, U., FRAAS, K., GEIBEL, C., and STEGLICH, F., 1992, *Phys. Rev.* B, **45,** 5740.
[80] NAKAMOTO, G., TAKABATAKE, T., FUJII, H., MINAMI, A., MAEZAWA, K., OGURA, I., and MENOVSKY, A. A., 1995, *J. phys. Soc. Jpn.*, **64,** 4834.
[81] KYOGAKU, M., KITAOKA, Y., NAKAMURA, H., ASAYAMA, K., TAKABATAKE, T., TESHIMA, F., and FUJII, H., 1990, *J. phys. Soc. Jpn.*, **59,** 1728.
[82] KYOGAKU, M., KITAOKA, Y., NAKAMURA, H., ASAYAMA, K., TAKABATAKE, T., and FUJII, H., 1991, *Physica* B, **171,** 235.
[83] BRUCKL, A., NEUMAIER, K., PROBST, CH., ANDRES, K., FLASCHIN, S. J., KRATZER, A., KALVIUS, G. M., and TAKABATAKE, T., 1997, *Physica* B, **240,** 199.
[84] IKEDA, H., and MIYAKE, K., 1996, *J. phys. Soc. Jpn.*, **65,** 1769.
[85] SATO, T., KADOWAKI, H., YOSHIZAWA, H., EKINO, T., TAKABATAKE, T., FUJII, H., REGNAULT, L. P., and ISIKAWA, Y., 1995, *J. Phys. condens. Matter*, **7,** 8009.
[86] MASON, T. E., AEPPLI, G., RAMIREZ, A. P., CLAUSEN, K. N., BROHOLM, C., STUECHLI, N., BUCHER, E., and PALSTRA, T. T. M., 1992, *Phys. Rev. Lett.*, **69,** 490.
[87] TAKABATAKE, T., NAGASAWA, M., FUJII, H., KIDO, G., SUGIYAMA, K., SENDA, K., KINDO, K., and DATE, M., 1992, *Physica* B, **177,** 177.
[88] IZAWA, K., SUZUKI, T., KITAMURA, M., FUJITA, T., TAKABATAKE, T., NAKAMOTO, G., FUJII, H., and MAEZAWA, K., 1996, *J. phys. Soc. Jpn.*, **65,** 3119.
[89] IZAWA, K., SUZUKI, T., KITAMURA, M., FUJITA, T., TAKABATAKE, T., NAKAMOTO, G., and FUJII, H., 1997, *Physica* B, **230–232,** 670.
[90] IZAWA, K., SUZUKI, T., KITAMURA, M., FUJITA, T., TAKABATAKE, T., NAKAMOTO, G., FUJII, H., and MAEZAWA, K., 1998, *J. magn. magn. Matter*, **177–181,** 395.
[91] IZAWA, K., SUZUKI, T., KITAMURA, M., FUJITA, T., TAKABATAKE, T., NAKAMOTO, G., FUJII, H., and MAEZAWA, K., 1999, *Phys. Rev.* B, **59,** 2599.
[92] NISHIGORI, S., SUZUKI, T., FUJITA, T., TANAKA, H., TAKABATAKE, T., and FUJII, H., 1994, *Physica* B, **199–200,** 473.
[93] TAKABATAKE, T., TANAKA, H., BANDO, Y., FUJII, H., NISHIGORI, S., SUZUKI, T., FUJITA, T., and KIDO, G., 1994, *Phys. Rev.* B, **50,** 623.
[94] NAKAMURA, K., KITAOKA, Y., ASAYAMA, K., TAKABATAKE, T., TANAKA, H., and FUJII, H., 1994, *J. phys. Soc. Jpn.*, **63,** 433.
[95] NISHIGORI, S., SUZUKI, T., FUJITA, T., TANAKA, H., TAKABATAKE, T., and FUJII, H., 1996, *J. phys. Soc. Jpn.*, **65,** 2614.
[96] TAKABATAKE, T., NAKOMOTO, G., YOSHINO, T., FUJII, H., IZAWA, K., NISHIGORI, S., GOSHIMA, H., SUZUKI, T., FUJITA, T., MAEZAWA, K., HIRAOKA, T., OKAYAMA, Y., OGURA, I., MENOVSKY, A. A., NEUMAIER, K., BRUCKL, A., and ANDRES, K., 1996, *Physica* B, **223–224,** 413.
[97] MALIK, S. K., MENON, L., PECHARSKY, V. K., and GSCHNEIDNER JR, K. A., 1997, *Phys. Rev.* B, **55,** 11471.
[98] AOKI, Y., SUZUKI, T., FUJITA, T., KAWANAKA, H., TAKABATAKE, T., and FUJII, H., 1990, *J. magn. magn. Matter*, **90–91,** 496.
[99] AOKI, Y., SUZUKI, T., FUJITA, T., KAWANAKA, H., TAKABATAKE, T., and FUJII, H., 1993, *Phys. Rev.* B, **47,** 15060.
[100] FUJII, H., TAKABATAKE, T., SUZUKI, T., FUJITA, T., SAKURAI, J., and SECHOVSKY, V., 1993, *Physica* B, **192,** 219.
[101] KAWANAKA, H., FUJII, H., NISHI, M., TAKABATAKE, T., MOTOYA, K., UWATOKO, Y., and ITOH, Y., 1989, *J. phys. Soc. Jpn.*, **58,** 3481.

[102] YETHIRAJ, M., ROBINSON, R. A., RHYNE, J. J., GOTAAS, J. A., and BUSCHOW, K. H. J., 1989, *J. magn. magn. Matter*, **79,** 355.
[103] FUJII, H., KAWANAKA, H., TAKABATAKE, T., SUGIURA, E., SUGIYAMA, K., and DATE, M., 1990, *J. magn. magn. Matter*, **87,** 235.
[104] SEVERING, A., THOMPSON, J. D., CANFIELD, P. C., FISK, Z., and RISEBOROUGH, P. S., 1991, *Phys Rev.* B, **44,** 6832.
[105] FISK, Z., private communication.
[106] MANDRUS, D., SARRAO, J. L., MIGLIORI, A., THOMPSON, J. D., and FISK, Z., 1995, *Phys. Rev.* B, **51,** 4763.
[107] ARUSHANOV, E., RESPAUD, M., BROTO, J. M., LEOTIN, J., ASKENAZY, S., KLOC, CH., BUCHER, E., and LISUNOV, K., 1997, *Phys. Rev.* B, **55,** 8056.
[108] ANDRAKA, B., 1994, *Phys. Rev.* B, **49,** 348.
[109] ADROJA, D. T., RAINFORD, B. D., NEVILLE, A. J., MANDAL, P., and JANSEN, A. G. M., 1996, *J. magn. magn. Matter*, **161,** 157.
[110] KASUYA, T., KOJIMA, K., and KASAYA, M., 1977, *Valence Instabilities and Related Narrow Band Phenomena*, edited by R. D. Parks (New York: Plenum), p. 137.
[111] IGA, F., KASAYA, M., and KASUYA, T., 1985, *J. magn. magn. Matter*, **52,** 279.
[112] IGA, F., SHIMIZU, N., and TAKABATAKE, T., 1988, *J. magn. magn. Matter*, **177–181,** 337.
[113] KASAYA, M., IGA, F., TAKIGAWA, M., and KASUYA, T., 1985, *J. magn. magn. Matter*, **47–48,** 429.
[114] FUJII, H., KAWANAKA, H., TAKABATAKE, T., KURISU, M., YAMAGUCHI, Y., SAKURAI, J., FUJIWARA, H., FUJITA, T., and OGURO, I., 1989, *J. phys. Soc. Jpn.*, **58,** 2495.
[115] KWEI, G. H., LAWRENCE, J. M., CANFIELD, P. C., BEYERMANN, W. P., THOMPSON, J. D., FISK, Z., LAWSON, A. C., and GOLDSTONE, J. A., 1992, *Phys. Rev.* B, **46,** 8067.
[116] TAKKE, R., NIKSCH, M., ASSMUS, W., LUTHI, B., POTT, R., SCHEFZYK, R., and WOHLLEBEN, D. K., 1981, *Z. Phys.* B, **44,** 33.
[117] KAISER, A. B., and FULDE, P., 1988, *Phys. Rev.* B, **37,** 5357.
[118] FISK, Z., CANFIELD, P. C., THOMPSON, J. D., and HUNDLEY, M. F., 1992, *J. Alloys Compounds*, **181,** 369.
[119] KWEI, G. H., LAWRENCE, J. M., and CANFIELD, P. C., 1994, *Phys. Rev.* B, **49,** 14708.
[120] MANDRUS, D., SARRAO, J. L., THOMPSON, J. D., HUNDLEY, M. F., MIGLIORI, A., and FISK, Z., 1994, *Physica* B, **199–200,** 471.
[121] SARRAO, J. L., MANDRUS, D., MIGLIORI, A., FISK, Z., and BUCHER, E., 1994, *Physica* B, **199–200,** 478.
[122] UWATOKO, Y., OOMI, G., TAKABATAKE, T., TESHIMA, F., and FUJII, H., 1991, *J. Jpn. Inst. Met.*, **6,** 135.
[123] UWATOKO, Y., OOMI, G., TAKABATAKE, T., and FUJII, H., 1992, *J. magn. magn. Matter*, **104–107,** 643.
[124] HOLTMEIER, S., HAEN, P., and ISIKAWA, Y., 1996, *Physica* B, **223–224,** 429.
[125] HOLTMEIER, S., HINKLE, C., AIGNER, M., BRULS, G., FINSTERBUSCH, D., WOL, B., ASSMUS, W., and LUTHI, B., 1997, *Physica* B, **230–232,** 658.
[126] SUZUKI, T., NOHARA, M., FUJISAKI, H., FUJITA, T., NAGASAWA, M., TAKABATAKE, T., and FUJII, H., 1992, *J. magn. magn. Matter*, **104–107,** 1293.
[127] TARASCON, J. M., ISIKAWA, Y., CHEVALIER, B., ETOURNEAU, J., HAGENMULLER, P., and KASAYA, M., 1980, *J. Phys.* (Paris), **41,** 1145.
[128] ALEKSEEV, P. A., IVANOV, A. S., DORNER, B., KIKOIN, K. A., MISCHENKO, A. S., LAZUKOV, V. N., KONOVALOVA, E. S., PADERNO, YU. B., RUMYANTSEV, A. YU., and SADIKOV, I. P., 1989, *Europhys. Lett.*, **10,** 457.
[129] H. E. KING JR, S. J. LA PLACA. T. PENNEY, and Z. FISK, 1981, *Valence Fluctuations in Solids*, edited by L. M. Falicov, W. Hanke and M. B. Maple (Amsterdam: North Holland), p. 333.
[130] NAKAMURA, S., GOTO, T., TAMAKI, A., KUNII, S., IWASHITA, K., and KASAYA, M., 1993, *Physica* B, **186–188,** 627.
[131] NAKAMURA, S., GOTO, T., KASAYA, M., and KUNII, S., 1991, *J. phys. Soc. Jpn.*, **60,** 4311.

[132] SUZUKI, T., AKAZAWA, T., NAKAMAURA, F., TANAKA, Y., FUJISAKI, H., AONO, S., FUJITA, T., TAKABATAKE, T., and FUJII, H., 1994, *Physica* B, **199–200,** 483.
[133] FUJITA, T., AKAZAWA, T., GOSHIMA, H., TAHARA, T., SUZUKI, T., TAKABATAKE, T., and FUJII, H., 1998, *Physica* B, **246–247,** 445.
[134] AKAZAWA, T., SUZUKI, T., NAKAMURA, F., FUJITA, T., TAKABATAKE, T., and FUJII, H., 1996, *J. phys. Soc. Jpn.*, **65,** 3661.
[135] THOMPSON, J. D., BEYERMANN, W. P., CANFIELD, P. C., FISK, Z., HUNDLEY, M. F., KWOK, G. H., LACERDA, A., LAWRENCE, J. M., and SEVERING, A., 1993, *Proceedings of the Hiroshima Workshop on f Electron Systems*, edited by H. Fujii, T. Fujita and G. Oomi (New York: Plenum) p. 35.
[136] HUNDLEY, M. F., THOMPSON, J. D., CANFIELD, P. C., and FISK, Z., 1994, *Physica* B, **199–200,** 443.
[137] COOLEY, J. C., ARONSON, M. C., and CANFIELD, P. C., 1997, *Phys. Rev.* B, **55,** 7533.
[138] HUNDLEY, M. F., LACERDA, A., CANFIELD, P. C., THOMPSON, J. D., and FISK, Z., 1993, *Physica* B, **186–188,** 425.
[139] TAKABATAKE, T., IGA, F., YOSHINO, T., ECHIZEN, Y., KATOH, K., KOBAYASHI, K., HIGA, M., SHIMIZU, N., BANDO, Y., NAKAMOTO, G., FUJII, H., IZAWA, K., SUZUKI, T., FUJITA, T., SERA, M., HIROI, M., MAEZAWA, K., MOCK, S., LOHNEYSEN, H. V., BRUCKL, A., NEUMAIER, K., and ANDERS, K., 1998, *J. magn. magn. Matter*, **171–181,** 277.
[140] SALES, B. C., JONES, E. C., CHAMOUKOS, B. C., FERNANDEZ-BACA, J. A., HARMON, H. E., SHARP, J. W., and VOLKMANN, E. H., 1994, *Phys. Rev.* B, **50,** 8207.
[141] HUNT, M. B., CHERNIKOV, M. A., FELDER, E., OTT, H. R., FISK, Z., and CANFIELD, P. C., 1994, *Phys. Rev.* B, **50,** 14933.
[142] LUNKENHEIMER, P., KNEBEL, G., VIANA, R., and LOIDL, A., 1995, *Solid State Commun.*, **93,** 891.
[143] LISUNOV, K. G., ARUSHANOV, E. K., KLOC, CH., BROTO, J., LEOTIN, J., ROKOTO, H., RESPAUD, M., and BUCHER, E., 1996, *Physica* B, **229,** 37.
[144] FREIMELT, K., DITUSA, J. F., BUCHER, E., and AEPPLI, G., 1996, *Ann. Phys.*, **5,** 175.
[145] BUSCHINGER, B., GEIBEL, C., STEGLICH, F., MANDRUS, D., YOUNG, D., SARRAO, J. L., and FISK, Z., 1997, *Physica* B, **230–232,** 784.
[146] PASCHEN, S., FELDER, E., CHERNIKOV, M. A., DEGIORGI, L., SCHWER, H., and OTT, H. R., 1997, *Phys. Rev.* B, **56,** 12916.
[147] KURISU, M., TAKABATAKE, T., and FUJIWARA, M., 1988, *Solid State Commun.*, **65,** 595.
[148] KURISU, M., TAKABATAKE, T., and FUJII, H., 1992, *Proceedings of the Hiroshima Workshop on Transport and Thermal Properties of f Electron Systems*, Hiroshima, edited by H. Fujii, T. Fujita and G. Oomi (New York: Plenum).
[149] HIRAOKA, T., KINOSHITA, E., TAKABATAKE, T., TANAKA, H., and FUJII, H., 1994, *Physica* B, **199–200,** 440.
[150] YAMAGUCHI, Y., SAKURAI, J., TESHIMA, F., KAWANAKA, H., TAKABATAKE, T., and FUJII, H., 1990, *J. Phys. condens. Matter*, **2,** 5715.
[151] TAKABATAKE, T., and FUJII, H., 1992, *Jpn. J. appl. Phys.*, **8,** 86.
[152] TAKABATAKE, T., NAGASAWA, M., FUJII, H., NOHARA, M., SUZUKI, T., FUJITA, T., KIDO, G., and HIRAOKA, T., 1992, *J. magn. magn. Matter*, **108,** 155.
[153] ECHIZEN, Y., and TAKABATAKE, T., 1999, *Physica* B, **259–261,** 292.
[154] KOBAYASHI, K., TAKABATAKE, T., NAKOMOTO, G., HIGA, M., YOSHINO, T., FUJII, H., and SERA, M., 1997, *Physica* B, **230–232,** 676.
[155] SHIBAUCHI, T., KATASE, N., TAMEGAI, T., UCHINOKURA, K., TAKABATAKE, T., NAKOMOTO, G., and MENOVSKY, A. A., 1997, *Phys. Rev.* B, **56,** 8277.
[156] INADA, Y., AZUMA, H., SETTAI, R., AOKI, D., ONUKI, Y., KOBAYASHI, K., TAKABATAKE, T., NAKOMOTO, G., FUJII, H., and MAEZAWA, K., 1996, *J. phys. Soc. Jpn.*, **65,** 1158.
[157] SUGIYAMA, K., FUJITA, M., KINDO, K., NAKOMOTO, G., KOBAYASHI, K., TAKABATAKE, T., and FUJII, H., 1997, *Physica* B, **230–232,** 683.
[158] INADA, Y., ISHIDA, T., AZUMA, H., AOKI, D., SETTAI, R., ONUKI, Y., KOBAYASHI, K., TAKABATAKE, T., NAKOMOTO, G., FUJII, H., and MAEZAWA, K., 1997, *Physica* B, **230–232,** 690.

[159] ADROJA, D., and RAINFORD, B., 1994, *J. magn. magn. Matter*, **135,** 333.
[160] UWATOKO, Y., ISHII, T., OOMI, G., TAKAHASHI, H., MORI, N., THOMPSON, J. D., SHERO, J. L., MANDRUS, D., and FISK, Z., 1996, *J. phys. Soc. Jpn.*, **65,** 27.
[161] HIRAOKA, T., OKAYAMA, Y., YOSINO, N., TAKABATAKE, T., and FUJII, H., 1996, *Physica* B, **223–223,** 441.
[162] HIRAOKA, T., KINOSHTA, E., TANAKA, H., TAKABATAKE, T., and FUJII, H., 1996, *J. magn. magn. Matter*, **153,** 124.
[163] NICKERSON, J. C., WHITE, R. M., LEE, K. N., BACHMAN, R., GEBALLE, T. H., and HULL JR, G. W., 1971, *Phys. Rev.* B, **3,** 2030.
[164] BEILLE, J., MAPLE, M. B., WITTIG, J., FISK, Z., and DELONG, L. E., 1983, *Phys. Rev.* B, **28,** 7397.
[165] COOLEY, J. C., ARONSON, M. C., FISK, Z., and CANFIELD, P. C., 1995, *Phys. Rev. Lett.*, **74,** 1629.
[166] COOLEY, J. C., ARONSON, M. C., LACERDA, A., FISK, Z., CANFIELD, P. C., and GUERTIN, R. P., 1995, *Phys. Rev.* B, **52,** 7322.
[167] KEBEDE, A., ARONSON, M. C., BUFORD, C. M., CANFIELD, P. C., JIN HYUNG CHO, COLES, B. R., COOLEY, J. C., COULTER, J. Y., FISK, Z., GOETTEE, J. D., HULTS, W. L., LACERDA, A., MCLENDON, T. D., TIWARI, P., and SMITH, J. L., 1996, *Physica* B, **223–223,** 256.
[168] TANAKA, T., NISHITANI, R., OSHIMA, C., BANNAI, E., and KAWAI, S., 1980, *J. appl. Phys.*, **51,** 3877.
[169] ROMAN, J., PAVLIK, V., FLACHBART, K., HERRMANNSDORFER, TH., REHMANN, S., KONOVALOVA, E. S., and PADERNO, YU. B., 1997, *Physica* B, **230–232,** 715.
[170] BATKO, I., FARKASOVSKY, P., FLACHBART, K., KONOVALOV, E. S., and PADERNO, YU. B., 1993, *Solid State Commun.*, **88,** 405.
[171] COOLEY, J. C., private communication.
[172] COOLEY, J. C., ARONSON, M. C., FISK, Z., and CANFIELD, P. C., 1994, *Physica* B, **199–200,** 486.
[173] LACERDA, A., RICKEL, D., HUNDLEY, M. F., CANFIELD, P. C., THOMPSON, J. D., FISK, Z., HAEN, P., and LAPIERRE, F., 1994, *Physica* B, **199–200,** 469.
[174] COOLEY, J. C., ARONSON, M. C., LACERDA, A., CANFIELD, P. C., FISK, Z., and GUERTIN, R. P., 1995, *Physica* B, **206–207,** 377.
[175] IGA, F., KASAYA, M., SUZUKI, H., OKAYAMA, Y., TAKAHASHI, H., and MORI, N., 1993, *Physica* B, **186–188,** 419.
[176] SUGIYAMA, K., OHYA, A., DATE, M., IGA, F., KASAYA, M., and KASUYA, T., 1985, *J. magn. magn. Matter*, **52,** 283.
[177] SUGIYAMA, K., IGA, F., KASAYA, M., KASUYA, T., and DATE, M., 1988, *J. phys. Soc. Jpn.*, **57,** 3946.
[178] SUGIYAMA, K., and DATE, M., 1989, *Physica* B, **155,** 253.
[179] DIEHL, J., FISCHER, H., KOEHLER, R., GEIBEL, C., STEGLICH, F., MAEDA, Y., TAKABATAKE, T., and FUJII, H., 1993, *Physica* B, **186–188,** 708.
[180] ISIKAWA, Y., MORI, K., OGISO, Y., OYABE, K., and SATO, K., 1991, *J. phys. Soc. Jpn.*, **60,** 2514.
[181] SERA, M., KOBAYASHI, N., YOSHINO, T., KOBAYASHI, K., TAKABATAKE, T., NAKOMOTO, G., and FUJII, H., 1997, *Phys. Rev.* B, **55,** 6421.
[182] ALIEV, F. G., VILLAR, R., VIEIRA, S., LOPEZ DE LA TORRE, M. A., SCOLOZDRA, R. V., and MAPLE, M. B., 1993, *Phys. Rev.* B, **47,** 769.
[183] BUCHER, B., SCHLESINGER, Z., CANFIELD, P. C., and FISK, Z., 1994, *Phys. Rev. Lett.*, **72,** 522.
[184] SEVERING, A., PERRING, T., THOMPSON, J. D., CANFIELD, P. C., and FISK, Z., 1994, *Physica B*, **199–200,** 480.
[185] ARKO, A. J., private communication.
[186] KILIBARDA-DALAFAVE, S., NG, H. K., YUEN, T., LIN, C. L., CROW, J. E., and TANNER, D. B., 1993, *Phys. Rev.* B, **48,** 297.
[187] SCHLESINGER, Z., FISK, Z., ZHANG, H.-T., MAPLE, M. B., DITUSA, J., and AEPPLI, G., 1993, *Phys. Rev. Lett.*, **71,** 1748.
[188] SHIRANE, G., FISCHER, J. E., ENDOH, Y., and TAJIMA, K., 1987, *Phys. Rev. Lett.*, **59,** 351.

[189] TAJIMA, K., ENDOH, Y., FISCHER, J., and SHIRANE, G., 1988, *Phys. Rev.* B, **38,** 6954.
[190] PARK, C., SHEN, Z. X., LOESER, A. G., DESSAU, D. S., MANDRUS, D. G., MIGLIORI, A., SARRAO, J. L., and FISK, Z., 1995, *Phys. Rev.* B, **52,** 16981.
[191] BREUER, K., MESSERLI, S., PURDIE, D., GARNIER, M., HENGSBERGER, M., BAER, Y., and MIHALIK, M., 1997, *Phys. Rev.* B, **56,** 7061.
[192] OHTA, H., TANAKA, R., MOTOKAWA, M., KUNII, S., and KASUYA, T., 1991, *J. phys. Soc. Jpn.*, **60,** 1361.
[193] GORSHUNOV, B., SLUCHANKO, N., VOLKOV, A., DRESSEL, M., KNEBEL, G., LOIDL, A., and KUNII, S., 1999, *Phys. Rev.* B, **59,** 1808.
[194] ALEKSEEV, P. A., LAZUKOV, V. N., OSBORN, R., RAINFORD, B. D., SADIKOV, I. P., KONOVALOVA, E. S., and PADERNO, YU. B., 1993, *Europhys. Lett.*, **23,** 347.
[195] OKAMURA, H., KIMURA, S., SHINOZAKI, H., NANBA, T., IGA, F., SHIMIZU, N., and TAKABATAKE, T., 1998, *Phys. Rev.* B, **58,** 7496.
[196] BOUVET, A., KASUYA, T., BONNET, M., REGNAULT, L. P., ROSSAT-MIGNOD, J., IGA, F., FAK, B., and SEVERING, A., 1998, *J. Phys. condens. Matter*, **10,** 5667.
[197] SULEWSKI, P. E., SIEVERS, A. J., MAPLE, M. B., TORIKACHVILI, M. S., SMITH, J. L., and FISK, Z., 1988, *Phys. Rev.* B, **38,** 5338.
[198] DONOVAN, S., SCHWARTZ, A., and GRUNER, G., 1997, *Phys. Rev. Lett.*, **79,** 1401.
[199] DEGIORGI, L., 1999, *Rev. mod. Phys.*, **71,** 687.
[200] URASAKI, K., and SASO, T., 1998, *Phys. Rev.* B, **58,** 15528.
[201] DAMASCELLI, A., SCHULTE, K., VAN DER MAREL, D., and MENOVSKY, A. A., 1997, *Phys. Rev.* B, **55,** 4863.
[202] VAN DER MAREL. D., DAMASCELLI, A., SCHULTE, K., and MENOVSKY, A. A., 1998, *Physica* B, **244,** 138.
[203] OHTA, H., KIMURA, S., KULATOV, E., HALILOV, S., NANBA, T., MOTOKAWA, M., SATO, M., and NAGASAKA, K., 1994, *J. phys. Soc. Jpn.*, **63,** 4206.
[204] OHTA, H., KIMURA, S., KULATOV, E., HALILOV, S. V., NANBA, T., and MOTOKAWA, M., 1995, *J. magn. magn. Matter*, **140–144,** 121.
[205] DAMASCELLI, A., SCHULTE, K., VAN DER MAREL, D., FATH, M., and MENOVSKY, A. A., 1997, *Physica* B, **230–232,** 787.
[206] DEGIORGI, L., HUNT, M. B., OTT, H. R., DRESSEL, M., FEENSTRA, B. J., GRUNER, G., FISK, Z., and CANFIELD, P. C., 1994, *Europhys. Lett.*, **28,** 341.
[207] KOHN, W., 1964, *Phys. Rev.* A, **171,** 133.
[208] CHERNIKOV, M. A., DEGIORGI, L., FELDER, E., PASCHEN, S., BIANCHI, A. D., and OTT, H. R., 1997, *Phys. Rev.* B, **56,** 1366.
[209] TRAVAGLINI, G., and WACHTER, P., 1984, *Phys. Rev.* B, **29,** 893.
[210] NANBA, T., OHTA, H., MOTOKAWA, M., KIMURA, S., KUNII, S., and KASUYA, T., 1993, *Physica* B, **186–188,** 440.
[211] KIMURA, S., NANBA, T., TOMIKAWA, M., KUNII, S., and KASUYA, T., 1992, *Phys. Rev.* B, **46,** 12196.
[212] KIMURA, S., NANBA, T., KUNII, S., and KASUYA, T., 1994, *Phys. Rev.* B, **50,** 1406.
[213] DRESSEL, M., GORSHUNOV, B., SLUCHANKO, N., VOLKOV, A., KNEBEL, G., LOIDL, A., and KUNII, S., 1999, *Physica* B, **259–261,** 347.
[214] OKAMURA, H., KIMURA, S., SHINOZAKI, H., NANBA, T., IGA, F., SHIMIZU, N., and TAKABATAKE, T., 1999, *Physica* B, **259–261,** 317.
[215] KILIBARDA-DALAFAVE, S., NG, H. K., CROW, J. E., PERNAMBUCO-WISE, P., YUEN, T., and LIN, C. L., 1993, *Physica* B, **186–188,** 989.
[216] NYHUS, P., COOPER, S. L., and FISK, Z., 1995, *Phys. Rev.* B, **51,** 15626.
[217] UDAGAWA, M., FUJITA, Y., OGITA, N., YOSHINO, T., TAKABATAKE, T., and FUJII, H., 1999, *Physica* B, **259–261,** 290.
[218] NYHUS, P., COOPER, S. L., FISK, Z., and SARRAO, J., 1995, *Phys. Rev.* B, **52,** 14308.
[219] ALEKSEEV, P. M, MIGNOT, J.-M., ROSSAT-MIGNOD, J. M., LAZUKOV, V. N., and SADIKOV, I. P., 1993, *Physica* B, **186–188,** 384.
[220] ALEKSEEV, P. A., MIGNOT, J.-M., ROSSAT-MIGNOD, J. M., LAZUKOV, V. N., SADIKOV, I. P., KONOVALOVA, E. S., and PADERNO, YU. B., 1995, *J. Phys. condens. Matter*, **7,** 289.
[221] EKINO, T., UMEDA, H., KATOH, K., TAKABATAKE, T., and FUJII, H., 1998, *J. magn. magn. Matter*, **177–181,** 379.

[222] LAUBE, F., GOLL, G., OBERMAIR, C., PIETRUS, T., and LOHNEYSEN, H. V., 1999, *Physica* B, **259–261,** 303.
[223] FATH, M., AARTS, J., MENOVSKY, A. A., NIEUWENHUYS, G. J., and MYDOSH, J., 1998, *Phys. Rev.* B, **58,** 15483.
[224] EKINO, T., TAKABATAKE, T., TANAKA, H., and FUJII, H., 1995, *Phys. Rev. Lett.*, **75,** 4262.
[225] EKINO, T., TAKABATAKE, T., and FUJII, H., 1997, *Physica* B, **230–232,** 635.
[226] EKINO, T., YOSHINO, T., TAKABATAKE, T., and FUJII, H., 1996, *Physica* B, **223–224,** 444.
[227] KOHGI, M., OHOYAMA, K., OSAKABE, T., and KASAYA, M., 1992, *J. magn. magn. Matter*, **108,** 358.
[228] DAVYDOV, D. N., KAMBE, S., JANSEN, A. G. M., WYDER, P., WILSON, N., LAPERTOT, G., and FLOQUET, J., 1997, *Phys. Rev.* B, **55,** 7299.
[229] FRANKOWSKI, I., and WACHTER, P., 1982, *Solid State Commun.*, **41,** 577.
[230] GUNTHERODT, G., THOMPSON, W. A., HOLTZBERG, F., and FISK, Z., 1982, *Phys. Rev. Lett.*, **49,** 1030.
[231] KUNII, S., and KAGAYA, O., 1985, *J. magn. magn. Matter*, **52,** 165.
[232] AMSLER, B., FISK, Z., SARRAO, J. L., VON MOLNAR, S., MEISEL, M. W., and SHARIFI, F., 1998, *Phys. Rev.* B, **57,** 8747.
[233] MOSER, M., WACHTER, P., HULLINGER, F., and ETOURNEAU, J. R., 1985, *Solid State Commun.*, **54,** 241.
[234] EKINO, T., UMEDA, H., IGA, F., SHIMIZU, N., TAKABATAKE, T., and FUJII, H., 1999, *Physica* B, **259–261,** 315.
[235] KJEMS, J., and BROHOLM, C., 1988, *J. magn. magn. Matter*, **76–77,** 371.
[236] ROSSAT-MIGNOD, J., REGNAULT, L. P., JACOUD, J. L., VETTIER, C., LEJAY, P., FLOQUET, J., WALKER, E., JACAARD, D., and AMATO, A., 1988, *J. magn. magn. Matter*, **76–77,** 376.
[237] KOHGI, M., OHOYAMA, K., OSAKABE, T., KASAYA, M., TAKABATAKE, T., and FUJII, H., 1993, *Physica* B, **186–188,** 409.
[238] KADAWAKI, H., SATO, T., YOSHIZAWA, H., EKINO, T., TAKABATAKE, T., FUJII, H., REGNAULT, L. P., and ISIKAWA, Y., 1994, *J. phys. Soc. Jpn.*, **63,** 2074.
[239] MASON, T. E., *et al.* unpublished.
[240] SEVERING, A., THOMPSON, J. D., CANFIELD, P. C., FISK, Z., and RISEBOROUGH, P., 1992, *J. Alloys Compounds*, **181,** 211.
[241] RAYMOND, S., MURANI, A. P., FAK, B., REGNAULT, L. P., LAPERTOT, G., ALEKSEEV, P. A., and FLOQUET, J., 1998, *J. magn. magn. Matter*, **190,** 245.
[242] RAYMOND, S., REGANULT, L. P., SATO, T., KADOWAKI, H., PYKA, N., NAKAMOTO, G., TAKABATAKE, T., FUJII, H., ISIKAWA, Y., LAPERTOT, G., and FLOQUET, J., 1997, *J. Phys. condens. Matter*, **9,** 1599.
[243] RAYMOND, S., REGNAULT, L. P., KADOWAKI, H., NAKAMOTO, G., TAKABATAKE, T., and FLOQUET, J., 1997, *Physica* B, **230–232,** 667.
[244] KAGAN, YU., KIKOIN, K. A., and MISCHENKO, A. S., 1997, *Phys. Rev.* B, **55,** 12348.
[245] KAGAN, YU., KIKOIN, K. A., and MISCHENKO, A. S., 1997, *Physica* B, **230–232,** 680.
[246] PARK, J.-G., ADROJA, D. T., MCEWEN, K. A., BI, Y. J., and KULDA, J., 1999, *Physica* B, **259–262,** 288.
[247] PARK, J.-G., ADROJA, D. T., MCEWEN, K. A., BI, Y. J., and KULDA, J., 1999, *Phys. Rev.* B, **58,** 3167.
[248] SATO, T., KADOWAKI, H., YOSHIZAWA, H., TAKABATAKE, T., FUJII, H., and ISIKAWA, Y., 1996, *J. Phys. condens. Matter*, **8,** 7127.
[249] SATO, T., KADOWAKI, H., YOSHIZAWA, H., NAKAMOTO, G., EKINO, T., TAKABATAKE, T., FUJII, H., REGNAULT, L. P., and ISIKAWA, Y., 1996, *Physica* B, **223–224,** 432.
[250] SCHROEDER, A., AEPPLI, G., MASON, T. E., and BUCHER, E., 1997, *Physica* B, **234–236,** 861.
[251] KUMAGAI, K., FURUKAWA, Y., OOI, K., RAINFORD, B., and YAKUBOVSKII, A., 1999, *Physica* B, **259,** 294.
[252] NAKAMURA, K., KITAOKA, Y., ASAYAMA, K., TAKABATAKE, T., NAKOMOTO, G., TANAKA, H., and FUJII, H., 1996, *Phys. Rev.* B, **53,** 6385.
[253] ADROJA, D., and RAINFORD, B., 1994, *Physica* B, **199–200,** 498.

[254] ADROJA, D. T., DEL MORAL, A., DE TERESA, J. M., IBARRA, M. R., and RAINFORD, B. D., 1995, *J. magn. magn. Matter*, **140–144,** 1219.
[255] SATO, T., KADOWAKI, H., TAKABATAKE, T., FUJII, H., and ISIKAWA, Y., 1996, *J. Phys. condens. Matter*, **8,** 8183.
[256] KADOWAKI, H., SATO, T., NAKAMOTO, G., TAKABATAKE, T., FUJII, H., and ISIKAWA, Y., 1997, *Physica* B, **230,** 664.
[257] OHOYAMA, K., KOHGI, M., YOSHINO, T., TAKABATAKE, T., HAHN, W., and ECCLESTON, R. S., 1999, *Physica* B, **259–261,** 283.
[258] HOLLAND-MORITZ, E., and KASAYA, M., 1986, *Physica* B, **136,** 424.
[259] ALEKSEEV, P. A., 1993, *Physica* B, **186–188,** 365.
[260] VON MOLNAR, S., THEIS, T., BENOIT, A., BRIGGS, A., FLOQUET, J., RAVEX, J., and FISK, Z., 1982, *Valence Instabilities*, edited by P. Wachter and H. Boppart (Amsterdam: North Holland), p. 389.
[261] KIKOIN, K. A., and MISCHENKO, A. S., 1990, *J. Phys. condens. Matter*, **2,** 6491.
[262] AONO, M., and KAWAI, S., 1979, *J. phys. Chem. Solids*, **40,** 797.
[263] REYES, A. P., HEFFNER, R. H., CANFIELD, P. C., THOMPSON, J. D., and FISK, Z., 1994, *Phys. Rev.* B, **49,** 16321.
[264] TAKAGI, S., YASUOKA, H., OGAWA, S., and WERNICK, J. H., 1981, *J. phys. Soc. Jpn.*, **50,** 2539.
[265] MAIR, S., KRUG VON NIDDA, H.-A., LOHMANN, M., and LOIDL, A., prepint.
[266] KITAOKA, Y., KYOGAKU, M., NAKAMURA, K., ZHENG, G.-Q., NAKAMURA, H., ASAYAMA, K., TAKABATAKE, T., TANAKA, H., FUJII, H., and SUZUKII, T., 1993, *Physica B*, **186–188,** 431.
[267] NAKAMURA, K., KITAOKA, Y., ASAYAMA, K., TAKABATAKE, T., NAKOMOTO, G., and FUJII, H., 1996, *Phys. Rev.* B, **54,** 6062.
[268] OHAMA, T., YASUOKA, H., and ISIKAWA, Y., 1995, *J. phys. Soc. Jpn.*, **64,** 4566.
[269] PENA, O., LYSAK, M., MACLAUGHLIN, D. E., and FISK, Z., 1981, *Solid State Commun.*, **40,** 539; PENA, O., MACLAUGHLIN, D. E., LYSAK, M., and FISK, Z., 1981, *J. appl. Phys.*, **52,** 215.
[270] TAKIGAWA, M., YASUOKA, H., KITAOKA, Y., TANAKA, T., NOZAKI, H., and ISHIZAWA, Y., 1981, *J. phys. Soc. Jpn.*, **50,** 2525.
[271] KUNII, S., UEMURA, T., CHIBA, Y., KASUYA, T., and DATE, M., 1985, *J. magn. magn. Matter*, **52,** 271.
[272] KOJIMA, K., HUKUDA, Y., KAWANAKA, H., TAKABATAKE, T., FUJII, H., and HIHARA, T., 1990, *J. magn. magn. Matter*, **90–91,** 505.
[273] KRATZER, A., KALVIUS, G. M., TAKABATAKE, T., NAKAMOTO, G., FUJII, H., and KREITZMAN, S. R., 1992, *Europhys. Lett.*, **19,** 649.
[274] KRATZER, A., KALVIUS, G. M., FLASCHIN, S. J., NOAKES, D. R., WAPPLING, R., BRUCKL, A., NEUMAIER, K., ANDRES, K., TAKABATAKE, T., KOBAYASHI, K., NAKOMOTO, G., and FUJII, H., 1997, *Physica B*, **230–232,** 661.
[275] KALVIUS, G. M., KRATZER, A., MUNSCH, K. H., WAGNER, F. E., ZWIRNER, S., KOBAYASHI, K., TAKABATAKE, T., NAKOMOTO, G., FUJII, H., KREITZMAN, S. R., and KEIFL, R., 1993, *Physica* B, **186–188,** 412.
[276] FLASCHIN, S. J., KRATZER, A., BURGHART, F. J., KALVIUS, G. M., WAPPLING, R., NOAKES, D. R., KADONO, R., WATANABE, I., TAKABATAKE, T., KOBAYASHI, K., NAKAMOTO, G., and FUJII, H., 1996, *J. Phys. condens. Matter*, **8,** 6967.
[277] KALVIUS, G. M., TAKABATAKE, T., KRATZER, A., WAPPLING, R., NOAKES, D. R., FLASCHIN, S. J., BURGHARDT, F. J., BRUCKL, A., NEUMAIER, K., ANDERS, K., KADONO, R., WATANABE, I., KOBAYASHI, K., NAKOMOTO, G., and FUJII, H., 1997, *Physica* B, **230–232,** 655.
[278] KALVIUS, G. M., TAKABATAKE, T., KRATZER, A., WAPPLING, R., NOAKES, D. R., FLASCHIN, S. J., BURGHARDT, F. J., KADONO, R., WATANABE, I., BRUCKL, A., NEUMAIER, K., ANDERS, K., KOBAYASHI, K., NAKOMOTO, G., and FUJII, H., 1997, *Hyperfine Interactions*, **104,** 157.
[279] PARK, J.-G., SCOTT, C., MCEWEN, K. A., and CYWINSKI, R., 1997, *Physica* B, **230–232,** 673.
[280] PARK, J.-G., COLES, B. R., and SARKISSIAN, B. V. B., 1994, *Physica* B, **199–200,** 475.

[281] ALLEN, J. W., 1992, *Synchrotron Radiation Research, Advances in Surface and Interface Science,* Vol. 1, *Techniques*, edited by R. Z. Bachrach (New York: Plenum Press), p. 252.
[282] ARKO, A. J., RISEBOROUGH, P. S., ANDREWS, A. B., JOYCE, J. J., TAHVILDAR-ZADEH, A. N., and JARRELL, M., 1998, *Handbook on the Physics and Chemistry of the Rare Earths*, edited by K. A. Gschneidner Jr and L. R. Eyring (Amsterdam: Elsevier Publishers).
[283] SEKIYAMA, A., SUGA, S., SAITOH, Y., UEDA, S., HARADA, H., MATSUSHITA, T., NAKATANI, T., IWASAKI, T., MATSUDA, K., KOTSUGI, M., IMADA, S., TAKABATAKE, T., YOSHINO, T., ADROJA, D. T., TAKAYAMA, R., SAKAI, O., HARIMA, H., and NANBA, T., 1999, *Solid State Commun.*, **111,** 373.
[284] GARNIER, M., PURDIE, D., HENGSBERGER, M., BREUER, K., and BAER, Y., 1999, *Physica* B, **259–261,** 1095.
[285] BREUER, K., MESSERLI, S., PURDIE, D., HENGSBERGER, M., PANACCIONE, G., BAER, Y., TAKAHASHI, T., YOSHII, S., KASAYA, M., KATOH, K., and TAKABATAKE, T., 1998, *Europhys. Lett.*, **41,** 565.
[286] SAITOH, T., SEKIYAMA, A., MIZOKAWA, T., FUJIMORI, A., ITO, K., NAKAMAURA, H., and SHIGA, M., 1995, *Solid State Commun.*, **95,** 307.
[287] SUSAKI, T., MIZOKAWA, T., FUJIMORI, A., OHNO, A., TONOGAI, T., and TAKAGI, H., 1998, *Phys. Rev.* B, **58,** 1197.
[288] OH, S. J., *et al.*, 1987, *Phys. Rev.* B, **35,** 2267.
[289] CHAINANI, A., YOKOYA, T., MORITO, T., TAKAHASHI, T., YOSHII, S., and KASAYA, M., 1994, *Phys. Rev.* B, **50,** 8915.
[290] NOHARA, S., NAMATAME, H., FUJIMORI, A., and TAKABATAKE, T., 1992, *Phys. Rev.* B, **47,** 1754.
[291] SLEBARSKI, A., JERZIERSKI, A., ZYGMUNT, A., MAHL, S., NEUMANN, M., and BORSTEL, G., 1996, *Phys. Rev.* B, **54,** 13551.
[292] KANG, J.-S., OLSON, C. G., INADA, Y., ONUKI, Y., KWON, S. K., and MIN, B. I., 1998, *Phys. Rev.* B, **58,** 4426.
[293] KANG, J.-S., INADA, Y., ONUKI, Y., OLSON, C. G., KWON, S. K., and MIN, B. I., 1999, *Physica* B, **259–261,** 1116.
[294] NOHARA, S., NAMATAME, H., FUJIMORI, A., and TAKABATAKE, T., 1992, *Physica* B, **186–188,** 403.
[295] SLEBARSKI, A., JERZIERSKI, A., ZYGMUNT, A., MAHL, S., NEUMANN, M., and BORSTEL, G., 1998, *Phys. Rev.* B, **58,** 4367.
[296] HIESS, A., ZOBKALO, I., BONNET, M., SCHWEIZER, J., LEVLIEVRE-BERNA, E., TASSET, F., ISIKAWA, Y., and LANDER, G. H., 1997, *J. Phys. condens. Matter*, **9,** 9321.
[297] HIESS, A., ZOBKALO, I., BONNET, M., SCHWEIZER, J., LEVLIEVRE-BERNA, E., TASSET, F., ISIKAWA, Y., and LANDER, G. H., 1997, *Physica* B, **230–232,** 687.
[298] KUMIGASHIRA, H., SATO, T., YOKOYA, Y., TAKAHASHI, T., YOSHII, S., and KASAYA, M., 1999, *Phys. Rev. Lett.*, **82,** 1943.
[299] SUSAKI, T., SEKIYAMA, A., KOBAYASHI, K., MIZOKAWA, T., FUJIMORI, A., TSUNEKAWA, M., MURO, T., MATSUSHITA, T., SUGA, S., ISHII, H., HANYU, T., KIMURA, A., NAMATAME, H., TANIGUCHI, M., MIYAHARA, T., IGA, F., KASAYA, M., and HARIMA, H., 1996, *Phys. Rev. Lett.*, **77,** 4296.
[300] SUSAKI, T., SEKIYAMA, A., KOBAYASHI, K., MIZOKAWA, T., FUJIMORI, A., TSUNEKAWA, M., MURO, T., MATSUSHITA, T., SUGA, S., ISHII, H., HANYU, T., KIMURA, A., NAMATAME, H., TANIGUCHI, M., MIYAHARA, T., IGA, F., KASAYA, M., and HARIMA, H., 1997, *Phys. Rev. Lett.*, **78,** 1832.
[301] JOYCE, J. J., and ARKO, A. J., 1997, *Phys. Rev. Lett.*, **78,** 1831.
[302] SUSAKI, T., TAKEDA, Y., MAMIYA, K., FUJIMORI, A., SHIMADA, K., NAMATAME, H., TAMIGUCHI, M., SHIMIZU, N., IGA, F., and TAKABATAKE, T., 1999, *Phys. Rev. Lett.*, **82,** 992.
[303] KASAYA, M., KIMURA, H., ISIKAWA, Y., FUJITA, T., and KASUYA, T., 1981, *Valence Fluctuations in Solids*, edited by L. M. Falicov, W. Hanke and M. B. Maple (Amsterdam: North Holland), p. 251.

[304] IGA, F., HIURA, S., KLIJN, J., SHIMIZU, N., TAKABATAKE, T., ITO, M., MATSUMOTO, Y., MASAKI, F., SUZUKI, T., and FUJITA, T., 1999, *Physica* B, **259–261,** 312.
[305] FISK, Z., SARRAO, J. L., COOPER, S. L., NYHUS, P., BOEBINGER, G. S., PASSNER, A., and CANFIELD, P. C., 1996, *Physica* B, **223–224,** 409.
[306] BEILLE, J., VOIRON, J., and ROTH, M., 1983, *Solid State Commun.*, **47,** 399.
[307] BEILLE, J., VOIRON, J., TOWFIQ, F., ROTH, M., and ZHANG, Z. Y., 1981, *J. Phys.* F, **11,** 2153.
[308] CHERNIKOV, M. A., FELDER, E., PASCHEN, S., BIANCHI, A. D., OTT, H. R., SARRAO, J. L., MANDRUS, D., and Z. FISK, Z., 1997, *Physica* B, **230–232,** 790.
[309] BAUER, E., BOCELLI, S., HAUSER, R., MARABELLI, F., and SPOLENAK, R., 1997, *Physica* B, **230–232,** 794.
[310] PASCHEN, S., PUSHIN, D., OTT, H. R., YOUNG, D. P., and FISK, Z., 1999, *Physica* B, **259,** 864.
[311] BUSCHINGER, B., WEIDEN, M., TROVARELLI, O., HELLMANN, P., GEIBEL, C., and STEGLICH, F., 1998, *J. Phys. condens. Matter*, **10,** 2021.
[312] ALEKSEEV, P. A., CLEMENTYEV, E. S., LAZUKOV, V. N., SADIKOV, I. P., GOREMYCHKIN, E. A., and SASHIN, I. L., 1993, *Physica* B, **186–188,** 416.
[313] MENON, L., and MALIK, S. K., 1977, *Physica* B, **230–232,** 695.
[314] MENON, L., and MALIK, S. K., 1977, *Solid State Commun.*, **101,** 779.
[315] MENON, L., and MALIK, S. K., 1977, *Phys. Rev.* B, **55,** 14100.
[316] MALIK, S. K., MENON, L., GHOSH, K., and RAMAKRISHNAN, S., 1995, *Phys. Rev.* B, **51,** 399.
[317] MARTIN, R. M., and ALLEN, J. W., 1979, *J. appl. Phys.*, **50,** 7561; 1980, *J. appl. Phys.*, **53,** 2143.
[318] MARTIN, R. M., 1982, *Phys. Rev. Lett.*, **48,** 362.
[319] MCQUEEN, P. G., HESS, D. W., and SERENE, J. W., 1994, *Phys. Rev.* B, **50,** 7304.
[320] MORENO, J., and COLEMAN, P., 1999, *Physica* B, **259–261,** 190.
[321] COLEMAN, P., 1987, *Phys. Rev.* B, **35,** 5072.
[322] MILLIS, A. J., and LEE, P. A., 1987, *Phys. Rev.* B, **35,** 3394.
[323] SANCHEZ-CASTRO, C., BEDELL, K., and COOPER, B. R., 1993, *Phys. Rev.* B, **47,** 6897.
[324] TOVAR COSTA, M. V., DE OLIVIERA, N. A., JAPIASSU, G. M., CONTINENTINO, M. A., and TROPER, A., 1998, *J. magn. magn. Matter*, **177–181,** 331.
[325] CONTINENTINO, M. A., JAPIASSU, G. M., and TROPER, A., 1995, *J. magn. magn. Matter*, **140–144,** 1251.
[326] DONIACH, S., FU, C., and TRUGMAN, S., 1994, *Physica* B, **199–200,** 450.
[327] DUAN, J. M., AROVAS, D. P., and SHAM, L. J., 1997, *Phys. Rev. Lett.*, **79,** 2097.
[328] RASUL, J. W., 1995, *Phys. Rev.* B, **51,** 2576.
[329] SASO, T., 1997, *Physica* B, **230–232,** 711.
[330] LAWRENCE, J. M., and MILLS, D. L., 1991, *Comments Cond. Mat. Phys.*, **15,** 163.
[331] SCHLOTTMANN, P., 1998, *Current Problems in Condensed Matter: Theory and Experiment*, edited by J. L. Moran-Lopez (New York: Plenum Press).
[332] ALIEV, F. G., MOSCHALKOV, V. V., KOZYRKOV, V. V., ZALYALYUTDINOV, M. K., PRYADUN, V. V., and SCOLOZDRA, R. V., 1988, *J. magn. magn. Matter*, **76–77,** 295.
[333] RISEBOROUGH, P. S., 1994, *Physica* B, **199–200,** 466.
[334] READ, N., 1985, *J. Phys.* C, **18,** 2651.
[335] RASUL, J. W., 1997, *Phys. Rev.* B, **56,** 163.
[336] HOUGHTON, A., READ, N., and WON, H., 1987, *Phys. Rev* B, **37,** 3782.
[337] DONIACH, S., 1987, *Phys. Rev.* B, **35,** 1814.
[338] WANG, Z., LI, X. P., and LEE, D. H., 1993, *Phys. Rev.* B, **47,** 11935.
[339] YU, C., and WHITE, S. R., 1993, *Phys. Rev. Lett.*, **71,** 3866.
[340] KARBOWSKI, J., 1996, *Phys. Rev.* B, **54,** 728.
[341] DORIN, V., and SCHLOTTMANN, P., 1992, *Phys. Rev.* B, **46,** 10800.
[342] DONIACH, S., and FAZEKAS, P., 1992, *Phil. Mag.* B, **65,** 1171.
[343] RISEBOROUGH, P. S., 1998, *Phys. Rev* B, **58,** 15534.
[344] FU, C., and DONIACH, S., 1995, *Phys. Rev.* B, **51,** 17439.
[345] JARRELL, M., AKHLAGHPOUR, H., and PRUSCHKE, TH., 1993, *Phys. Rev. Lett.*, **70,** 1670.

[346] TSVELIK, A. M., 1994, *Phys. Rev. Lett.*, **71,** 3866.
[347] COLEMAN, P., MIRANDA, E., and TSVELIK, A., 1993, *Phys. Rev. Lett.*, **70,** 2960; 1993, *Physica* B, **186–188,** 362.
[348] TAKAHASHI, Y., and MORIYA, T., 1979, *J. phys. Soc. Jpn.*, **46,** 1451.
[349] EVANGELOU, S. N., and EDWARDS, D. M., 1980, *J. Phys.* C, **16,** 2121.
[350] JARLBORG, T., 1995, *Phys. Rev.* B, **51,** 11106.
[351] TAKAHASHI, Y., 1994, *J. Phys. condens. Matter*, **6,** 7063.
[352] TAKAHASHI, Y., 1997, *J. Phys. condens. Matter*, **9,** 2593.